Cullin5 and SOCS Protein Regulation of Receptor Tyrosine Kinases

Carissa Pilling

A dissertation

submitted in partial fulfillment of the

requirements for the degree of

Doctor of Philosophy

University of Washington
2017

Reading Committee:

Jonathan A. Cooper, Chair

William M. Grady

Bruce E. Clurman

Program Authorized to Offer Degree:

Molecular and Cellular Biology

University of Washington

Abstract

Cullin5 and SOCS Protein Regulation of Receptor Tyrosine Kinases

Carissa Pilling

Chair of the Supervisory Committee:
Jonathan A. Cooper, Ph.D.
Biochemistry

Suppressors of cytokine signaling (SOCS) proteins are a family of eight proteins that can inhibit signal transduction through receptor tyrosine kinases (RTKs) by serving as substrate receptors in Cullin5-RING E3 ubiquitin ligase (CRL5) and through a variety of CRL5-independent mechanisms. We have shown that Cul5, SOCS2 and SOCS6 inhibit epithelial cell transformation. To identify heretofore-uncharacterized substrates of $CRL5^{SOCS2}$ and $CRL5^{SOCS6}$, we performed multiple mass spectrometry-based screens. First, a quantitative phosphoproteomic comparison of WT and Cul5-depleted cells identified increased abundance of phosphotyrosine (pY) peptides from the activation loop of the insulin receptor (INSR) and insulin-like growth factor receptor I (IGF-IR). Using western blotting we found pY1135 in the activation loop of INSR or IGF-IR was indeed increased in Cul5-depleted cells, suggesting that activation of either the INSR or IGF-IR or both are negatively regulated by $CRL5^{SOCS1}$-depletion. Second, we

identified proteins that interact with SOCS2 and SOCS6 using two parallel proteomics techniques: BioID and Flag affinity purification mass spectrometry. We found that the receptor tyrosine kinase ephrin type-A receptor 2 (EphA2) interacted with SOCS2. Furthermore, SOCS2-EphA2 binding required the SOCS2 SH2 domain and autophosphorylation of a tyrosine in the activation loop of EphA2 induced by the ligand Ephrin A1 (EfnA1). SOCS2 interaction only occured with EphA2 that was internalized into endosomes following EfnA1 stimulation. Moreover, SOCS2 overexpression induces EfnA1 expression, and increased EfnA1 decreases the steady-state level of EphA2. Collectively, this suggests that SOCS2 may contribute to trafficking of EphA2. Third, we examined the relationship between Cul5 and the receptor tyrosine kinase epidermal growth factor receptor (EGFR) in mammary epithelial cells. Unlike control cells, Cul5-depleted cells grow independent of added epidermal growth factor (EGF) in the media. However, we found that the growth of Cul5-depleted cells in EGF-free media required EGFR ligand binding and EGFR kinase activity. Cul5-depleted cells showed increased expression of some EGFR ligands in EGF-free media and increased phosphorylation of EGFR, consistent with an autocrine requirement of EGFR signaling. Taken together, our results demonstrate new mechanisms by which Cul5-depletion or SOCS protein over-expression may regulate receptor tyrosine kinases in epithelial cells.

TABLE OF CONTENTS

LIST OF FIGURES

LIST OF TABLES

ACKNOWLEDGEMENTS

I am thankful to Jon Cooper for his training over the past six years. Jon I appreciate your time and patience while answering all my questions on background information, protocols, and future directions. You have taught me how to think critically and how to design well-controlled experiments that directly address the hypothesis. I am always amazed at your wealth of knowledge on tyrosine kinase biology and biochemistry techniques, and appreciate you sharing this knowledge with me over the past six years. Your excitement and passion for science is infectious and drove me to keep going even when my project took unexpected turns. I enjoyed and benefited immensely from our weekly, sometimes daily, discussions about my project and other projects in the lab. I also greatly appreciate your willingness to allow me to take time off at the beginning and end of my Ph.D. to complete two internships in industry. Your thoughtful discussions with me on my career path after my Ph.D. were valuable and will instruct my next steps. Finally, thank you for dealing with my terrible paper/dissertation writing and for taking the time to teach me how to write more clearly. I know sometimes it wasn't easy, but I truly appreciate it.

I would also like to thank Anjali Teckchandani for her helpful experiment suggestions and in lab mentorship. I knew that I could always go to her with any experimental questions or confusing result and she would make time to teach me. She was not only a fantastic mentor to me, but also taught me how to mentor other people through our many conversations.

I would also like to thank members of my thesis committee for their thoughtful advice on experiments, careers, and general help navigating through the Ph.D. process. More specifically I would like to thank Bruce Clurman, William Gray and Jon Cooper for taking the time to read and comment on my dissertation.

I am also very grateful to Julio Vasquez and Dave McDonald of the Fred Hutch Scientific Imaging Core for assistance with microscopy and image analysis; the staff of the Fred Hutch Flow Cytometry Core for their assistance with cell sorting and flow analysis; Phil Gafken and

the staff of the Fred Hutch Proteomics facility for running the affinity purification mass spectrometry samples; ChenWei Lin of the Paulovich lab for running the affinity purification mass spectrometry samples through MaxQuant to obtain label-free quantification data; Wade Harper, Anne-Claude Gingras and Rob Lawrence for helpful discussions on mass spectrometry screening techniques and approaches; the Koch Institute Swanson Biotechnology Center for technical support, specifically Amanda Del Rosario and the Proteomics Core Facility, for running the quantitative phosphotyrosine mass spectrometry experiment; Sergey Ovchinnikov and Kyle Stahley for their helpful discussions and assistance with the mass spectrometry data analysis; Sherry Yen for GPS constructs and helpful discussion about the GPS screening approch; Wade Harper, Sergi Simo, Bruce Huang, Sascha Strait, Hironori Katoh, Amilcar Flores-Morales and Anne-Claude Gringras for DNA constructs; Zoe Maltzer for her technical assistance with qPCR; Fariha Ahmed-Qadi and Zoe Maltzer for their technical assistance with the growth assay experiments; Jason Berndt for construction of the clonal CRISPR/Cas9 Cul5 MCF10A cell line; George Laszlo and Khyati Shah for their initial observations and work studying EGFR in EV & shCul5 MCF10A cells; and Jason Berndt for his critical review of the dissertation. Carissa Pilling was supported by a NSF graduate research fellowship. The work in this dissertation was supported by grant R01-GM109463 from the US Public Health Service.

DEDICATION

This work is dedicated to my family members who have passed away due to cancer: Albert Pilling, Neville Pilling, Margret Cheatham, Mimi O'Leary, and James O'Leary.

Chapter 1. GENERAL INTRODUCTION

1.1 TYROSINE KINASES

Cells receive signals from the extracellular environment and respond dynamically to maintain homeostasis. One key way cells respond to their environment is through transmembrane receptors expressed on the surface of the cell that bind to extracellular cues. Extracellular molecule binding to these receptors results in the activation of the enzymes intrinsic to or associated with the receptor on the cytosolic side of the cell. The receptors then activate signaling cascades that translate the information from the environment to the interior of the cell triggering a physiological response.

Kinases are one group of enzymes that can be activated by receptors or are transmembrane receptors themselves. There are 500 kinases in the human genome. In eukaryotic species kinases transfer a phosphate moiety from ATP primarily to the amino acids serine (S), threonine (T) or tyrosine (Y) (*1*). Receptors that use tyrosine kinases to relay extracellular information have been shown to play a significant role in cell migration, immune cell signaling, cellular responses to hormones and growth factors, and virtually all other cellular processes (*2*). Thus, tyrosine kinases are important modulators of cell behavior.

There are 90 tyrosine kinases in the human genome (*3*), which can be subdivided into two families: receptor tyrosine kinases (RTKs) and non-receptor tyrosine kinases (NRTKs). RTKs are the largest family of tyrosine kinases with 58 members grouped into 20 families base on ligand binding properties (*2, 4*).

1.1.1 *Receptor Tyrosine Kinases(RTKs)*

Most RTKs are single-pass transmembrane proteins composed of extracellular ligand binding domains and intracellular cytoplasmic domains. In the absence of ligand binding, most RTKs are monomeric. The exception is the insulin receptor (INSR) and insulin-like growth factor receptor (IGF-R) receptor family, members which dimerize in the absence of ligand due to the presence of disulfide bonds that link two monomers. The extracellular side of RTKs is primarily devoted

to ligand binding and sometimes dimerization. On the cytosolic side, RTKs have a juxtamembrane region, of varying length, followed by a tyrosine kinase domain and varying c-terminal domains/regions. In the unstimulated state, monomeric RTKs have intramolecular (*cis*) interactions that inhibit the kinase domain (*5*).

Ligand binding results in a molecular cascade that activates intrinsic RTK kinase activity. RTKs bind to extracellular soluble or membrane-bound ligands. Ligand binding causes dimerization or oligomerization, bringing the kinase domains of each RTK monomer near one another. The close proximity causes *trans*-phosphorylation of each receptor in the oligo which relieves *cis*-inhibition of the kinase domain. This event is followed by autophosphorylation of a conserved tyrosine(s) in the kinase activation loop. Phosphorylation of the activation loop results in a kinase domain in a stable conformation that binds ATP and substrate proteins (*1, 2, 5, 6*). Active RTKs autophosphorylate on tyrosine residues in the carboxy-terminus creating binding sites for downstream signaling proteins.

Downstream signaling proteins are recruited to the RTKs through Src homology 2 (SH2) or phosphotyrosine-binding (PTB) domains (*2*). SH2 domains bind to the phosphorylated tyrosine and three to five amino acids c-terminal to the phosphorylated tyrosine. Individual SH2 domains can be characterized by the sequence of the consensus binding motif to which it binds (*7*). PTB domains bind to phosphotyrosine and three amino acids N-terminal to the phosphotyrosine. Some PTB domains directly recruit to the phosphotyrosine-containing protein; however, the majority of PTB domain-containing proteins rely on other domains in *cis* to colocalize with substrates and secondarily bind phosphotyrosines (*8*). RTKs activate downstream signaling by either phosphorylating bound proteins or through the simultaneous binding of signaling proteins or both.

1.1.2 *Non-Receptor Tyrosine Kinases (NRTKs) and their associated receptors*

NRTKs are distinct from RTKs in localization but have similar mechanisms of activation. NRTKs are cytosolic, or anchored to the membrane through N-terminal myristoylation or palmitoylation. In addition to the kinase domain, NRTKs often have other domains or motifs that

promote interaction with macromolecules within the cell. The most common of which are SH2, SH3, and PH domains that mediate interactions with other proteins or membranes.

Activation of NRTKs is similar to RTKs. Many NRTKs are *cis*-inhibited and removal of this inhibition leads to phosphorylation of tyrosine in the kinase domain activation loop by homo- or hetero-*trans*-phosphorylation with another NRTK. Activation loop phosphorylation activates the kinase. Moreover, NRTKs can be recruited to and phosphorylate RTKs (*2, 6*).

Some transmembrane receptors that lack intrinsic enzymatic activity can use NRTKs to transmit extracellular signals. These receptors are separated into three groups (cytokine receptors, antigen receptors, and integrins) based on the type of NRTK used to transmit extracellular cues (*1*). Cytokine receptors use the JAK family of NRTKs to transmit signals. JAK proteins contain a domain that constitutively targets them to the cytoplasmic tail of the cytokine receptor (*2*). In the ligand-free state cytokine receptors form a weak homo or heterodimer on the membrane. Two JAKs associated with the receptor dimer bind one another resulting in dual *trans*-inhibition. Ligand binding pulls the cytoplasmic tails of each receptor apart, breaking the JAK-JAK inhibitory interaction and resulting in JAK *trans*-phosphorylation and activation (*9*). The activated JAKs then phosphorylate tyrosine residues in the cytokine receptor, creating binding sites for downstream signaling proteins, including members of the STAT family of transcription factors, which are a major downstream target of cytokine receptors. STATs bind to phosphorylated cytokine receptors using a SH2 domain. Upon receptor binding STATs are phosphorylated by JAK, they then dissociate from the receptor, and dimerize. STAT proteins can hetero or homodimerize through a SH2 phosphotyrosine interactions. The activated STAT dimers move into the nucleus and activate or repress transcription (*1, 10*).

Antigen receptors are a second class of NRTK-associated transmembrane receptors that include the T-cell, B-cell and Fc receptors. These receptors partner with the Src family of NRTKs (SFKs; c-Src, Lck, Hck, Lyn, Blk, Fgr, Fyn, Yes, and Yrk) to activate downstream signaling (*1, 11*). Myristoylization of the N-termini of SFKs results in constitutive targeting to the plasma membrane. All SFKs have a SH3, SH2, short linker, and kinase domains. Before activation, the SH2 domain of SFKs is bound to a phosphorylated tyrosine residue in the C-terminal tail, and

the SH3 domain is bound to a linker region near the N-terminus. The folding of SFKs inactivates the kinase domain and blocks the SH2 and SH3 domain binding interfaces of the SFK. Dephosphorylation of the c-terminal phosphotyrosine in SFKs releases the SH2 and SH3 domain intramolecular interactions, activates the kinase domain, and promotes autophosphorylation of the activation loop tyrosine (*12*).

Integrins are NRTK-associated transmembrane receptors that connect the intracellular cytoskeleton to the extracellular matrix. Integrin engagement with the extracellular matrix, changes integrin receptor conformation resulting in the aggregation of integrins and the formation of a complex of structural and signaling proteins, called a focal adhesion. The NRTKs FAK and Src are both transiently activated upon integrin engagement and essential for the formation of multiprotein complexes that connect the cell and the extracellular matrix, called focal adhesions (*13*).

1.1 Endocytosis and Endosomal Trafficking of Receptor Tyrosine Kinases

Inactivation of RTKs occurs by at least two distinct mechanisms, both of which involve post-translational modifications. First, RTKs are dephosphorylated by protein tyrosine phosphatases (PTPs). PTPs have the ability to both activate and inhibit tyrosine kinases because depending on the specific tyrosine, phosphorylation can either activate or inhibit kinase activity (*14*).

The second and major mechanism of negative regulation of RTKs involves ubiquitin-mediated endocytosis and degradation. Ubiquitylation refers to the post-translational addition of ubiquitin, a 76-amino acid protein, to lysine residues of target proteins. Ubiquitylation occurs using a three-step enzyme cascade. First, ubiquitin (Ub) is added to a cysteine on an Ub-activating enzyme (E1) in ATP dependent manner. The ubiquitin-charged E1 then transfers the ubiquitin to a cysteine on an Ub-conjugating enzyme (E2). Finally, the ubiquitin-charged E2 binds to an Ub-ligase (E3) that is bound to the target substrate protein (*15*). For the really interesting new gene (RING) family of E3 Ub-Ligases, the E2 will transfer the ubiquitin onto a lysine in the target proteins. For the homologous to the E6-AP carboxyl terminus (HECT) family of E3s the ubiquitin is transferred to a cysteine in the E3, before transfer to the lysine in the target protein.

The E3 is responsible for binding proteins that will ultimately be ubiquitylated, i.e. substrates (*16*).

Ubiquitin can be added to one (mono) or more lysines (multi-mono) in a target protein. A second ubiquitin can be added to one of the seven lysines in ubiquitin in a process called polyubiquitylation. Monoubiquitylation, multi-monoubiquitylation and the different polyubiquitylation linkages each serve a different function in the cell. Some linkage-specific functions have been well worked out, such as Lys-48 and Lys-11 polyubiquitylation that targets proteins to the 26S proteasome for degradation (*17*). Multi-monoubiquitylation and Lys-63 polyubiquitylation regulate endocytosis and target proteins to the lysosome (*18, 19*). Proteins that possess ubiquitin-binding domains (UBDs) recognize ubiquitylated proteins and execute the physiological function of these linkages (*17*).

RTK endocytosis can lead to lysosomal degradation or ligand dissociation and recycling back to the plasma membrane. Endocytosis serves two roles: it can shut off the signaling from RTKs through degradation or it can fine-tune the type and duration of signaling downstream of the receptor.

Endocytosis of RTKs has been shown to proceed through both a clathrin-dependent pathway and multiple clathrin-independent pathways, including caveolin-dependent, clathrin- and caveolin-independent, macropinocytic, fast endophilin-mediated, and other mechanisms (Figure 1.1) (*20, 21*). Nevertheless, the majority of RTK endocytosis after ligand binding is thought to occur through the clathrin-dependent mechanism (*18, 19*).

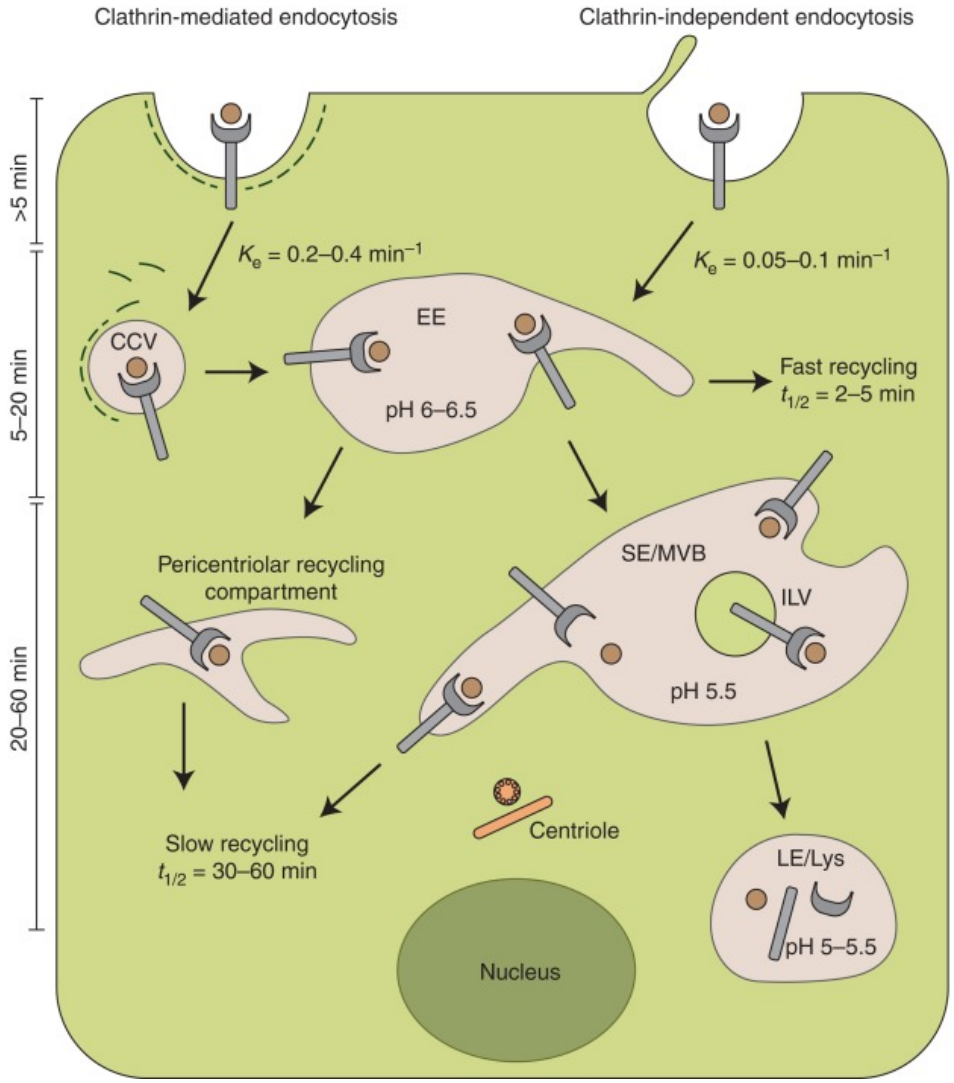

FIGURE 1.1 RTK ENDOCYTOSIS, RECYCLING AND LYSOSOMAL DEGREDATION

RTK are endocytosed through a clathrin-dependent or multiple clathrin-independent mechanisms. RTK-containing endocytic vesicles first enter the early endosome (EE), where endocytic cargo is sorted into downstream compartments. A RTK can be recycled back to the plasma membrane from the early endosome in a process called fast recycling. When a RTK recycles from the multi vesicular body (MVB) it is called slow recycling. Any RTKs incorporated into the intraluminal vesicles (ILV) inside the MVB will be degraded by the lysosome. Figure is from the paper in this citation (*18*).

Clathrin-dependent endocytosis of RTKs can be constitutive or ligand-induced (*22*). Constitutive endocytosis involves incorporation of RTKs into clathrin-coated pits (CCP) independent of ligand stimulation. Constitutive association with CCPs requires a cytoplasmic motif, including

the acidic dileucine [DE]xxxL[LI] internalization motif and the YxxΦ motifs, both of which bind to the adaptor protein AP-2 (*23*). AP-2 binds to clathrin, nucleating the formation of a clathrin lattice and clusters of receptors in CCPs at the plasma membrane (*18*). PTB-domain containing CCP adaptor proteins, such as Dab2, ARH, and Numb, bind to [FY]xNPx[FY] motifs in some RTKs. These adaptors interact with AP-2 and bring RTKs into CCPs (*24*). Even though, some RTKs have AP-2, Dab2, ARH, and Numb binding motifs constitutive endocytosis does not to play a significant role in RTK internalization (*25-29*). Instead, the major way RTKs are incorporated into CCPs is through ligand-simulated ubiquitylation of the receptor.

RTKs are rapidly ubiquitylated after ligand-mediated activation, and this causes binding of the CCP adaptor proteins epsin-1/-2, Eps15, and Eps15R through respective UBDs. The epsin-1/2, Eps15, and Eps15R adaptors bind to clathrin via AP-2. Therefore, ubiquitylated receptors are sequestered by epsin-1/2, Eps15, and Eps15R adaptors on the plasma membrane in CCPs until a clathrin coated vesicle is pinched off of the membrane (*18, 23*). Eps15/15R can also be monoubiquitylated after acute RTK stimulation, and Eps15/15R ubiquitylation may play a role in the formation of RTK-containing CCPs (*30, 31*). Additionally, a clathrin-independent lipid-raft-dependent method of endocytosis of EGFR requires ubiquitylation, Eps15, and Epsin (*32*).

After internalization, a RTK-containing vesicle enters the endosomal system that is responsible for trafficking the receptors to different locations in the cell. A RTKs face one of three fates in the endosomal system: recycling via the slow or fast recycling pathways or trafficking to multivesicular bodies (Figure 1.1). Endosomes are trafficked to these locations along microtubules and as endosome matures and grows the pH on the inside steadily decreases. Acidification can cause dissociation of the ligand from the receptor, depending on the affinity of the receptor-ligand interaction, leading to decreased kinase activity and RTK ubiquitylation (*18, 19*). The early endosome is the first compartment a RTK enters in the endosomal system.

The early endosome gathers and sorts cargo to downstream compartments. Early endosomes are characterized by the presence of the GTPase Rab5 and its effectors EEA1, APPL1, and APPL2. There are three different types of early endosomes: those that have EEA1 only, APPL only or both EEA1 and APPL. APPL1 early endosomes are the precursor to EEA1-positive early

endosomes (*33*). These small early endosomes undergo fission and fusion reactions as they move towards the nucleus increasing the endosome size.

After trafficking through early endosomes, RTKs can be recycled back to the membrane and the ligand binding status is thought to mediate this. A RTK that released its ligand in the early endosome is deubiquitylated and is recycled back to the plasma membrane, via the fast recycling pathway (*34*). RTK recycling provides repeated activation of RTK signaling pathways because the recycled receptor can be repeatedly activated by any ligand present outside of the cell.

Another destination for endocytic vesicles containing RTKs in the early endosome is the lysosomal degradation pathway. If the receptor is not recycled, then the early endosome continues on to become a late endosome. Late endosomes eventually become multivesicular bodies (MVB). Intraluminal vesicles (ILVs) inside the MVB are formed by pinching membrane off the late endosome into the lumen of the late endosome. The primary signal that sorts proteins into ILVs is protein ubiquitylation (*35, 36*).

The endosomal sorting complex required for transport (ESCRT) complex of proteins recognize, cluster, and pass ubiquitylated proteins along the late endosome/MVB membrane until a ILV is ultimately pinched off. Four ESCRT complexes act sequentially: ESCT-0, ESCRT-I, ESCRT-II, ESCRT-III. ESCRT-0 is recruited to the endosomes by binding to the PI(3)P lipid that is enriched in the early endosome and MVB membranes. ESCRT-0 binds to ubiquitylated cargo on the endosomal membrane and then sequentially recruits ESCRT-I followed by ESCRT-II and finally ESCRT-III, to form a ESCRT complex that will pinch off the ILV. Cargo is deubiquitylated before ILV scission from the MVB membrane, to prevent degradation of ubiquitin (*18, 37*).

ESCRT binding to a ubiquitylated RTK dictates if a RTK will be degraded or recycled via the slow recycling pathway. The ESCRT complexes are able to bind to ubiquitylated cargo through a variety of ubiquitin-binding domains. ESCRT-0 complex members HRS and STAM1/2 have ubiquitin-interacting motifs (UIMs). ESCRT-I complex members TSG101 and VSP23 have a ubiquitin E2 variant (UEV) domain that can bind ubiquitin. ESCRT-II complex member VPS36

has a GRAM-like ubiquitin binding on Eap45 (GLUE) domain that can bind to phosphorylated phosphatidylinositol lipids and ubiquitin (*36*). Any RTKs not captured by ESCRT and left on the outer membrane of MVB are recycled back to the plasma membrane via the slow recycling process. The receptors captured in ILVs are degraded when the MVB fuses with the lysosome (*23*). Therefore, MVBs turn off receptor signaling by isolating the c-terminal domain of an RTK from the cytosol and irreversibly degrading the receptor through fusion with the lysosome.

Multi-monoubiquitylation and Lys-63 polyubiquitylation are the ubiquitin linkages that signal for RTK incorporation into a ILV. The evidence supporting these two types of ubiquitylation comes from a few key observations. First, the TrkA RTK has been shown to be Lys-63 polyubiquitylated (*38*) and the majority of ubiquitin bound to epidermal growth factor receptor (EGFR) after acute EGF stimulation was found to be Lys-63 polyubiquitylation (*39*). Second, the ubiquitin-associated domain (UBA) from Rad23 recognizes multi-monoubiquitylation and Lys-63 polyubiquitylation in a similar manner (*40, 41*).

To maintain the high level of ubiquitylation needed to be captured in an ILV, a RTK must retain ligand binding, kinase activity, and E3 ligase binding. Receptors that remain on the surface of the MVB have low amount of ubiquitylation and cannot be trapped by ESCRT. These receptors will be recycled back to the plasma membrane via the slow recycling pathway (*42-44*).

There are many factors that have been shown to affect the fate of a RTK after endocytosis, including the degree of ligand stimulation. For the EGFR RTK it has been proposed that the fate of the receptor depends on the amount of ligand the receptor receives. A low physiological dose of ligand results in fast clathrin-mediated endocytosis that recycles receptors efficiently (*45*). When the fast CME pathway is saturated by high physiological doses of ligand, a slow clathrin-independent endocytosis (CIE) pathway targets the receptor mostly to the lysosome (*32*). However, the endocytic route EGFR takes and when EGFR takes a specific endocytic route may be cell-type specific because other reports in other cell have given conflicting results (*46, 47*).

RTK routing in the endocytic pathway can also depend on the specific ligand-receptor pair. As mentioned previously, RTKs are classified into subfamilies of related receptors based on ligand

binding properties. Each RTK in the family generally can bind to most/all of the ligands associated with the family, with varying ligand affinities (*4*). It has been shown that each ligand-receptor pair will dissociate at a different pH depending on the affinity of the interaction (*44, 48*). Some receptor-ligand pairs will dissociate as soon as the endosomal pH starts to drop and others will remain bound at the very low pH of the MVB. Receptors that release their ligand will recycle back to the membrane following inactivation of the kinase domain that leads to a termination of receptor ubiquitylation. Recycling via the fast vs. slow recycling pathway depends on the pH at which the ligand in dissociated i.e., ligand release in the early endosome results in fast recycling. A receptor that remains ligand bound will be targeted to the lysosome for degradation (*49, 50*). RTK heterodimerization with other receptors in the cell can dictate the fate of the RTK e.g., recycling vs. degradation. For example, some VEGFR ligands cause NRP-1 coreceptor binding and endosomal routing to the recycling pathway. VEGFR only endosomes are routed for degradation (*51*).

RTKs can also be activated and endocytosed by a variety of ligand-independent mechanisms. For example, hypoxic conditions and increased RTK density at the plasma membrane can active the kinase domain of some RTKs. Spontaneous activation targets the RTK to a perinuclear region for dephosphorylation followed by recycling of the inactive RTK back to the membrane (*49, 52, 53*). Activation of signaling pathways such as the SFK, MAPK, and PKC can also mediate ligand-independent endocytosis of RTKs (*54-57*). These methods of activation and internalization typically cause recycling of the receptor, rather than degradation of the receptor.

While RTK recycling vs. degradation dictates the length and strength of a RTK signaling event there is evidence that the location of the RTK in the endosomal system can dictate the type of signaling pathways activated by the RTK. After endocytosis, a RTK is cut off from extracellular ligand after endocytosis, but its cytosolic domain is exposed to different interactions partners as it traffics through the different endosome compartments and some downstream signaling components are preferentially recruited to distinct endosomal compartments (*33*). Recruitment of signaling proteins may be mediated by the different lipid composition and proteins located on each type of endosome. Therefore, a receptor may not be able to activate some signaling pathways until it reaches the appropriate endosomal compartment where downstream signaling

components are located (*49, 58*). For example, the RTK MET cannot activate Rac-1 until it reaches the Rac-1 guanine nucleotide exchange factor (GEF) Tiam1 located at early endosomes (*59*). Oncogenic MET mutants display increased Rac activity and increased stability caused by a high rate of endocytosis and recycling through the early endosome (*60*). Therefore, removal of a RTK from the surface of the cell does not immediately inactivate downstream signaling.

1.2 TYROSINE KINASE UBIQUITYLATION

Most RTKs that have been shown to bind to multiple E3 ubiquitin ligases. However, there are two E3 ubiquitin ligases, Cbl and $CRL5^{SOCS}$, that can bind to most families of RTKs. As of right now, it is not clear why RTKs bind to multiple E3 ligases and if the functions of each E3 are unique or redundant.

1.2.1 *Cbl E3 ubiquitin ligase*

Most RTKs and NRTKs bind to and are ubiquitylated by the Cbl family of RING E3 ubiquitin ligases. The Cbl family of proteins has three members c-Cbl, Cbl-b, Cbl-c. The c-Cbl and Cbl-b isoforms are ubiquitously expressed, while Cbl-c is primarily expressed in epithelial cells. At the n-terminus, the Cbl proteins have a tyrosine-kinase-binding domain (TKB), which binds phosphotyrosine residues, followed by a RING domain responsible for ubiquitylation. C-Cbl and Cbl-b have an additional proline-rich region, which serves as a docking site for SH3 domains, and a c-terminal ubiquitin-associated domain (UBA) (*61, 62*).

The majority of our understanding of Cbl regulation of RTKs comes from in-depth studies on c-Cbl regulation of EGFR. Cbl may control EGFR endocytosis in some cell types by ubiquitylating EGFR and by recruiting and ubiquitylating endocytic adaptors. C-Cbl binds to EGFR directly and indirectly (via another protein, Grb2) after ligand-induced activation of EGFR. C-Cbl binding to EGFR has three effects: it can inhibit downstream signaling though competition for a phosphorylation site, it can act as an adaptor for signaling proteins, and it can serve as an E3 ubiquitin ligase. For the adaptor functions, c-Cbl binds to the adaptor proteins CIN85 and CD2AP that concentrate the phosphatidylinositide-phosphate lipids (PIPs) needed for endocytosis near activated EGFR and these adaptors bind to the endocytic adaptor AP-2. C-Cbl

can also multimono-ubiquitylate EGFR at the plasma membrane, triggering binding of the endocytic adaptors Eps15 and Epsin (*61, 63*). C-Cbl may also transfer ubiquitin onto endocytic adaptors near EGFR (*61*).

All of these functions indicate that c-Cbl coordinates clathrin-dependent endocytosis of EGFR and one paper has supported this model. The authors showed c-Cbl binding and ubiquitylation of EGFR are required for clathrin-mediated endocytosis of EGFR (*64*). However, some other papers have shown that c-Cbl overexpression does not enhance EGFR internalization (*65, 66*) and c-Cbl/Cbl-b double knockout cells or cells expressing a form of EGFR that cannot bind c-Cbl or Cbl-b can still endocytose EGFR into the cell (*37, 64, 67*). These conflicting results could be cell line specific effects, but Cbl most likely plays a role in endocytosis of EGFR and other RTKs.

Cbl proteins have been shown to be required for the lysosomal degradation of RTKs (*37*). Cbl accompanies RTK cargo to the early endosome, where its continued activity is essential for lysosomal degradation of RTKs (*68-71*) and Cbl can be recruited to the MVB as well (*72*). C-Cbl null cells can internalize EGFR properly into the cell, but fail to ubiquitylate and degrade EGFR (*68*). Thus, Cbl is a major factor implicated in RTK endocytosis and trafficking to the lysosome.

1.2.2 *$CRL5^{SOCS}$ E3 ubiquitin ligase*

In addition to Cbl family proteins, there are many more E3s that can bind to and ubiquitylate RTKs. For example, the substrate adaptors for the Cullin-RING-ligase 5 (CRL5) E3 have been shown to bind RTKs from many different families and may play an important role in RTK biology.

The Cullin-RING-ligases (CRL) are a family of multi-subunit E3 ubiquitin ligases that have similar domain architecture and regulation. The Cullin protein is the core complex member, it acts as the protein-scaffold on which the components of the E3 ligase assemble. One end of the Cullin backbone binds to a RING protein (Rbx1 or Rbx2) that will bind a charged E2 protein, while the other end of the Cullin recruits substrates for ubiquitylation by binding to

interchangeable substrate receptor proteins. There are six typical CRL E3 ligase complexes CRL1, CRL2, CRL3, CRL4A, CRL4B, and CRL5 (*73*).

Cullin activity is regulated by post-translation modification. Activation of the CRLs is regulated by the addition of the ubiquitin-like protein Nedd8 to a lysine residue in the Cullin protein. The COP9 signalosome is a complex of proteins that is responsible for removing the Nedd8 protein a process called deneddylation. CAND1 binds to CRLs and aids in the exchange of substrate receptors (*74*).

CRL5 specifically binds the RING protein Rbx2 at the C-terminus (*74*) and recruits substrates via the SOCS substrate adaptor proteins at the N-terminus. SOCS proteins are recruited to CRL5 by the heterodimer Elongin B/C, which binds to the SOCS-BC box domain in SOCS proteins and the N-terminus of Cul5 (*73*). There are 40 human proteins known to contain a C-terminal SOCS-BC box. These 40 substrate adaptors can be categorized into subgroups based on the domain(s) responsible for substrate binding, which are found N-terminal to the SOCS-BC box (*75*).

The SOCS family of proteins possess a central SH2 domain that binds phosphorylated tyrosine residues. There are 8 SOCS proteins in the human genome, SOCS1-7 and CisH (*75*). The SOCS SH2 domains have specificity for the residues upstream and downstream of the phosphorylated tyrosine residue (*76-79*). This is different from standard SH2 domain binding that recognizes the four to five amino acids downstream of the phosphorylated tyrosine residue (*7*). Moreover, the SOCS SH2 domains can be paired based on amino acid sequence homology: SOCS4 and SOCS5 have 92% homology, SOCS6 and SOCS7 have 56% homology, SOCS2 and CisH have 45% homology, and finally, SOCS1 and SOCS3 have 35% homology (*80*). The sequence homology between the SH2 domains may allow them to bind similar substrates and serve redundant functions. Indeed, many of the paired SOCS proteins share a handful of substrates; however, it is still unclear if this overlap leads to redundancy in the cell.

The SOCS family of proteins also each possess a unique N-terminal region of unknown structure and function. The sequence and length of the N-terminal region is different for each SOCS,

SOCS1-3 and CisH have relatively short N-termini, while SOCS4-7 have much longer N-termini. The N-termini of SOCS proteins may bind substrates (*81*) and the unique sequence of the N-terminus may give each SOCS a distinct function. Therefore, CRL5 can recognize and target tyrosine-phosphorylated and potentially non-phosphorylated substrates for degradation using the SOCS family substrate receptors.

1.2.3 *SOCS protein interactions with cytokine receptors and cytosolic proteins*

The classic function of SOCS proteins is the negative regulation of cytokine signaling, where they were first discovered and characterized. Acute cytokine stimulation activates the JAK/STAT signal pathway and induces the transcription of SOCS proteins, in a STAT-dependent manner. The SOCS protein then negatively regulates cytokine signaling using both CRL5-dependent and CRL5-independent mechanisms in a classical negative feedback loop (*82*).

SOCS proteins can inhibit cytokine signaling in a variety of ways: by competing for binding sites on the cytokine receptor, by inhibiting the JAK kinase domain and through proteasomal degradation of JAK and maybe STAT proteins as well. Early after the discovery of SOCS proteins it was proposed that SOCS2 and CISH compete with STAT proteins for the same phosphotyrosine binding site on cytokine receptors (*83, 84*). Most papers show SOCS overexpression alters STAT activation kinetics after cytokine stimulation. Suggesting that SOCS binding to a cytokine receptor acts to control the duration of STAT activation. However, the competitive inhibition model does not have much experimental support and needs further testing (*85*). There is evidence that SOCS3 competes with the PTP SHP2 for a phosphotyrosine-binding site on a cytokine receptor, thus limiting the activation of the phosphatase (*86*). SOCS proteins can also directly inhibit JAK kinase activity. SOCS1, 3, and 5 all have a region in their N-terminus that inhibits the kinase activity of the JAK family of kinases. For SOCS1 and 3 binding of the kinase inhibitory region (KIR) to the JAK kinase domain induces a conformational change in the catalytic pocket that prevents phosphate transfer (*87-90*). SOCS5 has a conserved region in the N-terminus, called JAK interaction region (JIR), that inhibits the autophosphorylation of JAK1 and JAK2 by an unknown mechanism (*91*). Finally, there is some evidence that SOCS proteins target JAK kinases to the proteasome through their SOCS-BC box and presumably

CRL5. Overexpression of SOCS1 increases the polyubiquitylation of JAK2 in a SOCS-box dependent manner (*92*). SOCS3 null cells have increased pY-JAK that may be regulated by the proteasome in a SOCS-Box dependent manner (*86*). CRL5-SOCS3 can ubiquitylate JAK *in vitro* (*93*). The SOCS proteins inhibit JAK-STAT signaling through direct JAK/STAT binding or through cytokine receptor binding or binding to both at the same time.

Table 1.1 outlines and details the many SOCS-cytokine receptor interactions identified in the literature. A large number of these interactions are mediated through SOCS SH2 domain binding to a phosphorylated tyrosine residue on the cytoplasmic tail of the receptor. While most papers have shown binding, the exact function of SOCS-cytokine receptor interactions has not been convincingly pinned down. The function of SOCS binding to cytokine receptors is thought to primarily be the regulation of JAK/STAT activity through the mechanisms outlined above (kinase inhibition, JAK/STAT ubiquitylation and competitive binding). However, there is one paper that showed SOCS2 binding to the growth hormone cytokine receptor regulates the receptor rather than the associated JAK/STAT. In this paper, the authors show that SOCS2-depletion increases the protein levels and half-life of growth hormone receptor. Interestingly the authors only see effects on the mature form of growth hormone receptor of (*94*) that is thought to reside at the plasma membrane (*95*). While there are plenty of SOCS-cytokine receptor binding interactions and insights into potential functions more work is needed to fully understand exact role of SOCS-cytokine receptor binding.

Table 1.1 SOCS interactions with Cytokine Receptors

SOCS	CYTOKINE RECEPTOR	FUNCTION	METHOD	REFERENCE
SOCS1	IFNGR1	Binding to Y441; Overexpression inhibits pY-STAT1 and slight inhibition of pY-JAK2, Y441F expressing cells have longer pY-STAT1 after INFγ stimulation.	Overexpression	(*96, 97*)
SOCS1	IFNAR1	Binds through Tyk2; Overexpression inhibits K63 ubiquitylation of Tyk2; Increased pY-STAT1 activation when SOCS1 is knocked out; Biology, increased antiviral and proinflammatory actions independent of Interferon-γ.	Overexpression Endogenous Knockout (signaling)	(*98, 99*)
SOCS1	IL-2-R gamma	Biology only.		(*100-105*)
SOCS1	IL-12-R	Biology only.		(*106*)

SOCS2	Growth Hormone Receptor	Binding; KO mouse biology; Overexpression decreases levels and siRNA, KO increases levels & half-life.	Overexpression Knockdown	(*94, 107, 108*)
SOCS2	Prolactin Receptor	Binding; SOCS2 OE blocks SOCS1 inhibition of pY-JAK2; Biology SOCS2 knockdown inhibits mammary gland growth; KO increased pY-STAT5 dependent on PLR.	Overexpression Knockdown	(*109, 110*)
SOCS2	Leptin receptor	Binding.	MAPPIT	(*111*)
SOCS2	IL-7 Receptor/CD127	Binding.	Endogenous	(*112*)
SOCS2	EPO-R	Binding.	MAPPIT	(*113*)
SOCS3	G-CSF-R	Decreased ligand mediated pY-STAT5 activation.	Overexpression	(*114-116*)
SOCS3	Gp130	Binding Y757; Knockout of SOCS3 increases duration of pY-STAT1 and pY-STAT3; Biology, Y757F have increased proliferation and SOCS3 knockout increases $CD8^+$ proliferation.	In Vitro Biochem Knockout	(*117-119*)
SOCS3	Leptin Receptor	Overexpression of SOCS3 inhibits signaling.	Overexpression	(*120*)
SOCS3	EPO-R	Binding to Y401, Y429, Y431; Decreased pY-EpoR by inhibition of JAK2, Decreased STAT5 transcription.	Overexpression	(*121, 122*)
SOCS3	IL-12Rb2	Binding to Y800; Decreased STAT4 DNA binding and transcription.	Overexpression	(*85*)
SOCS5	IL-4R	Binding; Overexpression inhibits ligand-mediated STAT6 activation; Biology, overexpression inhibits helper T cell differentiation.	In Vitro Overexpression	(*123*)
CisH	CD127	Binding; Knockdown prevents down-regulation.	Knockdown	(*112*)
CisH	Leptin Receptor	Binding.	MAPPIT	(*111*)
CisH	Erythropoietin Receptor	Binding to Y401.	Overexpression	(*124, 125*)
CisH	IL-3 Receptor	Binding.	Overexpression	(*125*)
CisH	Prolactin Receptor	Binding; Overexpression inhibits PRL induced pY-STAT5a; Biology, mice overexpressing Cis fail to remodel breast in preparation for lactation and don't lactate.	Overexpression	(*126, 127*)
CisH	IL-2 Receptor	Binding in a SH2-independent manner; OE blocks pY of the receptor by Lck.	Overexpression	(*83, 128*)

In addition to inhibiting cytokine signaling, SOCS proteins have been found to bind to and regulate tyrosine phosphorylated proteins in the cytosol (Table 1.1). The main function of SOCS binding to cytosolic targets is thought to be ubiquitylation that leads to proteasomal degradation. Some SOCS substrates such as IRS and p85 PI3K can be activated downstream of JAK kinases, so they might be a part of the JAK/STAT negative feedback loop (*10*). Most of the SOCS

proteins bind to cytosolic partners using their SH2 domain, but there are some exceptions. The SFK family member Lck binds to a region in the N-terminus of SOCS6 (*129*). The SH3 domains from many tyrosine-phosphorylated cytosolic proteins have been shown to bind to a proline-rich motif in the N-terminus of SOCS1 *in vitro*; however, there has not been follow-up work to show to binding in *in vivo* system (*130*). SOCS3 has been reported to be tyrosine phosphorylated at the very N-terminus in response to many growth factors and cytokines. Phosphorylation at this site inhibits p120 Ras GAP hours after the stimulation of the cells thus sustaining MAPK activation for longer (*131*). The examples of n-terminal binding give hints to the function of the n-terminus; however, further work is needed to understand the binding partners and function of this region fully.

Table 1.2 SOCS interactions with Cytosolic Proteins

SOCS	Cytosolic Protein	FUNCTION	METHOD	REFERENCE
SOCS1	VAV	Ub mediated degradation via proteasome	Overexpression	(*132*)
SOCS1	Tec	Binding SOCS1 N-term binding to kinase domain of Tec suppresses kinase activity.	Overexpression	(*133*)
SOCS1	P65/RelA	Ub mediated degradation via proteasome.	Overexpression Knockdown	(*134*)
SOCS1	IRS1/2	Ub mediated degradation using SOCS box.	Overexpression	(*135*)
SOCS1	FAK	Binding Y397 (activation loop Y) to SH2 and KIR; Overexpression inhibits kinase activity, increases Ub and turnover.	Overexpression	(*136*)
SOCS2	Pyk2	Ub mediated degradation.	Knockdown	(*137*)
SOCS2	NDR1/STK38	K48 ubiquitylation leading to proteasomal degradation. S2 inhibits TNFα induce cytokine transcription.	Overexpression Knockdown	(*138*)
SOCS3	IRS2	Overexpression decreases total IRS2.	Overexpression	(*135*)
SOCS3	p120 RasGAP	pY221 in SOCS3 binds to p120; Overexpressed pY-SOCS3 activates ERK: OE biology.	Overexpression	(*131*)
SOCS3	TAK1 & TRAF6	Binding; Overexpression inhibits TRAF6 ubiquitylation & inhibits TAK1/TRAF6 interaction.	Overexpression	(*139*)
SOCS3	FAK	Binding Y397 (activation loop Y) to SH2 and KIR; Overexpression inhibits kinase activity, increases ubiquitylation and turnover of protein.	Overexpression	(*136*)
SOCS5	Shc-1	Shc pY317 binds SOCS5 SH2.	Overexpression	(*91*)
SOCS5	PI3K (p85 & p110)	Overexpressed SOCS5 and endogenous bind; SOCS5 depletion increases PI3K.	Overexpression siRNA	(*140*)
SOCS6	IRS4	Binding; KO mouse biology.	In Vitro Overexpression	(*141*)
SOCS6	PI3K P85	Binding.	Overexpression	(*141, 142*)
SOCS6	Lck	Binding; Degradation via proteasome; Overexpression of SOCS6 inhibits T-cell activation.	Yeast 2 Hybrid Overexpression Knockdown	(*129*)
SOCS6	Cas	Binding; Degradation via proteasome; Biology KD.	Knockdown	(*143*)
SOCS7	IRS1	Binding; Overexpression increases ubiquitylation and knockout increases levels; Biology, knockout mice have increased insulin sensitivity.	Overexpression Knockout	(*144*)
SOCS7	IRS-4	Binds to the SH2 domain.	In Vitro Binding	(*141*)
SOCS7	P85 PI3K	Binds to the SH2 domain.	In Vitro Binding	(*141*)
SOCS7	Dab1	Binding; Ubiquitylation that leads to CRL5-mediated degradation, protein increases when CRL5 or SOCS7 is knocked out; Biology, $CRL5^{SOCS7}$ regulates neuron growth through Dab1.	Knockout	(*145*)

CisH	PLC-γ	Binding; CisH knock out causes a decrease in endogenous ubiquitylation and an increase in phospho-PLC.	Knockout	(*146*)

1.2.4 *SOCS protein interactions with RTKs*

SOCS proteins bind to and negatively regulate RTKs and their downstream signaling through multiple mechanisms. Table 1.3 outlines all of the known SOCS-RTK interactions, the function of each interaction, and the method(s) used by the authors. The main function proposed by these studies is that SOCS overexpression decreases kinase activity or increases turnover of the RTK in a proteasomal-dependent manner (See SOCS1-MET, SOCS2-FLT3, SOCS5-EGFR, SOCS6-Kit, and SOCS6-Flt3 in Table 1.3).

However, decreased RTK protein upon SOCS overexpression could be caused by decreased gene expression rather than increased proteasomal turnover of the RTK. The authors of many of these studies did not report the mRNA abundance of the RTK or its associated ligand. Changes in mRNA expression could occur two ways. First, SOCS overexpression could decrease STAT-based transcription of endogenous RTK mRNA for any RTK genes with a STAT binding site in the promoter. Second, if the RTK was overexpressed using a plasmid then SOCS overexpression may inhibit one of the many signaling pathways known to activate transcription off of a plasmid promoter. Tyrosine kinase activation of plasmid transciption is an overexpression artifact we have observed in our lab and must be controlled for. Lack of transcription controls means these studies should be examined with care.

The claim that SOCS proteins promote proteasomal degradation of a RTK must also be taken with care for a few reasons. Many papers use proteasome inhibitors to show proteasome inhibition prevents the SOCS-induced decrease in the RTK abundance; implying the RTK is being degraded by the proteasome (Table 1.3). It is highly unlikely that a transmembrane protein is being targeted to the proteasome. Proteasomal degredation of a membrane protein would require removal of the receptor from the membrane as it is fed into the proteasome, presumably a very energy intensive process. It is most likely that these results are due to the indirect effects of proteasome inhibition. For example, if the RTK mRNA levels are increased upon SOCS overexpression then the proteasome inhibitor could directly inhibit the SOCS-STAT and/or

SOCS-pY-substrate mechanisms mentioned above, bringing the transcription of the RTK mRNA off the endogenous or plasmid promoter back to baseline. Additionally, blocking the proteasome results in a depletion of the free ubiquitin pool in the cell, leaving no free ubiquitin in the cell for other ubiquitin-dependent processes (*23*). If the RTK is targeted to the lysosome by $CRL5^{SOCS}$ Lys-63 or multi mono ubiquitylation, then proteasome inhibition would deplete the free ubiquitin leaving none for $CRL5^{SOCS}$ to use, leading to decreased lysosomal degradation of the RTK and therefore more RTK protein. Endocytosis and lysosomal degradation of EGFR have been shown to be sensitive to proteasomal inhibition, so this indirect effect is not unreasonable (*147*). It is clear that more work needs to be done to understand the exact function of SOCS binding to RTKs and to determine if SOCS binding to RTKs regulates degradation.

Table 1.3 SOCS interactions with Receptor Tyrosine Kinases

SOCS	RTK	FUNCTION & BIOLOGY	METHOD	REFERENCE
SOCS1	M-CSF-R	Binding, SH2 to Y691 &Y721; Biology, inhibition of ligand-stimulated growth.	Overexpression Yeast 2 Hybrid	(*148*)
SOCS1	Insulin R	Binding; Decreased ligand-induced pY-ERK, pS-AKT, pY-IRS.	Overexpression	(*149*)
SOCS1	MET	Biology; decreased ligand-mediated proliferation; Increased K48 ubiquitylation and proteasomal degradation.	Overexpression	(*150*)
SOCS1	KIT	Binding; Biology, inhibition of Kit-mediated growth, suppresses ligand-mediated anchorage-independent growth.	Overexpression, Yeast 2 Hybrid	(*130*)
SOCS1	Flt3	Binding when both are overexpressed.	Overexpression	(*130*)
SOCS1	FGFR	Binding; Decreased FGF induced pY-STAT1 and increased pY-MAPK.	Overexpression	(*151*)
SOCS1	EGFR	Binding; Decreased ubiquitylation, decreased pY-STAT1/3.	Overexpression	(*152*)
SOCS2	FLT3	Binding, SH2 to Y955 & Y589; Increased pY-Flt3, decreased pY-ERK and pY-STAT5; Weak data showing increased ubiquitylation and increased degradation; Biology, decreased colony formation.	Overexpression	(*153*)
SOCS2	IGF-IR	Binding when both are overexpressed.	Overexpression	(*154*)
SOCS2	EGFR	Binding; Decreased EGF induced pY-STAT5, Increased pY-EGFR.	Overexpression	(*155*)
SOCS2	PDGFR	Binding.	Yeast 2 hybrid	(*129*)
SOCS2	TrKA	Binding; S2 overexpression increases total & surface receptor; S2 KO regulated neurite outgrowth (Sholl analysis)	Overexpression	(*156*)
SOCS3	IGF-IR	Binding when both are overexpressed.	Overexpression	(*157*)
SOCS3	Insulin R	Colocalization when both are overexpressed.	Overexpression	(*158*)
SOCS3	FGFR	Binding.	Overexpression	(*151*)
SOCS3	EGFR	Binding; Decreased ubiquitylation, decreased pY-STAT1/3.	Overexpression	(*152*)
SOCS4	EGFR	Binding of the SH2 domain to a peptide.	In Vitro	(*76, 159*)
SOCS5	EGFR	Faster internalization, more ubiquitylation, increased degradation of the receptor (OE); Increase in EGFR in S5 KO lung; Decreased STAT3 transcription (OE); Biology, decreased EGF-induced growth (OE).	Overexpression Knockout	(*140, 159-161*)
SOCS6	KIT	Binding, SH2 to JM pY567 & Y569; Biology, decreased ligand-dependent proliferation; Increased ubiquitylation and faster turnover of the receptor.	Overexpression Yeast 2 Hybrid	(*78, 162*)
SOCS6	FLT3	Binding; Increased ubiquitylation and internalization of the receptor.	Overexpression	(*163*)
SOCS6	Insulin R	Binding; Decreased ligand-induced pY-ERK, pS-AKT, pY-IRS.	Overexpression	(*149*)

1.2.5 *Regulation of SOCS proteins*

In addition to SOCS protein regulation of RTKs, RTKs may also influence SOCS protein expression and/or post-translation modification. RTKs have also been shown to induce SOCS transcription. Most cell line have low basal expression of SOCS proteins and this could be one reason researchers have had trouble determining the function of endogenous SOCS-RTK interactions. However, SOCS 1-3 and CisH are rapidly induced 60-100 min after cytokine stimulation, sometimes to 100 times the steady state level. SOCS4-7 are thought to be less prone to rapid induction by cytokines, but still can be induced (*164*). RTKs, like cytokine receptors, can induce SOCS gene expression after acute stimulation. The RTK-ligand pairs that induce SOCS proteins include FGFR3-Fgf, Kit-SCF, FLT3-FLT3 ligand, INSR-Insulin, EGFR-EGF, and PDGFR-PDGF. Like cytokine receptors, RTKs are thought to induce SOCS gene expression through STAT transcription factors (*165*).

Some SOCS proteins may also be tyrosine phosphorylated after RTK activation. Some examples include Flt3-SOCS2, 6; EGFR-SOCS2, 3, 5, 6; and Kit-SOCS6 (*153, 159, 162, 163*). The function of SOCS protein tyrosine phosphorylation has not yet been elucidated, but SOCS phosphorylation could recruit additional signaling proteins to the receptor after ligand induction, assembling a large signaling complex on the receptor tail. One other potential function of SOCS phosphorylation would be SOCS-SH2 mediated degradation of other SOCS proteins.

Regulation of SOCS proteins by RTKs may be crucial for the spatiotemporal control of signaling. The half-life of SOCS proteins is very short (*78, 94*), which allows SOCS proteins to be transiently expressed after induction. Thus, the SOCS1 and 3 SH2 domains have PEST motifs that act as a signal for degradation (*164*). Additionally, SOCS2 has been shown to be able to bind to all of the other SOCS proteins and its overexpression causes decreased SOCS1 and SOCS3 protein expression, in a Cul5 proteasome-dependent manner (*166, 167*). There is also work that shows SOCS2 is induction is delayed compared to other SOCS proteins (*168*). Taken together these studies suggest that cells rapidly return to baseline levels of SOCS protein expression and this allows a RTK to receive another signal without immediate negative regulation by SOCS proteins.

1.1 CRL5^{SOCS} IN SRC-SPECIFIC SIGNALING

There is evidence from our lab that Cul5 and SOCS2, 4, 5, and 6 act as inhibitors of proliferation in MCF10A mammary epithelial cells and inhibitors of migration in many cell types (*143, 145, 169*). Cul5-depleted MCF10A cells display EGF-independent growth, transformation in 3D culture and increased migration. These characteristics suggest that Cul5 acts as a transformation suppressor in MCF10A cells. In the absence of Cul5, MCF10A cells also display a twofold increase in Src family kinase (SFK) activity compared with control cells. This increased SFK activity is required but appears not to be sufficient for the increased growth and migration of shCul5 MCF10A cells, because overexpression of active Src does not increase growth and migration. This suggests that Cul5 regulates not only SFK activity but also proteins/processes downstream of the SFK members (*143*). Additionally, we found that reduced Cul5 activity in HeLa cells and neurons of the developing brain results in increased migration. Like MCF10As, these cell types also display increased SFK activity, indicating that Cul5 may play a similar role in other cell types (Unpublished, (*143, 145, 170*)). The question remains as to which tyrosine-phosphorylated proteins downstream of the SFK are mediating the altered biology of Cul5-depleted cells.

To identify the SOCS proteins that mediate the transformation of Cul5-depleted MCF10A cells, changes in migration and proliferation were assayed after depletion of one or more SOCS proteins. We found that simultaneous knockdown of the four most highly expressed SOCS proteins in MCF10A cells, SOCS2, 4, 5 and 6, phenocopies the increased migration and EGF-independent growth found in Cul5-depleted MCF10A cells. Suggesting that the substrates of these four SOCS proteins are responsible for the changes in biology seen in Cul5-depleted MCF10A cells (*143*). In addition, we found that SOCS2 and SOCS6 inhibit microtubule-induced focal adhesion disassembly and traffic into the focal adhesions of HeLa cells (*171*). Although there are several known receptor tyrosine kinase and non-receptor tyrosine kinase substrates of SOCS2 and 6, none of these previously characterized substrates are sufficient to fully explain how SOCS2 and 6 regulate focal adhesion dynamics (*80, 163, 172, 173*).

This dissertation provides the first quantitative mass spectrometry analysis of phosphotyrosine proteins in Cul5-depleted cells and the first comprehensive interaction study of SOCS2 and SOCS6 proteins, confirming previously identified interaction partners and identifying new possible functions of SOCS proteins. Additionally, I go on to characterize $CRL5^{SOCS}$ regulation of three RTKs (IGF-IR, EGFR, and EphA2).

Chapter 2. CRL5 SUBSTRATE SCREENING & VALIDATION OF IGF-IR/INSR AS A CRL5^{SOCS1} SUBSTRATE

2.1 INTRODUCTION

It has become increasingly clear that SOCS2, 4, 5, and 6 negatively regulate signaling pathways involved in proliferation and migration; however, the substrates these SOCS proteins dynamically regulate remain unknown. Two types of screening approaches, genomic and proteomic, have been used to identify dynamically regulated substrates of CRLs successfully (175).

Only one genomic approach, global protein stability profiling (GPS), has been used to successfully screen for CRL substrates. This technique makes use of a library of 293T cells in which each cell expresses a mRNA encoding dsRED as a readout of transcription, an IRES for internal ribosome entry, and a fusion of GFP to a human open reading frame (ORF). ORF protein abundance is measured by taking the ratio of GFP (protein) to dsRED (mRNA) using a flow cytometer (*174, 175*). Cells are sorted into bins based on the GFP/dsRED ratio and the DNA is extracted from each bin. The relative abundance of each ORF in the respective bins provides a measure of its protein expression level. Since all ORFs are driven off the same promoter, and RNA expression is individually controlled, variations in ORF level are mostly due to changes in protein stability. GPS was used to globally identify CRL substrates by comparing cells treated with the CRL inhibitor, MLN4924, to untreated cells. This screen was followed by more targeted screens of Cul1, Cul3, and Cul4. In these screens, each Cullin was inhibited by overexpressing a dominant negative version of the Cullin with a lentivirus. Many of the GPS high-priority candidates identified in this screen were validated (*176*). Recently a Cul2 GPS screen was conducted, and it successfully identified selenoproteins as targets of CRL2 (*177*). Overall this method has been shown to work well to identify substrates of most of the CRL family members. In section 2.2.1 I present my attempts to apply GPS to identify phosphorylation-dependent CRL5 substrates.

Many proteomic methods have been applied to detect CRL substrates. They can be subdivided further into two groups: bulk and affinity approaches. Bulk approaches utilize quantitative proteomics methods, such as SILAC or TMT labeling, to compare cells with and without active CRLs. Proteins that increase in abundance when a CRL is inhibited or depleted are candidate substrates for that CRL. Ubiquitin remnant profiling allows the identification of proteins that are ubiquitylated under specific cellular conditions. This method makes use of an antibody that recognized the Gly-Gly sequence left on ubiquitylated peptides after trypsin digestion (*178*). This allows researchers to compare changes in ubiquitylated peptide abundance in presence and absence of a E3 ligase. While this is a useful advance the major caveat to this technique is that it requires either a significant amount of starting material, proteasome or lysosome inhibitors to accumulate ubiquitylated protein, or a stable tagged ubiquitin expressed to purify the ubiquitylated proteins before trypsin digestion (*178, 179*). However, proteasome inhibitors can disrupt important cellular processes and cause ubiquitin depletion preventing ubiquitylation of non-proteasomal targets, resulting in artifacts in the substrates identified. Nevertheless, this approach has been used to identify substrates of CRLs by comparing ubiquitylated peptides in cells treated with and without MLN4924, a CRL inhibitor and successfully captured many previously known CRL substrates (*176*). In section 2.2.2 I present results of applying a bulk quantitative proteomics approach to identify phosphoproteins that increase in abundance when Cul5 is depleted.

Proteomic methods have also been coupled to affinity purification methods to look for CRL substrates; a technique called affinity purification mass spectrometry (AP-MS/MS). In this method, the CRL substrate adaptor protein is tagged, immunoprecipitated from cells and the mass spectrometer is used to identify all of the associated proteins. There are some variations on this approach that have been designed to identify CRL substrates specifically. One of these techniques is called the ligase trap. The ligase trap has UBAs fused to the CRL substrate adaptor protein in addition to a small tag. The UBAs serve two functions: first, UBA binding increases the affinity of the substrate to the substrate adaptor by binding to the ubiquitin chain; second, the UBA binding prevents the ubiquitin from targeting the substrate to the proteasome or other cellular locations (*180, 181*). This method has been used in tissue culture cells to identify twelve previously identified $CRL1^{\beta\text{-}TrCP}$ substrates. The major downside to the ligase trap procedure is

that it requires a large amount of starting material. The authors report using lysate from $2.8x10^9$ cells for the affinity enrichment (*180*).

For CRLs the most commonly used AP-MS/MS method is the Parallel Adaptor Capture (PAC) method developed by the Harper lab. In this method, a substrate adaptor protein is tagged with Flag-HA, stably overexpressed in cells, and pulled out of lysate using the HA tag. Immunoprecipitated proteins are eluted using the HA peptide and identified using MS/MS. The Harper lab developed a software program called ComPASS (*182*) to filter the large number of non-specific interaction proteins that come down with this method and obtain a list of high confidence interactor proteins (HCIP). PAC has been used in combination with drugs and substrate adaptor mutants to successfully identify substrates of CRL1 (*183, 184*). For example, Tan et al. used PAC in cells that were treated with a CRL inhibitor, a proteasome inhibitor or left untreated to identify F-Box interacting proteins that are turned over by the proteasome (*183*). The Clurman lab used PAC to compare binding partners that came down with a F-box protein that could not bind substrates to the WT F-box protein. Using this approach, the Clurman lab was able to successfully identify and validate novel FBW7 interacting proteins (*184*). In Chapter 3, I present the results of my AP-MS/MS approaches used to identify SOCS2 and SOCS6-interacting proteins.

2.2 RESULTS

2.2.1 *GPS screening of pY CRL5 substrates*

We choose to use the GPS screening method to identify substrates of CRL5 that are also phosphorylated by a SFK. The GPS ORFeome library of 293T cells is currently only available at two locations in the world. Before I traveled to conduct this screen, proof of principle experiments were performed in our lab to ensure this method would work to identify tyrosine phosphorylated substrates of CRL5. To test if GPS could work in our hands I first made cell lines expressing GPS controls (D1-D24). These controls express the dsRED-IRES-GFP fused to an ornithine decarboxylase (ODC) degron that has been mutated to give specific half-life (D1 $t_{1/2}$=1hr, D4 $t_{1/2}$=4hr, D24 $t_{1/2}$=24hr). The D1, D4, and D24 stable cells were analyzed using flow

cytometry to obtain a GFP/dsRED ratio as a readout of protein abundance (Figure 2.1a). Our results from this experiment were identical to those obtained by the creator of GPS, Sherry Yen (*174*). This indicated that we were able to get the GPS method working in our lab.

Now that we knew the GPS method was working in our lab I made GPS cell lines expressing *bona fide* CRL5 substrates: POLR2A, a non-phospho CRL5 proteasomal substrate, and Cas, a CRL5 proteasomal substrate that requires SFK phosphorylation for degradation (*143, 174, 185*). The D1 cell line was used as a negative control because its degradation is independent of CRL5 (*186*).

Traditionally, CRL activity is inhibited in GPS screens by infecting the cells with high titer lentiviruses expressing a dominant negative Cullin. I chose to use drugs in my GPS pilot tests, due to their ease of use, before moving on to high titer viruses. First, I wanted to make sure tyrosine phosphorylation would decrease Cas half-life. The PTP inhibitor pervanadate was added to the three GPS control cell lines to increase tyrosine phosphorylation non-specifically. Pervanadate stimulation decreased the half-life of Cas, and this reduction was inhibited when the proteasome inhibitor MG132 was included (data not shown). The D1 and POLR2A controls were unaffected by PTP addition. This showed that GPS was able to detect the changes in a CRL5 substrate abundance after phosphorylation-induced degradation.

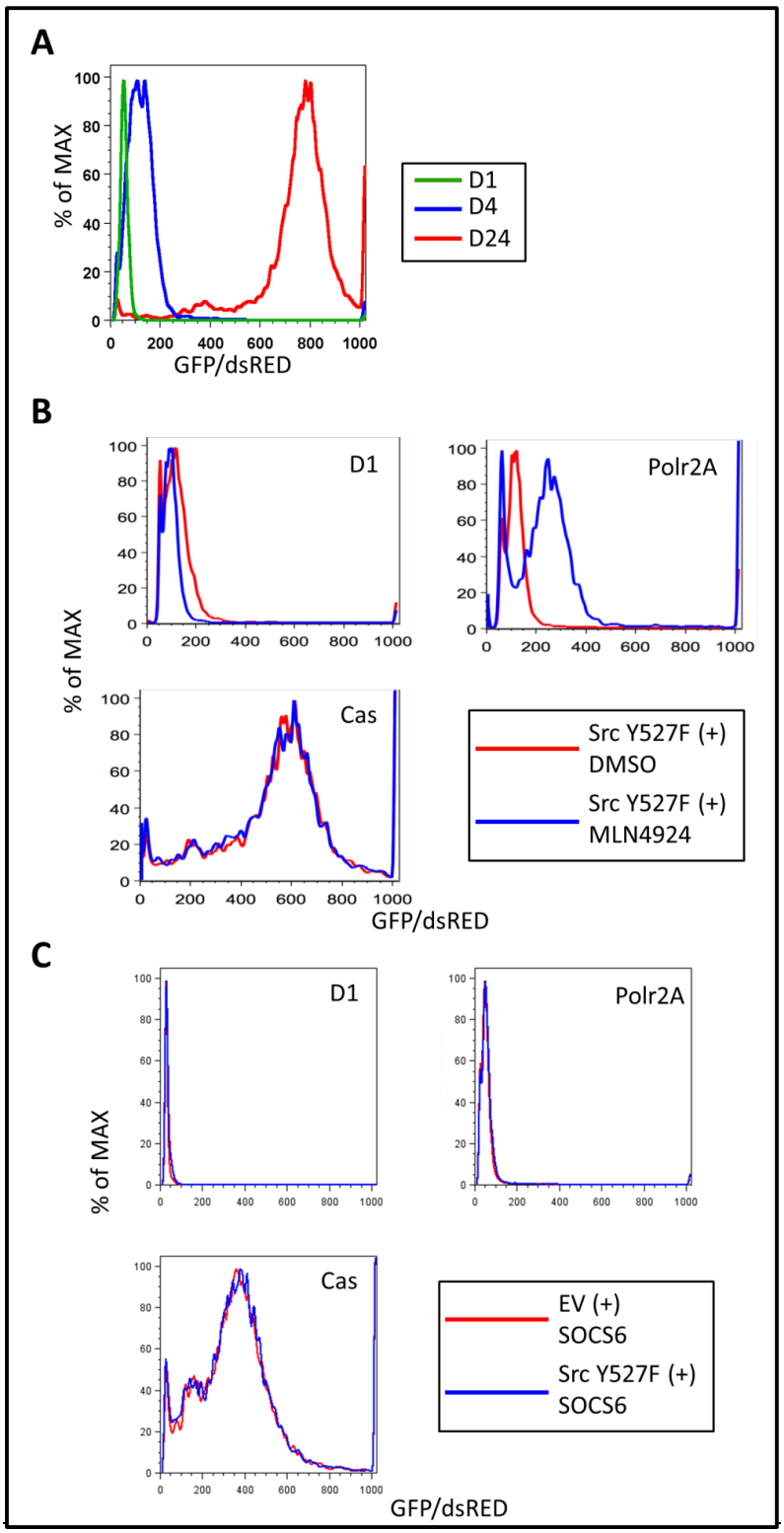

FIGURE 2.1 GPS SYSTEM DOESN'T WORK TO IDENTIFY TYROSINE PHOSPHORYLATED SUBSTRATES OF CRL5

(a) GPS controls correctly replicate previously published data. GFP and dsRED abundance was measured in 293T cells stably expressing the D1, D4 and D24 GPS

controls. (b) Non-phospho CRL5 substrate, but not the phospho substrate half-life increase when CRLs are inhibited. 293T cells stably expressing D1, POLR2A or p130Cas were transfected with constitutively active Src. 24 Hours later the cells were treated with 1μM MLN2924 for 4hours. The cells were then flow sorted for GFP and dsRED. (c) SOCS6 co-overexpression does not promote Cas turnover. 293T cells stably expressing D1, POLR2A or p130Cas were transfected with SOCS6 and either a control plasmid or constitutively active Src. The cells were then flow sorted for GFP and dsRED.

With this positive result, I moved on to test a more specific phosphorylation activator and CRL5 depletion/inhibitors. CRL5 degrades Cas after phosphorylation by Src at two sites (*143*). We expressed constitutively active Src (Src Y527F) in the three control cell lines to phosphorylate Cas at the CRL5 binding sites. Src activity was increased in these cells by Western blotting (data not shown). The GPS cells expressing Src Y527F were also treated with or without the CRL inhibitor MLN4924 (*187*). Changes in Cas, POLR2A and D1 protein abundance were analyzed by flow cytometry. As expected, MLN4924 increased levels of CRL substrate POLR2A but not negative control D1 (Figure 2.1b). These controls indicated that MLN4924 was specifically inhibiting CRL activity and not affecting non-CRL substrates. Surprisingly, however, the half-life of Cas did not change upon MLN4924 treatment.

We may not have seen an effect of MLN4924 on Cas levels because the MLN4924 treatment was only 4 hrs. The half-life of Cas in the presence of constitutively active SFKs is 2-3 hours long (*143*). Perhaps we did not see a large change in Cas abundance because the MLN4924 treatment only covered 1-2 Cas half-lives. To test this, we inhibited Cul5 through overexpression of dominant-negative Cul5 or depleted Cul5 with siRNA in the presence of constitutively active Src Y527F. Both of these methods provide plenty of time for Cas to protein to accumulate; however, Cas abundance did not change in either of these experiments (data not shown).

The GFP-Cas is overexpressed in the 293T cells and could be saturating endogenous SOCS6, the CRL5 substrate adaptor used to degrade Cas. GFP-POLR2A can be efficiently turned over by CRL5 by binding directly to CRL5 though its own SOCS box, independent of a substrate adaptor (*188*). To test this hypothesis the three control cell lines were analyzed in the presence of exogenous SOCS6 and the presence and absence of Src Y427F. Cas protein levels did not change upon addition of Src Y527F, even in the presence of exogenous SOCS6 (Figure 2.1c).

These results indicated that the CRL5 degradation of GFP-Cas, induced by Src Y527F phosphorylation, was absent or too low to detect using the GPS method. These challenges with the GPS screening method prompted us to change to a mass spectrometry (MS) based approach to identify tyrosine phosphorylated substrates degraded CRL5.

2.2.2 *Identification of phosphotyrosine peptides in Cul5-depleted cells*

Tyrosine phosphorylated proteins that are constitutively ubiquitylated and degraded in a CRL5-dependent manner should increase in abundance when Cul5 expression is depleted. To identify these proteins, we performed quantitative phosphotyrosine proteomics on control and Cul5-deficient cells. Three biological replicates of control (EV) and Cul5-depleted (shCul5) MCF10A cells were harvested for analysis (Supplementary Figure 1). Cells were lysed in 8 M urea containing 1 mM pervanadate as a phosphatase inhibitor. Proteins were reduced, alkylated and digested with trypsin and the peptides were labeled with isobaric TMT tags (Figure 2.2a). The digests were mixed, and phosphotyrosine peptides were enriched using anti-phosphotyrosine 4G10 beads followed by an immobilized metal affinity column (IMAC) (Figure 2.2a) (*189*). Phosphopeptides were analyzed and quantified by LC-MS/MS, followed by Mascot identification and computer-aided manual validation (*190, 191*). Overall this method identified and quantified 174 tyrosine phosphopeptides. Figure 2.2b shows a volcano plot of average fold change (FC) and P value for each peptide identified (n=3 EV and n=3 shCul5, one-sided Student t-test). 45 of the peptides were significantly increased ($P<0.05$) in Cul5-depleted cells. However, the fold changes in phosphopeptide abundance were small. This is most likely because the cells were grown in complete medium and were not acutely stimulated with ligand or incubated with phosphatase inhibitors to stimulate tyrosine phosphorylation.

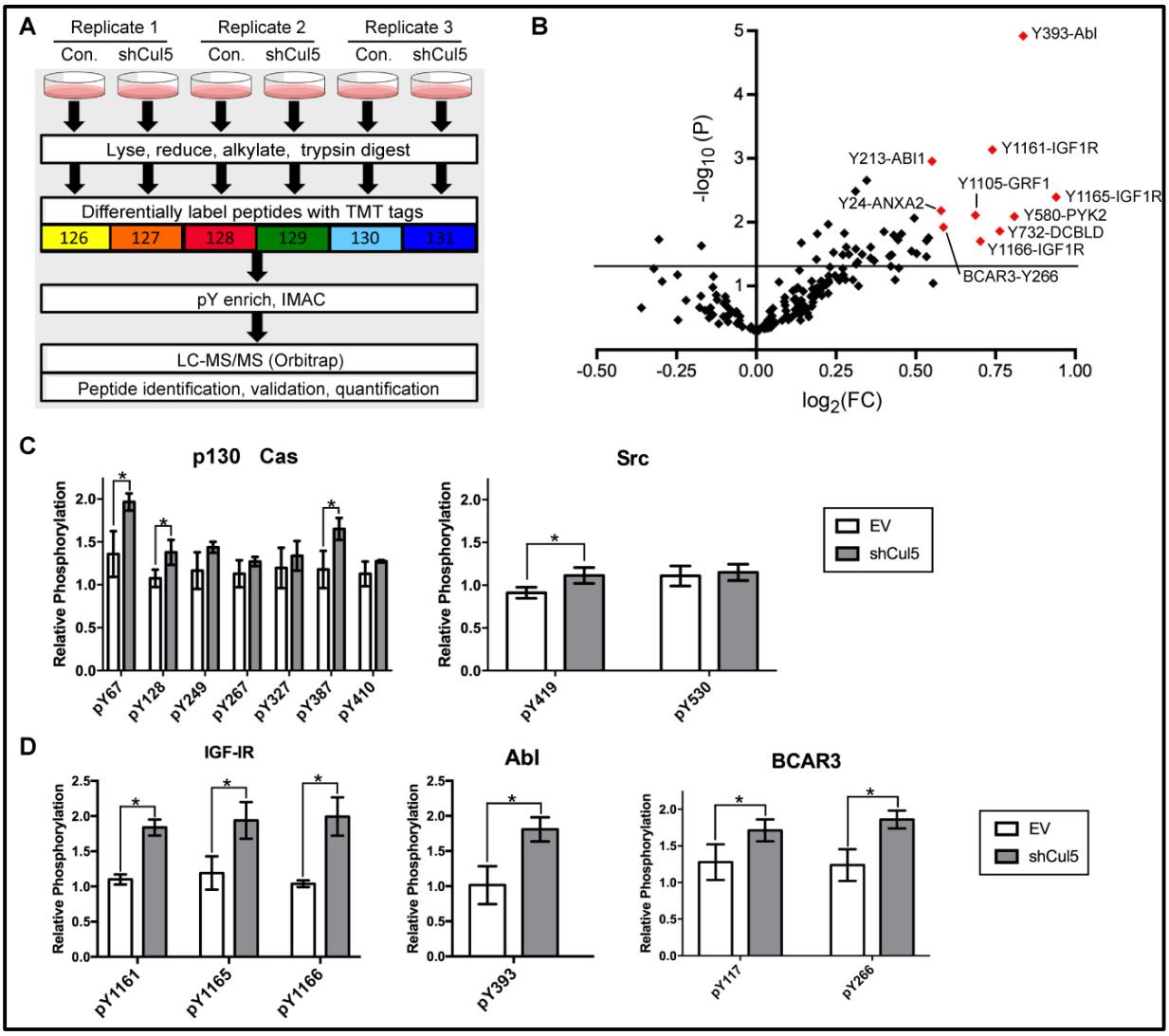

FIGURE 2.2 QUANTITATIVE PHOSPHOTYROSINE MASS SPECTROMETRY ON THE CONTROL AND CULLIN5-DEPLETED MCF10A CELLS IDENTIFIED PHOSPHORYLATION SITES THAT MAY BE REGULATED BY CULLIN5

(a) Flowchart of the quantitative phosphotyrosine mass spectrometry protocol used to identify phosphotyrosine sites regulated by Cullin5. Three biological replicates of control (EV) and Cul5-depleted (shCul5) MCF10A cells were harvested for analysis. Cells were lysed in 8 M Urea containing 1 mM pervanadate as a phosphatase inhibitor. Proteins were reduced, alkylated and digested with trypsin and the peptides were labeled with isobaric TMT tags. The digests were mixed, and phosphotyrosine peptides were enriched using anti-phosphotyrosine 4G10 beads followed by an immobilized metal affinity column (IMAC) enrichment. Phosphopeptides were analyzed and quantified by LC-MS/MS, followed by Mascot identification and computer-aided manual validation. (b) A volcano plot depicting the fold change (shCul5/EV) of each phosphopeptide verses the p-value, obtained through a one-sided two-sample equal variance T-Test in excel. Line at p=0.05. Red points have a fold change lager than 1.5-

fold. (c) Bar graphs depicting the fold change for every peptide found for p130Cas and Src. *, $p<0.05$. (d) Bar graphs depicting the fold change for every peptide found for IGF-IR, Abl and BCAR3, *$p<0.05$.

We scanned the results for phosphopeptides that we expected to be increased in Cul5-deficient cells. Previously, we detected increases in Src pY419, p130Cas pY165, and p130Cas total protein by immunoblotting (*143*). Two Src pY peptides were found in the proteomics experiment: the activation loop pY419 and inhibitory site pY530 (Figure 2.2c). As expected, only pY419 was significantly increased (Figure 2.2c). Seven p130Cas pY peptides were identified in the mass spectrometry experiments, three of which were significantly increased (Figure 2.2c). Six of the sites (but not pY67) are in the "substrate domain" of p130Cas, and, like pY165, are known to be phosphorylated by Src (*192, 193*). Our ability to detect these pY peptides suggests that Cul5-regulated phosphorylation could be detected by quantitative pY proteomics.

Several pY peptides were strongly increased in Cul5-deficient cells. Interestingly, the most significant increase was pY393 in the activation loop of the Abl tyrosine kinase (Figure 2.2d). Curiously, this site may be phosphorylated either by Abl (in trans) or Src (*194-196*). Phosphorylation of tyrosine kinase Pyk2 at Y580 was also increased. Pyk2 binds to and is regulated by SOCS2 (*137*). Pyk2 Y580 may be phosphorylated by SFKs (*197, 198*), so the increased Pyk2 phosphorylation in Cul5-deficient cells may be due to increased Src activity or decreased degradation of Pyk2. Other notable increases included a Src phosphorylation site in the DCBLD2 orphan scaffold receptor (*199*); Src phosphorylation site Y1105 of GRF1 (also known as ARHGAP35 and p190RhoGAP), which mediates binding to p120RasGAP (*200, 201*); Src phosphorylation site Y24 of ANXA2 (*202*); the major Abl phosphorylation site, Y213, of Abl-interacting protein ABI1, which inhibits Abl activity and is involved in cell migration and endocytosis and degraded by the proteasome (*203-208*); and Y266 of BCAR3, a p130Cas interaction partner and important focal adhesion protein (*209*) (Figure 2.2d). These changes indicate that the proteins phosphorylated at increased levels in Cul5-deficient cells are either phosphorylated by active Src, have increased activation loop phosphorylation and perhaps kinases activity, or are directly regulated by CRL5 in a pY-dependent manner.

2.2.3 *Potential significance of INSR/IGF-IR as a Cul5 substrate*

Our quantitative phosphotyrosine proteomics also showed that three phosphorylation sites in the insulin-like growth factor receptor-1 (IGF-IR) were phosphorylated at increased level when Cul5 was absent (Figure 2.2d). Even though Proteome Discoverer assigned these peptides to IGF-IR, they could equally well come from the insulin receptor (INSR). The INSR and IGF-IR are closely related but the IGF-IR binds more strongly to IGF1 and IGF2 ligands and the INSR binds more strongly to insulin (INS) ligand. The three phosphorylation sites (Y1131, Y1135, Y1136) are located in the kinase domain activation loop and are identical between the IGF-IR and INSR. These sites are the major sites of autophosphorylation and all must be phosphorylated for optimal kinase activity (*210*). Src can also phosphorylate these sites (*211*). After kinase activation, additional sites in IGF-IR and INSR are phosphorylated and leading to recruitment and activation of downstream signaling pathways (*212*).

We were interested in testing whether the INSR/IGF-IR is a bona fide Cul5 substrate for various reasons. First, the major mechanism of INSR/IGF-IR receptor signal termination is through endocytosis and recycling or targeting for degradation via the lysosome (*212*). Both endocytosis and degradation of IGF-IR receptor are regulated by ubiquitylation (*213*). Various E3 ubiquitin ligases that have been implicated in IGF-IR ubiquitylation, including β-arrestin/MDM2, Grb10/Nedd4, and c-Cbl (*214-218*). Two SOCS proteins, SOCS2 and SOCS3, also bind to IGF-IR; however, as of right now it is not known if they stimulate ubiquitylation or degradation (*154, 157*).

2.2.4 *Testing whether INSR and IGF-IR are Cul5 substrates*

We used Western blotting to test whether INSR or IGF-IR phosphorylation was increased in Cul5-deficient cells. We used a phospho-antibody that recognized pY1135 in the INSR which is equivalent to pY1150 in the IGF-IR. Henceforth, we call this antibody and site "pY1135". The phospho-antibody detects phosphorylation of a cleaved form of the INSR/IGF-IR known as the β chain. Both receptors are synthesized as a precursor that is cleaved into α and β subunits that are bound by disulfide bonds to form an $\alpha_2\beta_2$ functional receptor. The α-subunit is the extracellular

ligand binding moiety and the β-subunit has a short extracellular domain, a transmembrane domain and intracellular kinase domain, and contains the phosphorylation sites of interest.

The results showed that Cul5-depleted cells have increased phosphorylation at pY1135, confirming the quantitative phosphotyrosine mass spectrometry experiments (Figure 2.3a). Total levels of IGF-IR α and β chains may also increase slightly, but the increase was variable experiment to experiment.

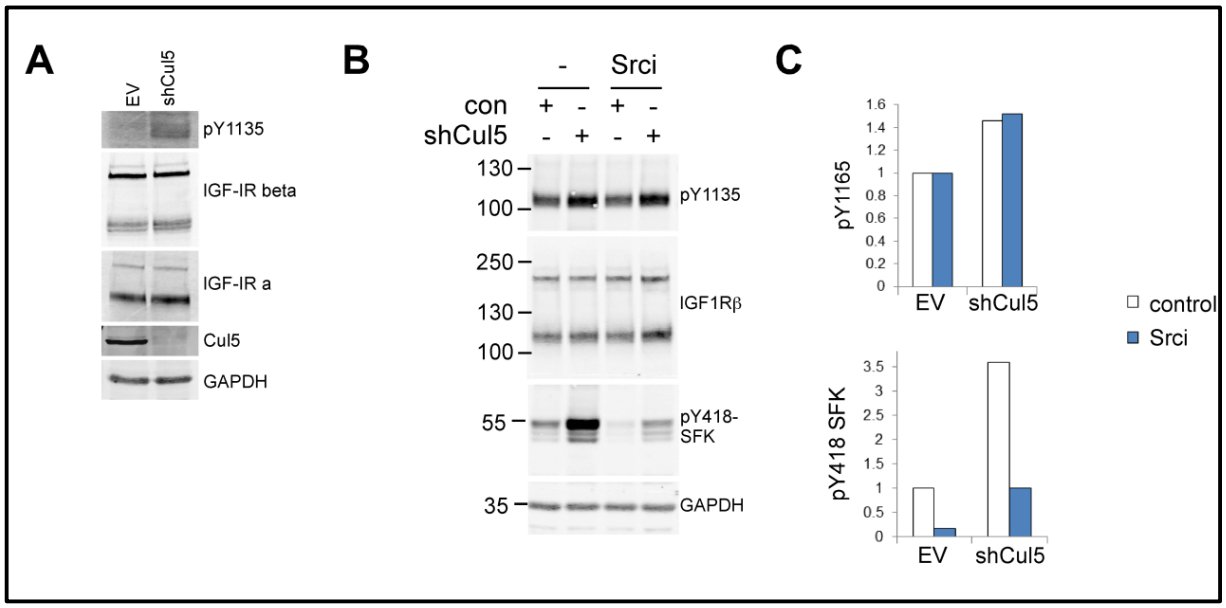

FIGURE 2.3 PY1135 IS INCREASED IN CUL5-DEPLETED CELLS INDEPENDENT OF SRC KINASE ACTIVITY

(a) pY1135 levels are increased in Cul5-depleted cells. Sub-confluent MCF10A cells were treated with 100 μM orthovanadate for 8hours prior to harvesting and analyzed by Western blotting. (b) Increase in pY1135 is independent of Src kinase activity. Sub-confluent MCF10A cells were treated with 100 μM orthovanadate and either DMSO or 10 μM SU6656 (Srci) for 8 hours before harvesting and analyzed by Western blotting. (c) Quantification of pY1135 and pY418-SFK activity, shows pY1135 levels are unchanged by Srci and pY418-SFK decreases when Srci is added to the cells. Western blots in panel b were quantified using ImageJ software. Bars represent the quantification of one biological replicate.

We wondered whether increased pY1135 phosphorylation reflected increased autophosphorylation or increased phosphorylation by another kinase. Cul5-depleted cells have increased SFK activity, and Src has been reported to phosphorylate IGF-IR at pY1135 (*143,*

211). To determine if the increase in pY1135 was due to Src phosphorylation or a change in pY-IGR-IR abundance or activity, we incubated control and Cul5-depleted cells in the presence of a Src inhibitor, SU6656. The Src inhibitor decreased SFK activity (pY418) in Cul5-depleted cells down to control cell levels but did not affect pY1135 levels in Cul5-depleted cells (Figure 2.3b,c). This suggested that pY1135 increased upon Cul5-depletion either because pY-IGF-IR/INSR degradation is directly regulated by CRL5 or CRL5 inhibits a pathway/protein that activates IGF-IR/INSR kinase.

IGF-IR has been reported to bind to SOCS2 and SOCS3 (*154, 157*), while INSR binds SOCS1 (*149*). To test which SOCS proteins bind IGF-IR, we expressed T7-tagged SOCS box mutants, SOCS1-7^{LCQQ} and CisH^{LCQQ}, which do not bind CRL5 and thus should not stimulate ubiquitylation and degradation (*167*). The T7-SOCS proteins were immunoprecipitated and Western blots were probed to detect binding of IGF-IRα and IGF-IRβ. IGF-IRα and IGF-IRβ bound strongly to SOCS1 and somewhat to SOCS2. The positive control, Cas, only bound only to SOCS6 as expected (*143*) indicating the immunoprecipitation was clean (Figure 2.4a). Our results suggest that SOCS1 and SOCS2 bind to IGF-IR and possibly bring it to CRL5 for ubiquitylation and degradation. To determine if SOCS1 or 2 are involved in the degradation of pY-IGF-IR, we knocked down SOCS1 and SOCS2 proteins individually or in combination in MCF10A cells and probed for total IGF-IRα, total IGF-IRβ and pY1135. Depletion of SOCS1 but not SOCS2 increased total IGF-IR and pY1135 levels (Figure 2.4b). This indicated that SOCS1 might be used by CRL5 to regulate pY-IGF-IR. To test whether IGF-IR ubiquitylation and degradation are directly regulated by CRL5^{SOCS1}, we would need to perform *in vitro* binding with SOCS1, [^{35}S] methionine pulse-chase degradation assays in Cul5- and SOCS1-depleted cells, and cell-based and *in vitro* ubiquitylation assays. Before starting these experiments, we first wanted to confirm that the increased pY1135 observed upon depletion of Cul5 with shRNA was due to Cul5 activity and not an off-target effect of the shRNA.

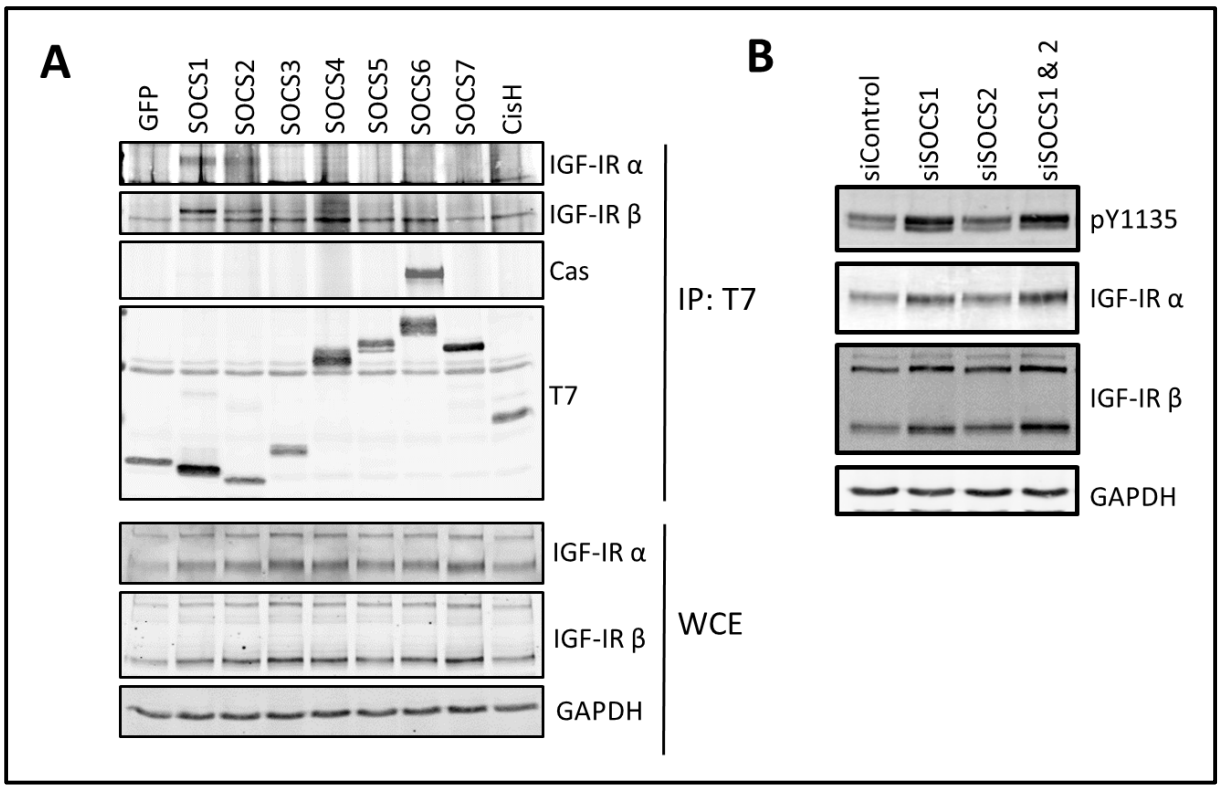

FIGURE 2.4 SOCS1 BINDS IGF-IR AND SOCS1 DEPLETION INCREASES PY1135

(a) Endogenous IGF-IR binds to overexpressed SOCS1 and SOCS2 in HeLa cells. HeLa cells were transiently transfected with T7-GFP or the indicated T7-SOCS^{LCQQ} constructs. Twenty-four hours later the cells were stimulated with 1 mM pervanadate for 30 minutes. The cells were lysed and immunoprecipitated with antibody to T7 and protein A/G beads. Western blots were probed with the indicated antibodies. (b) SOCS1-depletion causes an increase in pY1135 and total IGF-IR protein. MCF10A cells were transfected with siRNA to the indicated proteins two times over 72 hours. Four days after the first transfection the cells were then treated with 100 μM orthovanadate for 8 hours and then harvested and analyzed by Western blotting.

As a first step to testing whether the increase in pY1135 in Cul5-deficient cells might be an off-target effect of Cul5 shRNA, we tested whether inhibiting CRL activity using a Neddylation inhibitor, MLN4924, would also increase pY1135. We measured levels of another CRL5 substrate, BCAR3, as a positive control (unpublished). BCAR3 levels were increased by Cul5 knockdown or MLN4924 non-additively, suggesting that Cul5 knockdown inhibits BCAR3 degradation by a Neddylation-dependent process (Figure 2.5a). However, MLN4924 did not increase pY1135 levels in control or Cul5-deficient cells (Figure 2.5a). This suggested that either the observed increase in shCul5 cells is off-target or Cul5 is involved but independent of

Neddylation. Another possibility is that MLN4924 may not have been present for long enough to increase pY1135. The half-life of pY-IGF-IR in MCF10A cells is unknown, but most proteins have half-lives between 45 min and 22.5 hours and the MLN4924 was added for 24 hrs (*219*). Therefore, it is more likely that the observed increase in shCul5 cells is off-target or that pY-IGF-IR turnover is independent of Neddylation.

To further test for off-target effects, we treated MCF10A cells with individual or pooled siRNAs against Cul5. All of the individual and pooled siRNAs depleted Cul5 to a variable extent. Total levels of the control BCAR3 and pY1135 increased with every Cul5 siRNA sequence used (Figure 2.5b). This result provided evidence that the change in pY1135 may be specific to Cul5 and not an off-target. To perform one last off-target test, we checked the levels of total IGF-IR and INSR in MCF10A cells that have Cul5 knocked out with CRISPR/Cas9. The amount of our positive control BCAR3 increased in this cell line, and Cul5 protein was completely depleted. However, unexpectedly, the total quantity of IGF-IR was decreased by half in this cell line, and INSR levels remained constant (Figure 2.5c, d). Unfortunately, we did not probe these lysates for pY1135 to determine if pY1135 was increased or decreased. It is important to note that these Cul5 knockout cells are clonal and there may be additional mutations. The knockout line is still being validated. It is also important to note that changes in total IGF-IR were weak and somewhat variable and that we have not systematically tested for changes in total INSR. However, pY1135 is quite consistently increased when Cul5 or SOCS1 is knocked down, consistent with a Neddylation-independent regulation of IGF-IR or INSR phosphorylation by $CRL5^{SOCS1}$.

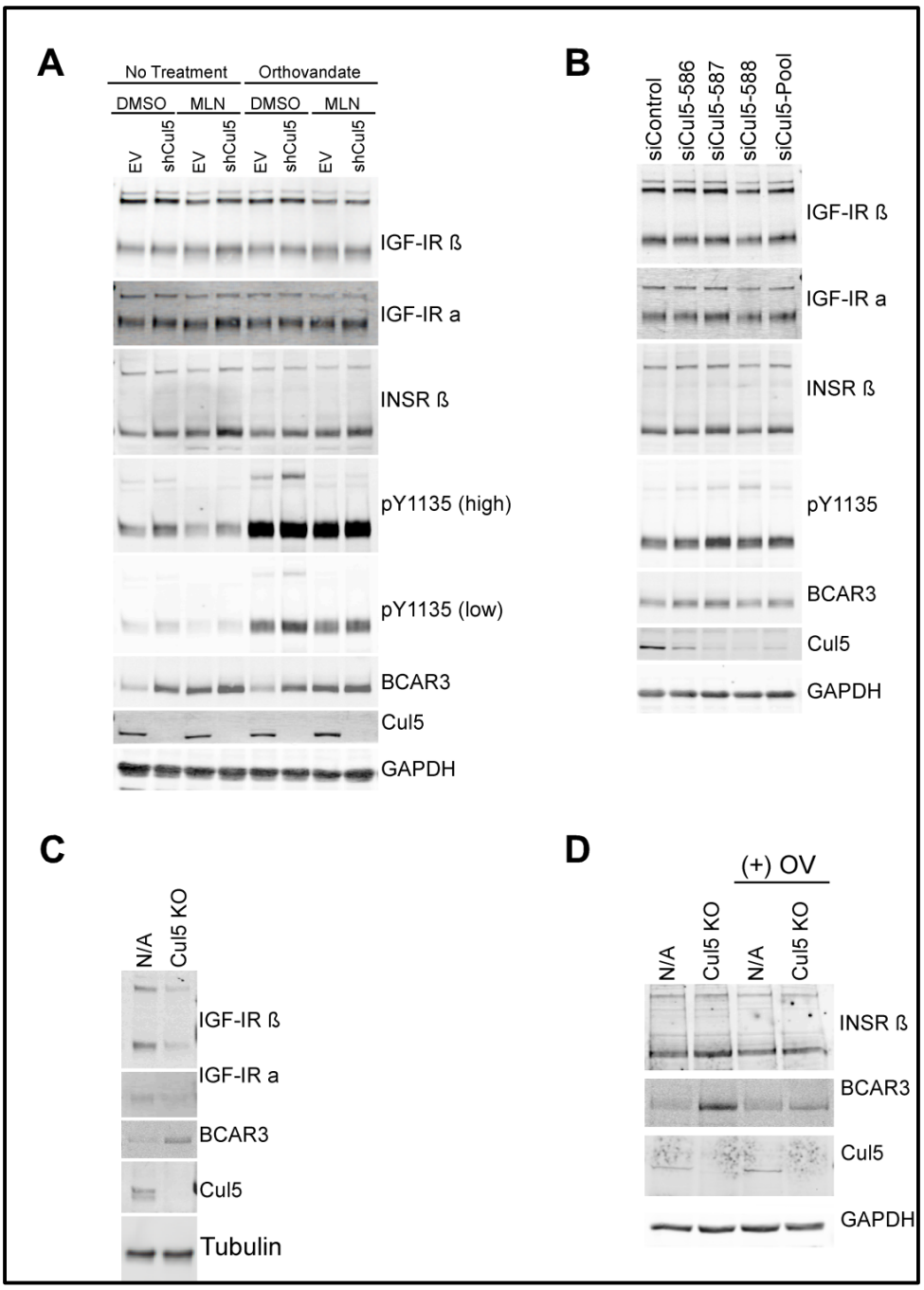

FIGURE 2.5 CUL5 DEPLETION, BUT NOT INHIBITION OF CRL5 NEDDYLATION INCREASES PY1135

(a) MLN4924 treatment does not increase pY1135 to the same levels as Cul5 shRNA. Twenty-four hours before lysis sub-confluent MCF10A cells were treated with 5 μM MLN4924 or an equivalent volume of DMSO. Eight hours before lysis the cells were treated with 0 or 100 μM orthovanadate. (b) Individual Cul5 siRNA sequences increase pY1135, but have variable effects on INSR and IGF-IR levels. MCF10A cells were transfected with the indicated siRNAs two times over three days. Four days after the first transfection the cells were treated with 100 μM orthovanadate for 8 hours. At the

end of the orthovanadate treatment, the cells were harvested and analyzed by Western blotting. (c) IGF-IR levels go down in Cul5 CRISPR knockout cells. Sub-confluent MCF10A cells were treated with 100 μM orthovanadate for 8 hours and then harvested. (d) INSR levels go up slightly in Cul5 CRISPR knockout cells. Sub-confluent MCF10A cells were treated with 100 μM orthovanadate for 8 hours and then harvested.

2.3 DISCUSSION

We set out to identify substrates of CRL5 that were dynamically turned over using GPS and global phosphotyrosine proteomics. The GPS method has been used to determine substrates of CRL1, CRL2, CRL3, and CRL4. In our hands, the GPS system allowed the detection of increased turnover of a CRL5 substrate, Cas, when the PTP inhibitor pervanadate was present to increase tyrosine phosphorylation. Moreover, pervanadate-induced Cas turnover was inhibited by the proteasome inhibitor MG132. Nevertheless, when constitutively active Src was used to induce phosphorylation of Cas, we were unable to see Cas turnover. This was true even in the presence of exogenous SOCS6 expression. Perhaps pervanadate induces Cas turnover by other E3 ligases in addition to $CRL5^{SOCS6}$. $CRL5^{SOCS6}$ might contribute to only a small percent of total Cas turnover. For example, $CRL5^{SOCS6}$ may only regulate Cas turnover in focal adhesions, and the amount of Cas in focal adhesions is such a small percent of the total Cas the GPS technique cannot detect it. Overall, these experiments demonstrated that GPS was not a feasible approach to screen for CRL5 substrates.

Quantitative phosphopeptide affinity enrichment has not been used yet to identify phosphorylation-dependent substrates of CRLs. Our results show that phosphopeptide enrichment is a viable method to identify proteins that are turned over in a pY-dependent manner by CRL5. This is evident by the identification of Cas and Src peptides in our screen that were previously validated by Western blotting. Moreover, we identified increases in phosphopeptides from BCAR3 and IGF-IR/INSR that were subsequently validated by Western blotting as potential CRL5 substrates (some data not shown). One important caveat with this screening approach is that the proteins identified may be indirect targets of Cul5, e.g., proteins that are phosphorylated downstream of a kinase that is directly regulated by CRL5. In future work, it will be important to determine which of the significantly increased peptides identified in this screen

are direct targets of Cul5 and which are indirect. This is even more important because many of the significantly increased peptides have been reported to be phosphorylated by the Src family kinases, whose activity is also increased in these cells. Src may be regulating some of these sites, however it is likely that additional kinases and/or proteins are regulated by Cul5 and play a role in MCF10A cell transformation because our previous work showed that Src activation was not sufficient to induce the same phenotypes as removal of Cul5.

The tyrosine-phosphorylated peptides that were increased significantly by Cul5 depletion had relatively small changes in abundance. This is most likely because constitutive tyrosine phosphorylation is low in actively growing cells, leading to a low amount of CRL5-based turnover in control cells. If we were to repeat this work, it would be best to include orthovanadate or pervanadate to increase tyrosine phosphorylation globally or to acutely stimulate the cells with an exogenous growth factor(s) to stimulate specific kinase pathways. This would result in more CRL5-based turnover in control cells, causing an increase in the fold changes observed between control and Cul5-depleted cells.

Phosphorylation of the three tyrosines (pY1131, pY1135, pY1136) located in the activation loop of the IGF-IR/INSR receptor were identified by our screen as significantly increased in our Cul5-depleted cells. We validated the increase in one of these peptides, pY1135, with Western blotting and showed that the increase was independent of Src kinase activity, suggesting that autophosphorylation is increased. pY1135 was also increased when Cul5 expression was inhibited by several Cul5 siRNAs, suggesting that the effects are not off-target.

IGF-IR had previously been reported to bind to SOCS2 and SOCS3 (*154, 157*). In our screen of SOCS binding interactions, we found IGF-IR bound to SOCS1 and SOCS2 after acute pervanadate stimulation. We did not check INSR binding in our screen, but the INSR has been reported to bind to SOCS1, 3, and 6 (*149, 158*). SOCS1, 2, 3 are all strongly induced after extracellular stimulation and thought to behave similarly, so this may be why IGF-IR can bind to all three of these proteins (*80*). SOCS1 depletion with pooled siRNAs increased the abundance of pY1135 in MCF10A cells. In future work, it will be interesting to confirm that the increase in

pY1135 is not off target by using individual siRNA constructs and stable shRNA cell lines to deplete SOCS1.

In conclusion, our results suggest that the GPS approach may not be viable for CRL5 substrates that require phosphorylation for degradation, but quantitative phosphotyrosine proteomics may be useful. Specifically, we detected increases in phosphorylation of known substrates (Src and Cas) and a new candidate, BCAR3 (data not shown). We also detected increased phosphorylation in the activation loop of the INSR/IGF-IR, which appears not to be off target. Further study of this latter phosphorylation seems justified. Specifically, we would like to determine which receptor is affected and if increased phosphorylation is caused by decreased degradation of the active receptor or through increased kinase activity. We note that MCF10A cells are routinely grown in the presence of high levels of insulin and both receptors may be activated. One control we did not perform was to check the RNA expression levels of the endogenous ligands IGF1, IGF2, and insulin to make sure there is not more autocrine stimulation of the receptor in the absence of CRL5 activity. If there is no change in ligand abundance, then a [^{35}S] methionine pulse-chase experiment should be done to determine if the half-life of pY1135 is changed upon Cul5 or SOCS1 depletion. Also, it will be critical to know if SOCS1 binds directly to IGF-IR and INSR to get assurance of the direct interaction. This could be followed by a cell-based and in vitro ubiquitylation assay to show CRL5 ubiquitylates IGF-IR/INSR directly.

One very interesting observation was that pY1135 was not affected by the CRL Neddylation inhibitor MLN4924. This suggests that pY1135 may be CRL5^{SOCS1}-dependent but Neddylation-independent. This indicates that CRL5^{SOCS1} regulation of pY1135 is independent of the ubiquitylation activity of CRL5. Perhaps the CRL5^{SOCS1} complex is an adaptor that mediates the binding of a protein that directly regulates INSR/IGF-IR kinase activity. This would be novel function of CRL5^{SOCS1} binding.

Chapter 3. SOCS2 BINDS TO & REGULATES EPHA2 THROUGH MULTIPLE MECHANISMS

3.1 INTRODUCTION

The Eph receptors are the largest family of receptor tyrosine kinases (*220*). They can be classified into two groups, EphA and EphB receptors, based on the similarity in their extracellular amino acid sequences. Eph's bind to Ephrins (Efn) ligands on the surfaces of adjacent cells. The EphA receptors preferentially to bind the GPI-linked EfnA ligands (Efn-A1-A5) and the EphB receptors preferentially to bind to the transmembrane EfnB ligands (EfnB1-B3), with a few exceptions. There are eight EphA receptors, EphA1-EphA8, and six EphB receptors, EphB1-EphB6 (*221, 222*). All of the Eph receptors are structurally similar: starting at the N-terminus they have a globular ligand binding domain, a cysteine-rich region, two fibronectin type III domains, followed by a transmembrane domain. On the intracellular side, they have a juxtamembrane region, tyrosine kinase domain, a SAM domain and PDZ binding motif (*220*).

Because their ligands are bound to adjacent cells, Eph-Efn signaling requires cell-to-cell contact and can elicit signaling in either the Eph-expressing cell, the Efn-expressing cell or both cells. Forward signaling refers to the signaling in the receptor cell after *trans* activation and reverse signaling refers to the signaling in the Efn cell after *trans* activation. Forward and reverse signaling is important for developmental processes that are regulated by Eph-Efn signaling, because both activate cytoskeletal changes that mediate cell repulsion or adhesion (*223*).

Similar to most other RTKs, the Eph receptors form dimers upon ligand engagement; however, unlike most other RTKs the Eph receptors must form higher order clusters to produce productive downstream signaling. Eph receptors must bind membrane bound or artificially clustered Efns in order to trigger productive receptor signaling (*220*). One Eph receptor binds to one Efn ligand, these then dimerize causing the rapid assembly of higher order clusters. Tetramers are needed for the activation and biological function of the receptor (*224*). These clusters are required to

activate forward signaling. Efn ligands can also act on receptors in the same cells in a process called *cis* interaction or activation. Cis-activation is speculated to reduce forward signaling by inhibiting the formation of large Eph receptor clusters (*225, 226*).

The juxtamembrane region of the Eph receptors contains two conserved tyrosine residues that regulate the kinase activity of the Eph receptor. When the two juxtamembrane tyrosines are un-phosphorylated the juxtamembrane region contacts the kinase domain preventing the kinase activation segment from forming the ordered conformation needed for productive kinase activity. Phosphorylation the juxtamembrane tyrosines results in a disordered juxtamembrane region causing release from the kinase domain allowing the kinase activation segment to form the correct conformation (*227-229*). The juxtamembrane tyrosines are phosphorylated in a processive order. The juxtamembrane tyrosine farthest from the membrane (JM2) is phosphorylated first followed by the juxtamembrane tyrosine closest to the membrane (JM1). It has been reported that JM2 serves as a better proxy for the kinase activity of the Eph receptor (*230*). Juxtamembrane phosphorylation is followed by autophosphorylation of a tyrosine residue in the kinase activation loop, causing full activation of the receptor (*231*).

Forward and reverse Eph-Efn signaling causes changes actin polymerization. Eph-Efn forward signaling activates NCK1, NCK2, phosphoinositide-3-kinase (PI3K), SFK, VAV2, VAV3, and Ephexin. Together these signaling proteins regulate actin polymerization and the cytoskeleton through their regulation of the Rho GTPases, Rac and Rho (*223*). Eph-Efn reverse signaling activates the SFKs and small GTPases to induce actin remodeling. The EfnA ligands lack a c-terminal tail, they are thought to act through the p75 and Ret receptors. The EfnB ligands stimulate changes in the cytoskeleton by activating Rac through DOCK180 (*223*).

Eph-Efn signaling is turned off through a process called trans-endocytosis. This describes the process where either the ligand or the receptor-expressing cell endocytose the receptor-ligand complex in addition to the membrane from the adjacent cell. The direction of this endocytosis seems to depend on the type of cells interacting. Ultimately this removes the cell-cell contact at the site of trans-endocytosis (*232*).

3.1.1 *Eph-Efn biology*

The Efn-Eph signaling pathway has been shown to be essential for many developmental processes including cell sorting at tissue boundaries and axon guidance (*223*). Early cell mixing studies demonstrated that cells overexpressing either WT EphB or WT Efn-B separated into two homogeneous populations with a sharp boundary between the two overexpressing cells. The cell sorting required the cytoplasmic domains of EphB and EfnB indicating that both forward and reverse Eph signaling contributed to the formation of cell boundaries (*233, 234*). Efn-Eph signaling is also necessary for neuronal topographic map formation in the auditory, somatosensory, motor, visual and olfactory systems (*235*). A topographic map is when the spatial position of the projection neuron matches the spatial position of the connection. The first crucial experiments showed that gradients of Eph receptors and Efns in retinal axons and their targets in the brain control where the axon will synapse. Efn-Eph interactions are also important for choice points, where neurons have to choose between areas of high Efn or no Efn expression (*235, 236*). In addition to neuron development, there are other developmental processes that Eph-Efn signals control, such as gastrulation, somitogenesis, and angiogenesis (*220*). Overall, the Eph receptors and Efn ligands are both modulators of development.

In the adult, Efn-Eph signaling has also been shown to be important for the formation and remodeling of the mammary ducts in mice. The mammary ducts have three different types of epithelial cells: luminal epithelial cells, the cells that line the duct that leads to the nipple; terminal end bud epithelial cells, these are the cells that form the bud at the other end of the duct; and myoepithelial cells, that surround these two-other cell types and make ECM components (*237*). At the onset of puberty and in preparation for lactation the ductal structures in the breast must undergo branching and morphogenesis to form or re-model the breast (*238*). EphA2 is expressed in the terminal end bud epithelial cells, where it regulates branching at the onset of puberty (*239*). EphB4 is expressed in luminal epithelial cells, and EfnB2 is expressed in the surrounding myoepithelial cells where they regulate these compartments. Loss of EfnB1 or increased expression of EphB4 changes differentiation and branching the breast ducts (*240-243*).

3.1.2 *EphA2 activation and ubiquitylation*

The EphA2 receptor can bind to all EfnA ligands but prefers EfnA1 (*220*). Upon ligand binding, EphA2 is phosphorylated at the juxtamembrane tyrosines Y588, Y594 and the activation loop tyrosine Y772 (*244*). Two E3 ubiquitin ligases have been shown to bind and ubiquitylate EphA2: Cbl and UBE4A.

Cbl binds through its TKB (tyrosine kinase binding) domain to ligand-activated pY-EphA2. Tyrosine 813 in EphA2 has been proposed to be the Cbl binding site in EphA2, based on similarity to other Cbl pY sites (*52*). However, co-immunoprecipitation experiments have not been done to definitively show this is the correct site. Overexpression of WT Cbl decreases the level of exogenous EphA2 protein, dependent on the Cbl RING domain (*245, 246*). Exogenous EphA2 can be ubiquitylated when Cbl is overexpressed in cells, and this ubiquitylation decreases when Y813 site is mutated to a phenylalanine (*52*). This early evidence suggested that Cbl may ubiquitylate and degrade EphA2 by binding to pY813 in EphA2 after ligand-mediated activation of the receptor.

Additional clues to the function of EphA2 regulation by Cbl come from studies of the Kaposi's sarcoma-associated herpesvirus (KSHV). KSHV binds to EphA2 as a way to gain entry into endothelial and human foreskin fibroblast cells. KSHV binding to EphA2 stimulates EphA2 phosphorylation leading to the activation of Src, FAK, and PI3K. EphA2-KSHV binding also results in EphA2 binding to the clathrin-coated pit adaptors Cbl, AP-2 and epsin and to clathrin itself. EphA2 is mono-ubiquitylated and Lys63 poly-ubiquitylated after virus stimulation in a Cbl-dependent manner. Moreover, EphA2 and KSHV cannot get into human foreskin fibroblast cells when Cbl is absent (*247, 248*). Therefore, KSHV binding to EphA2 stimulates Cbl ubiquitylation of EphA2 that leads to the clathrin-dependent endocytosis of viral-bound EphA2 into the cell. Cbl may also be required for the clathrin-dependent endocytosis of EphA2 in cells stimulated with EfnA1 ligand as well, but there is no direct evidence for this. It is not clear if Cbl is required for the lysosomal degradation of EphA2.

The adaptor protein Src-like adaptor protein (SLAP) is widely expressed in immune cells, where it acts as an adaptor protein downstream of antigen receptors. Recently SLAP was found to be

expressed in healthy colon epithelial cells and is down-regulated in colorectal cancer. SLAP binds to Y594 in the EphA2 juxtamembrane region and recruits the E3 Ub ligase UBE4A to EphA2. UBE4A-SLAP has been shown to ubiquitylate EphA2 in cells and *in vitro*. Knockdown of SLAP or UBE4A slightly increased total EphA2 protein in colorectal cancer cell lines. When SLAP is overexpressed total EphA2 decreases and knockdown of UBE4A rescues this decrease. This suggests that, in normal colon epithelial cells where SLAP expression is high, SLAP and UBE4A may regulate the turnover of EphA2. The authors suggest this turnover is proteasomal degradation because MG123, a proteasomal inhibitor, prevents the SLAP-induced decrease in total EphA2 (*249*). However, it seems this could be due to the depletion of ubiquitin that then prevents other ubiquitin-dependent process, as mentioned previously (*23*). Overall it seems like high levels of SLAP and UBE4A may be needed to get significant changes in total EphA2 levels or degradation rate.

EphA2 is overexpressed in metastatic tumors originating from a wide variety of tissues. As a result, many drugs and antibodies have been made to inhibit EphA2 activity. However, many tumors are promoted by EphA2 in a EfnA ligand-independent manner, making it a complex kinase to drug (*250, 251*). EphA2 has primarily been shown to be overexpressed in breast cancer cells and its overexpression correlates with decreased EfnA1 expression and loss of estrogen receptor expression (*252-254*). Increased EphA2 expression in Her2-positive breast cancer patients correlates with a decrease in disease-free and overall survival (*255*). Subsequent work showed EphA2 could bind to Her2, and EphA2 expression is required for tumor growth, cell migration and Rho activation in a Her2 overexpressing breast cancer mouse model (*239*). Over-expression of EphA2 in normal breast epithelial cells, MCF10A, has been shown to promote cell transformation (*256*).

In this chapter, I report screens for SOCS2 and SOCS6-interacting proteins, the finding that SOCS2 interacts with EphA2, and follow-up experiments to determine the significance of SOCS2-EphA2 interaction.

3.2 RESULTS

3.2.1 *Identification of SOCS2- and SOCS6-interacting proteins*

The PAC method was used to identify binding partners of F-box proteins which are substrate receptors for CRL1 (*183, 184*). Because it had worked for F-box proteins, we attempted to use the same method for SOCS2, 4, 5 and 6. These SOCS proteins were stably expressed in MCF10A cells with a Flag-HA tag. After an overnight serum starvation, the cells were stimulated with a high physiological amount of EGF (100 ng/mL) and insulin (10 µg/mL), to stimulate the association of substrates with the SOCS proteins, and CRL activity was inhibited with MLN4924 to promote stable complex formation. SOCS 2, 4, 5 and 6 were pulled out of cells using the HA tag, eluted with HA peptide, and sent to the Harper lab for LC-MS/MS identification and CompPASS filtering.

Unfortunately, there were very few (2-6) high confidence interacting proteins (HCIP) identified using this method and the CRL5 complex members were not enriched in any of the SOCS purifications. This failed attempt at PAC is most likely due to a few factors. First, there was lots of keratin contamination in this experiment that resulted in fewer real hits being identified. Next, we observed Flag-HA-SOCS protein expression is turned off over time in MCF10A cells, so we immunoprecipitated a lower amount of SOCS out of cells even though we started with the same number of cells as the Harper lab. SOCS protein expression is most likely turned off due to their inhibition of phosphotyrosine signaling. Cells that express lower levels of SOCS proteins will have less inhibition of phosphotyrosine signaling, which will provide a growth advantage. Finally, we had trouble recovering all of the Flag-HA-SOCS from the HA beads using the HA peptide elution. All of these problems together meant that we sent a small amount of a dirty SOCS material to be identified in the mass spectrometer. This method may have worked if we could have recovered a higher amount of a clean affinity purification.

As alternative approaches to identify SOCS2 and 6-interacting proteins, we used bait proteins whose expression was induced with doxycycline in Flp-In T-Rex HEK293 cells. The cells were maintained under non-inducing conditions to avoid negative selection, and only induced at the time of the experiment. We also used two unrelated affinity purification mass spectrometry (AP-

MS) methods: BioID and Flag AP-MS (*257, 258*). For BioID, a bait protein is fused to a promiscuous, mutated, biotin ligase, BirA (*257*). Biotin is then transferred to neighboring proteins, which may be isolated using streptavidin and identified using LC-MS/MS. Flag AP-MS is a more conventional affinity purification procedure in which the bait is fused to a Triple-Flag epitope tag and bound proteins are purified over anti-Flag antibody. These two methods identify overlapping sets of targets and have been used jointly to determine the substrates for another CRL, $CRL1^{\beta TrCP}$ (*258-260*).

We generated cell lines expressing SOCS2 and SOCS6 bearing Myc-BirA and Triple Flag tags, as well as Myc-BirA and Triple Flag tag vector cell lines as negative controls. Three biological replicates of SOCS2, SOCS6 and vector alone were performed for each procedure. The cells were incubated with doxycycline to induce expression of the bait proteins, and sodium orthovanadate was added to increase tyrosine phosphorylation globally. In addition, we added MLN4924 to inhibit CRL activity and thereby stabilize CRL substrates from ubiquitylation and degradation (*187*). The cells were lysed and the biotinylated or Flag proteins were purified. The proteins were eluted with on-bead trypsin digestion and analyzed with liquid chromatography-tandem mass spectrometry (LC-MS/MS). Peptides were identified and quantified using label-free quantification in MaxQuant (*261*). We estimated the abundance of each protein in each replicate by averaging the quantities of its top three peptides (*262*). The protein abundances from biological triplicate experiments were then analyzed statistically using SAINTq software (*263*). For each protein detected, abundances from the bait of interest were compared with those from the other bait and negative control, and P value, Bayesian False Discovery Rate (FDR), and average fold change (FC) were reported. Here we consider the interactions that had a Bayesian False Discovery rate of less than ten percent as being significant.

Figure 3.1 shows that 53 proteins interacted significantly with SOCS2 and 73 proteins interacted with SOCS6, colored according to their detection by BioID (red), Flag AP-MS (yellow) or both procedures (orange). The size of the symbol indicates the average FC over negative control from the biological triplicates. The lines represent protein-protein interactions previously reported in the STRING database (*264*). The two proteomics methods are complementary, identifying

different sets of interacting proteins. The Flag-AP-MS method identifies strong, easily solubilized interactions while the BioID method captures weaker, poorly solubilized proteins (*258, 259*). However, some proteins were identified by both methods, including the CRL5 complex members Cul5, TCEB1 (ElgC) and TCEP2 (ElgB), which were doubly identified with SOCS2 and SOCS6. This shows that both methods were able to identify known components of the CRL5 complex.

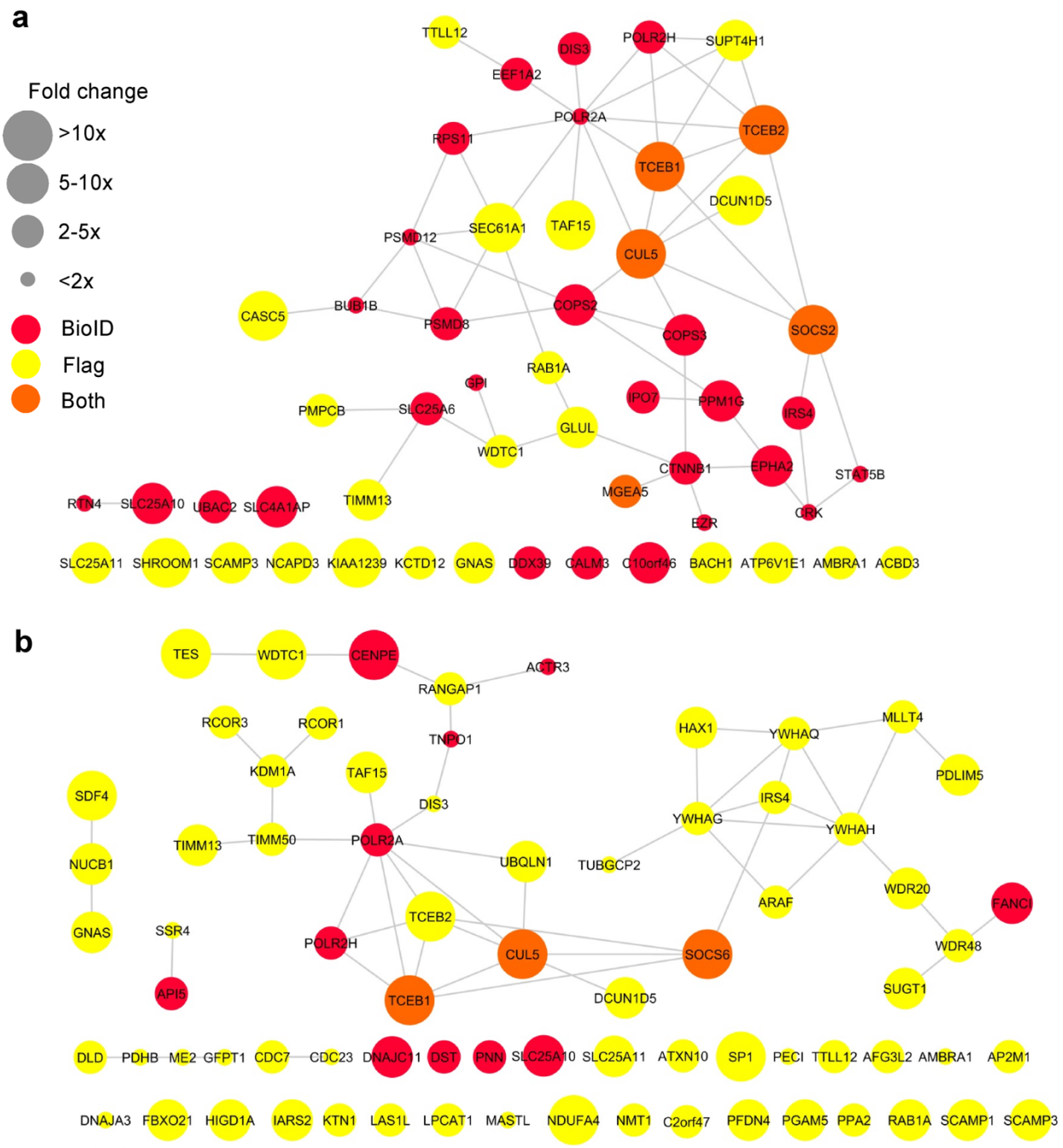

FIGURE 3.1 BIOID AND AFFINITY PURIFICATION MS IDENTIFIES SOCS2 AND SOCS6 INTERACTOMES

(a and b) SOCS2 and SOCS6 interactions identified using BioID and Triple-FLAG affinity purification mass spectrometry, with previously identified interactions added from the STRING database. Triple-FLAG or Myc-BirA tagged empty vector, SOCS2, or SOCS6 were stably integrated into Flp-In T-Rex 293 cells. The cells were treated with 75 μM sodium orthovanadate, 1 μM MLN4924, 1 μg/mL Doxycycline and 2 mM Biotin for 24 hr, lysed and immunoprecipitated with either Flag M2 magnetic beads (Flag) or streptavidin agarose beads (BirA). An on-bead tryptic digestion was performed, followed by sample desalting. The samples were run on a Orbitrap Elite and peptides were identified using MaxQuant label-free quantification. The average of the top three peptide intensities from each biological replicate were used to estimate protein abundance and then run through SAINTq program. Interacting proteins shown had a Bayesian false discovery rate <10%. The STRING app in Cytoscape was used to determine the interactions between the top hits and make the figure.

Other proteins implicated in general ubiquitylation or proteasome functions were detected as SOCS2 or 6 interactors. Both SOCS2 and 6 interacted with DCUN1D5 (DCNL5), a member of the DCN family of E3 Nedd8 ligases that transfer Nedd8 onto the Cullin backbone (*265, 266*). SOCS6 interacted with UBQLN1 (PLIC1), which interacts with many ubiquitin ligases and the proteasome (*267*). UBQLN1 contains ubiquitin-like and ubiquitin-associated UBA domains and is implicated in protein traffic, autophagy, aggresomes, and cell spreading (*268-270*). SOCS6 interacted with WDR40 and WDR28, which are deubiquitinase (DUB) activators (*271, 272*). SOCS2 interacted with COPS2 and COPS3, components of the COP9 signalsome that controls CRL neddylation (*273*).

Both SOCS2 and SOCS6 also interacted with the POLR2A and POLR2H subunits of RNA polymerase II (PolII) and various PolII-associated TAFs. POLR2A is known to bind to the ElgB/C adaptor subunits of CRL5 through Elongin A (ElgA), using a SOCS box in ElgA (*188, 274*). Our results suggest that SOCS2 and SOCS6 may interact with POLR2A-ElgA-ElgB/C, which is surprising because ElgB/C is only expected to bind one SOCS box protein at a time. SOCS2 and 6 also bound to the autophagy regulator, AMBRA1. AMBRA1 was reported to interact with ElgB/C and a variety of SOCS box proteins (*275*). It is not known how ElgB/C binds to AMBRA1 at the same time as SOCS proteins.

We were most interested in proteins that may require phosphorylation to bind to SOCS2/6 SH2 domains. A previous screen for SOCS6 SH2-binding proteins detected insulin receptor substrate (IRS)-2 and 4 and the p85α and p85β subunits of phosphatidylinositol 3' kinase (PI3K) (*141*). We detected IRS4 binding to SOCS2 and 6. Other SOCS-IRS family protein interactions have been reported, so SOCS-IRS binding may be quite general (*135, 141, 144*). However, SOCS6 gene disruption does not affect insulin signaling in mice (*141*). We also identified STAT5b using SOCS2 as bait. SOCS2 null mice have prolonged STAT5b signaling (*276*). Our results suggest that SOCS2 may bind phospho-STAT5b to directly negatively regulate signaling.

Known phosphotyrosine proteins that we detected binding to SOCS6 include LIM domain proteins TES and PDLIM5 (ENH), both of which are involved in cell-cell and cell-matrix attachments (*277-279*), as well as MLLT4 (afadin, AF6), a Ras/Rap-regulated protein which regulates cell-cell junctions (*280*). Known tyrosine-phosphorylated SOCS2-binding proteins include the apical membrane protein Shroom1 (*281, 282*), CTNNB1 (β-catenin), which regulates cell-cell junctions (*283*), Crk, a signaling adaptor protein (*284, 285*), Ezrin, a protein that cross-links the plasma membrane to the active cytoskeleton (*286*), and the RTK EphA2 .

Visual inspection of the SOCS2 and SOCS6 binding partners indicated that both proteins interact with a wide variety of integral membrane proteins and membrane trafficking proteins, including Rab1a, solute carrier family proteins SLC25A11, SLC25A10 and SLC25A6, Sec61 translocon component SEC61A1, Golgi secretory carrier family protein SCAMP3, and the vacuolar ATPase subunit ATP6V1E1. In addition, SOCS6 interacted with four different 14-3-3 family proteins (YWHAQ, YWHAG, YWHAH) and known 14-3-3 interactor A-Raf. Both SOCS proteins bound nuclear proteins and mitochondrial proteins. These interactions suggest that SOCS2 and 6 can enter a variety of cell compartments and interact with shared and private partners.

To validate some of our candidate SOCS2-interacting proteins in a different cell type, we repeated the BioID assay, transiently expressing Myc-BirA, Myc-BirA-SOCS6, Myc-BirA-SOCS2, and a SH2 domain-inactivating mutant, BirA-SOCS2^{R73K}, in HeLa cells. Cell lysates were purified with streptavidin, and probed for GAPDH as a negative control and Cul5 as a positive control (Supplementary Fig S2). None of the BirA fusion proteins stimulated GAPDH

biotinylation. All three BirA fusion proteins stimulated Cul5 biotinylation, as expected. If MLN4924 was omitted, the Cul5 band became a doublet of Neddylated and Un-Neddylated Cul5 (Supplementary Fig S2). We then tested candidate SOCS2-interacting proteins that have been reported to be tyrosine phosphorylated, including Ezrin, Crk, IRS4, EphA2, and β-Catenin. All of these proteins were strongly biotinylated in cells expressing BirA-SOCS2^{WT} but not by BirA alone, BirA-SOCS2^{R73K} or BirA-SOCS6 (Supplementary Fig S2). This suggests that they are in close proximity to SOCS2 and their interaction requires tyrosine phosphorylation.

3.2.2 *SOCS2 SH2 domain binds to EphA2 through autophosphorylation sites in the kinase domain*

We chose the candidate CRL5^{SOCS2} substrate, EphA2, for further study. EphA2 is over-expressed in breast cancer cells and its over-expression correlates with decreased EfnA1 expression and loss of estrogen receptor expression (*252-254*). Increased EphA2 expression in Her2-positive breast cancer patients correlates with decreased disease-free and overall survival (*255*). Although several RTKs have been reported to interact with SOCS proteins, interaction between an Eph family receptor and a SOCS protein has not been reported previously.

BioID validation experiments confirmed that EphA2 is in close proximity to BirA-SOCS2, when phosphatases are inhibited (Figure 3.2a). To determine if EphA2 forms a stable complex with SOCS2 or SOCS6, we tested for co-precipitation with T7-tagged SOCS box mutants, SOCS2^{LCQQ} and SOCS6^{LCQQ}, which do not bind CRL5 and thus should not stimulate ubiquitylation and degradation (*167*). Endogenous EphA2 co-precipitated with T7-SOCS2^{LCQQ} but not T7-SOCS6^{LCQQ} (Figure 3.2b). These results suggest that EphA2 and SOCS2 are not only in close proximity but form a stable complex. To determine if Cul5 also bound EphA2, inactive Cul5 (T7-Cul5^{K724R}) and Myc-EphA2 were co-expressed in Cul5-depleted HeLa cells. T7-Cul5^{K724R} co-precipitated Myc-EphA2 (Figure 3.2c). This suggests that CRL5^{SOCS2} associates with EphA2 when tyrosine phosphorylation is artificially stimulated with phosphatase inhibitors.

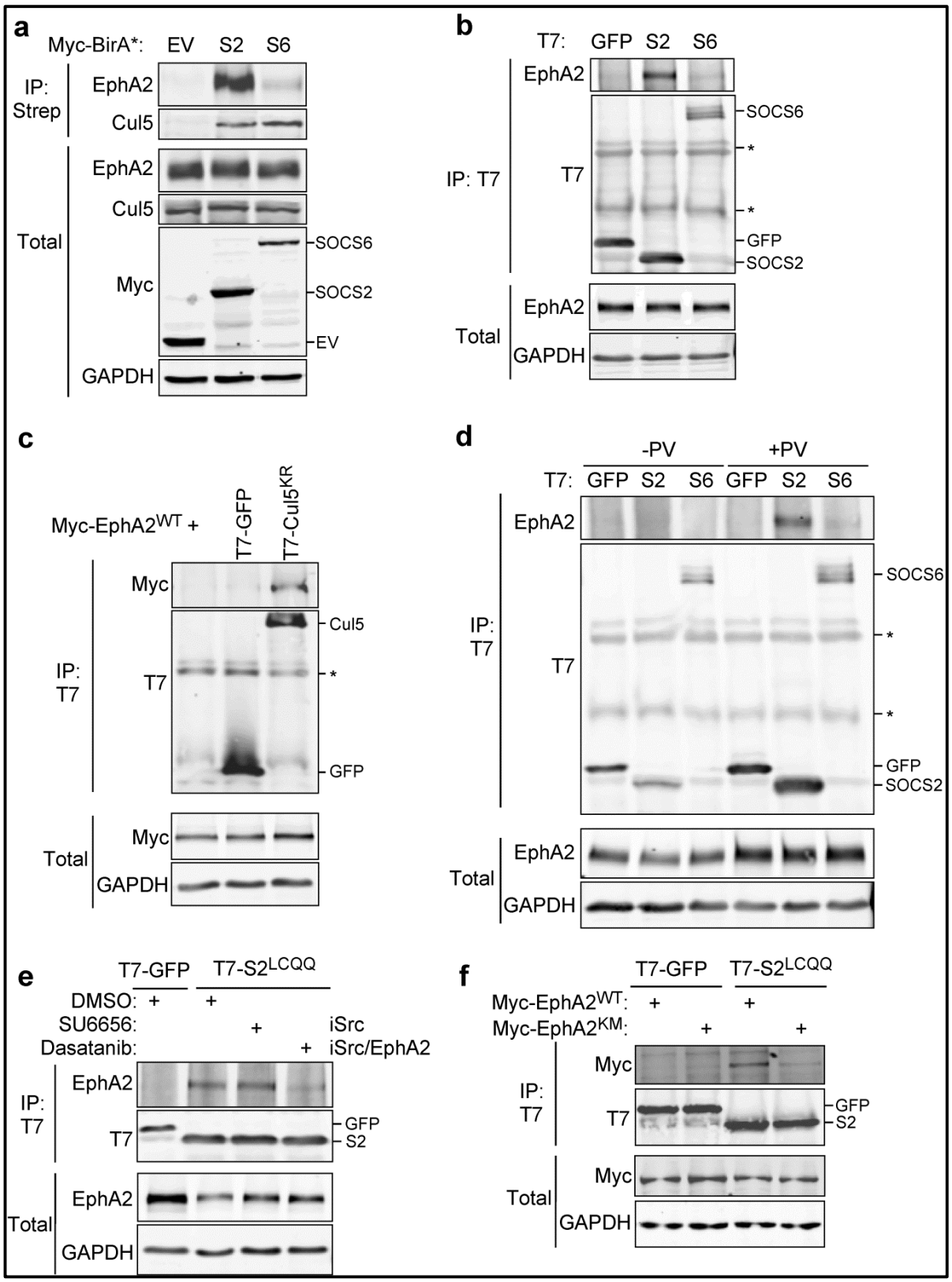
a
Myc-BirA*: EV S2 S6
IP: Strep
EphA2
Cul5
Total
EphA2
Cul5
Myc
GAPDH
SOCS6
SOCS2
EV
b
T7: GFP S2 S6
EphA2
IP: T7
T7
SOCS6
*
*
GFP
SOCS2
Total
EphA2
GAPDH
c
Myc-EphA2WT +
T7-GFP
T7-Cul5KR
Myc
IP: T7
T7
Cul5
*
GFP
Total
Myc
GAPDH
d
-PV
+PV
T7: GFP S2 S6 GFP S2 S6
EphA2
IP: T7
T7
SOCS6
*
*
GFP
SOCS2
Total
EphA2
GAPDH
e
T7-GFP
T7-S2LCQQ
DMSO: + +
SU6656: + iSrc
Dasatanib: + iSrc/EphA2
IP: T7
EphA2
T7
GFP
S2
Total
EphA2
GAPDH
f
T7-GFP
T7-S2LCQQ
Myc-EphA2WT: + +
Myc-EphA2KM: + +
IP: T7
Myc
T7
GFP
S2
Total
Myc
GAPDH

FIGURE 3.2 ENDOGENOUS EPHA2 FORMS A COMPLEX WITH SOCS2 AND CRL5, DEPENDENT ON EPHA2 KINASE ACTIVITY

(a) EphA2 is strongly biotinylated by BirA-SOCS2. 293T cells were transiently transfected with either Myc-BirA, Myc-BirA-SOCS2 or Myc-BirA-SOCS6. Twenty-four hours after transfection the cells were stimulated with 75 μM sodium orthovanadate, 1 μM MLN4924 and 2 mM Biotin for twenty-four hours. Following the stimulation, the cells were lysed and biotinylated proteins were purified using streptavidin agarose beads. The whole cell extract represents 1.5% of the lysate used for the pull down. (b) EphA2 binds T7-SOCS2. HeLa cells were transiently transfected with T7-GFP, T7-SOCS2^{LCQQ}, or T7-SOCS6^{LCQQ}. Twenty-four hours later the cells were stimulated with 75 μM vanadate, 1 μM MLN4924 for twenty-four hours. The cells were lysed and immunoprecipitated with antibody to T7 and protein A/G beads. The whole cell extract represents 5% of the lysate used for the pull down. (c) EphA2 binds to inactive Cul5 (Cul5^{K799R}). Cul5-depleted HeLa cells were transiently transfected with Myc-EphA2 and either T7-GFP or T7-Cul5^{K799R}. Twenty-four hours after transfection the cells were stimulated with 1 mM pervanadate for 30 min, lysed and immunoprecipitated with antibody to T7 and protein A/G beads. The whole cell extract represents 6% of the lysate used for the pull down. (d) Omission of PTP inhibitors prevented co-precipitation of T7-SOCS2^{LCQQ} with EphA2. HeLa cells were transiently transfected with T7-GFP, T7-SOCS2^{LCQQ}, or T7-SOCS6^{LCQQ}. Twenty-four hours after the transfection half of the cells were stimulated with 75 μM sodium orthovanadate or PBS for twenty-four hours. Cells were lysed and immunoprecipitated with antibody to T7 and protein A/G beads. The whole cell extract represents 7% of the lysate used for the pull down. (e) EphA2-SOCS2 interaction was inhibited by Dasatinib, but not by SU6656. HeLa cells were transiently transfected with T7-GFP or T7-SOCS2^{LCQQ}. Twenty-four hours after the transfection either DMSO, 1 μM SU6656 or 200 nM Dasatinib were added to the cells for two hours, then stimulated with 1 mM pervanadate for 30 min, lysed and immunoprecipitated with antibody to T7 and protein A/G beads. The whole cell extract represents 3.5% of the lysate used for the pull down. (f) Kinase-dead EphA2 (K646M) cannot bind to T7-SOCS2^{LCQQ} in EphA2-depleted cells. EphA2-depleted HeLa cells were transiently transfected with either Myc-EphA2^{WT} or Myc-EphA2^{K646M} and either T7-GFP or T7-SOCS2^{LCQQ}. Twenty-four hours after transfection the cells were stimulated with 1 mM pervanadate for 30 min, lysed and immunoprecipitated with antibody to T7 and protein A/G beads. The whole cell extract represents 3.5% of the lysate used for the pull down.

In all of our previous experiments the phosphotyrosine phosphatase inhibitors orthovanadate or pervanadate were added to the cells prior to lysis. To determine if phosphatase inhibition was required for EphA2-SOCS2 binding, we immunoprecipitated T7-SOCS2 in the presence and absence of inhibitors. EphA2 did not co-precipitate with T7-SOCS2^{LCQQ} when phosphatases were active, providing evidence that the interaction may require tyrosine phosphorylation (Figure 3.2d). EphA2 tyrosine phosphorylation may be catalyzed by EphA2, in an autophosphorylation reaction, or by cross-talk from another kinase. We used two approaches to test whether EphA2

activity is required for SOCS2 binding. First, we tested whether chemical inhibition of EphA2 would inhibit SOCS2 binding. A specific inhibitor of EphA2 is not available, so we used Dasatinib, which inhibits EphA2, Src and several other kinases (*287*). EphA2-SOCS2 interaction was inhibited by Dasatinib (Figure 3.2e) but not by SU6656, a semi-specific Src inhibitor. Second, we utilized a kinase dead version of Myc-EphA2, EphA2^{K646M}. When expressed in EphA2-depleted cells, Myc-EphA2^{K646M} was not phosphorylated on the Y588 autophosphorylation site and had decreased overall tyrosine phosphorylation (Supplementary Fig. S3). Myc-EphA2^{K646M} failed to bind to T7-SOCS2^{LCQQ} (Figure 3.2f), suggesting that EphA2 autophosphorylation is required to bind SOCS2.

To test whether EphA2-SOCS2 interaction involves the SH2 domain of SOCS2 we measured EphA2 binding to three SOCS2 mutants: an N-terminal deletion (ΔNT), an SH2 domain-inactivating mutant (R73K), and SOCS-Box deletion (ΔSB) (Figure 3.3a). These mutants were transiently expressed in HeLa cells. The Flag-SOCS2^{R73K} mutant failed to interact with endogenous EphA2, while Flag-SOCS ΔNT and ΔSB both bound strongly to EphA2 (Figure 3.3b). This suggests that the SOCS2 SH2 domain is binding to a phosphorylation site in EphA2.

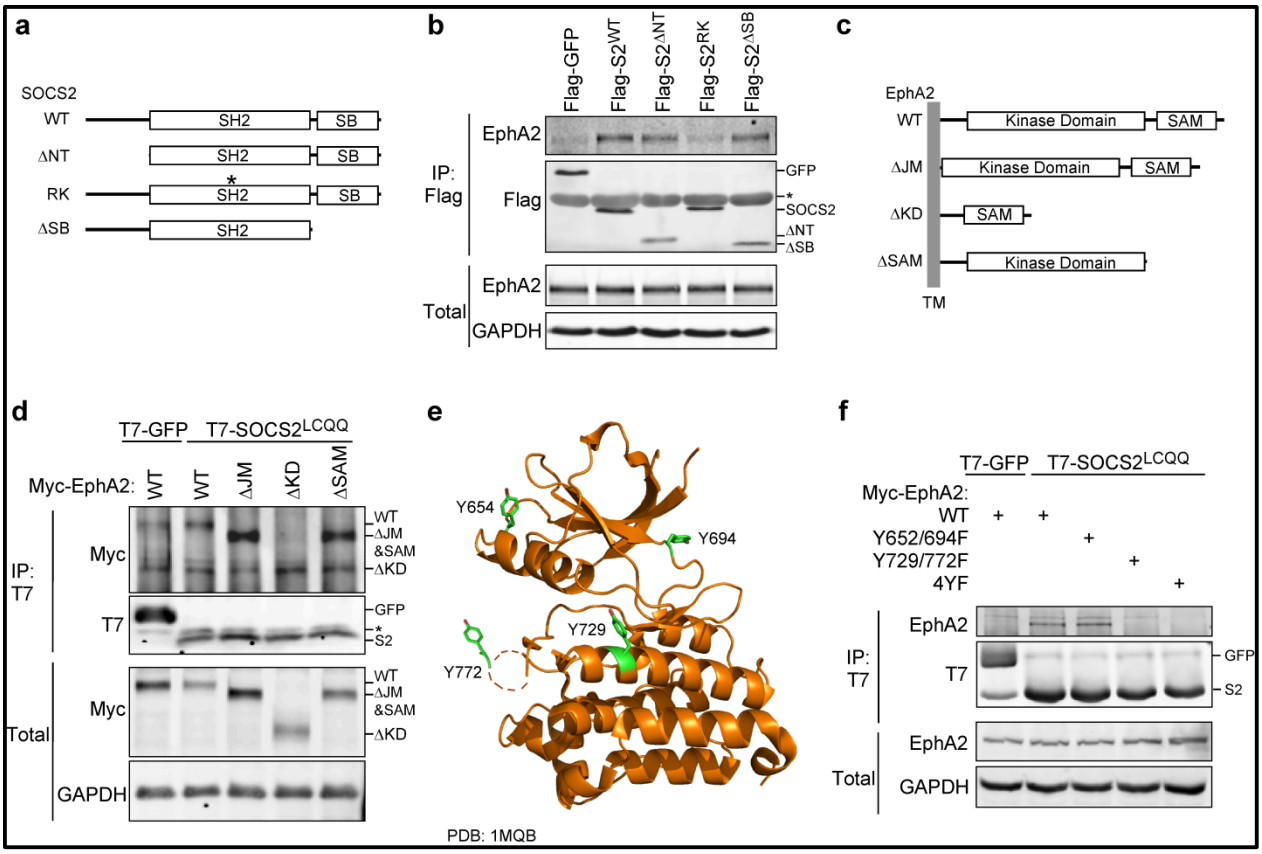

FIGURE 3.3 EPHA2 Y772 AND Y729 IN THE KINASE DOMAIN BIND TO THE SOCS2 SH2 DOMAIN

(a) Schematics of the SOCS2 deletion and point mutant constructs used: WT, full length SOCS2; ΔNT, lacking amino acids 1–37; RK, point mutation at R73 in the SH2 domain mutated to lysine; ΔSB, lacking amino acids 159–198. (b) The SOCS2 SH2 domain is required to bind EphA2. HeLa cells were transiently transfected with the indicated Flag-GFP or Flag-SOCS2 construct. Forty-eight hours after transfection the cells were stimulated with 1 mM pervanadate for 30 min, lysed and immunoprecipitated with Flag M2 magnetic beads. The whole cell extract represents 4% of the lysate used for the pull down. (c) Schematics depicting the cytosolic side of the EphA2 deletion mutants used: WT, full length EphA2; ΔJM, lacking amino acids 566–612; ΔKD, lacking amino acids 605–905; ΔSAM, lacking all amino acids after 886. (d) The EphA2 kinase domain is required for binding to SOCS2. HeLa cells were transiently transfected with T7-SOCS2^{LCQQ} and the indicated Myc-EphA2 construct. Forty-eight hours after transfection the cells were stimulated with 1 mM pervanadate for 30 min, lysed and immunoprecipitated with antibody to T7 and protein A/G beads. The whole cell extract represents 2% of the lysate used for the pull down. (e) Cartoon representation of the EphA2 kinase domain crystal structure (PDB: 1MQB)104, with Y654, Y694, Y729 and Y772 displayed as green sticks. (f) Y771 and Y729 in EphA2 are required for binding to SOCS2. 293T cells were transiently transfected with T7-SOCS2^{LCQQ} and either Myc-EphA2^{WT}, Myc-EphA2$^{Y652F/Y694F}$, Myc-EphA2$^{Y729F/Y772F}$, and Myc-EphA2$^{Y652F/Y694F/Y729F/Y772F}$. Twenty-four hours after transfection the cells were stimulated with 1 mM pervanadate for 30 min, lysed and immunoprecipitated with

antibody to T7 and protein A/G beads. The whole cell extract represents 7% of the lysate used for the pull down.

The Eph receptor cytoplasmic region can be divided into four domains: a juxtamembrane segment, a kinase domain, a sterile alpha motif (SAM), and a PDZ-binding motif (*288-290*). To narrow down the SOCS2 binding site in EphA2, we deleted the EphA2 juxtamembrane region (ΔJM), kinase domain (ΔKD), and SAM domain and PDZ-binding motif (ΔSAM) (Figure 3.3c). T7-SOCS2^{LCQQ} bound to the Myc-EphA2$^{\Delta JM}$ and Myc-EphA2$^{\Delta SAM}$ but not to Myc-EphA2$^{\Delta KD}$ (Figure 3.3d), suggesting that the SOCS2 binding site is located in the kinase domain of EphA2 and the JM and SAM regions are not required.

The EphA2 kinase domain contains eleven tyrosines. We mutated each of the eleven tyrosines individually to phenylalanine and tested binding to T7-SOCS2^{LCQQ} (Supplementary Fig. S4 a-c). SOCS2 bound to each single mutant, so we tested the effects of double (Y652/694F & Y729/772F) and quadruple (4YF) mutations at four reported autophosphorylation sites (*291*) (Figure 3.3e). The Y729/772F and 4YF mutants both failed to interact while WT and Y652/694F EphA2 bound to T7-SOCS2^{LCQQ} (Figure 3.3f). This suggests that both Y729 and Y772 are required for binding. Y772 is in the kinase activation loop, raising the possibility that the double mutant may have reduced autophosphorylation at multiple sites, leading to decreased binding. To exclude this possibility, we compared the phosphorylation of the single Y772F and double Y729/772F mutants (Supplementary Fig. S4d). Both mutants were phosphorylated similarly, but only the single Y772F mutant binds SOCS2, suggesting that both Y772 and Y729 are required for binding.

3.2.3 *EfnA1 induces EphA2 binding to SOCS2*

To test whether SOCS2 binds to EphA2 under physiological conditions, we stimulated cells with EfnA1-Fc, a dimer of EfnA1. HeLa cells were transfected with T7-SOCS2^{LCQQ}, serum starved, and incubated with either EfnA1-Fc or with control Fc for various times. T7-SOCS2^{LCQQ} was immunoprecipitated and associated EphA2 was detected by immunoblotting. EfnA1-Fc but not Fc stimulated co-precipitation of EphA2 with SOCS2, with maximal binding 90-120 min after stimulation (Figure 3.4a, b).

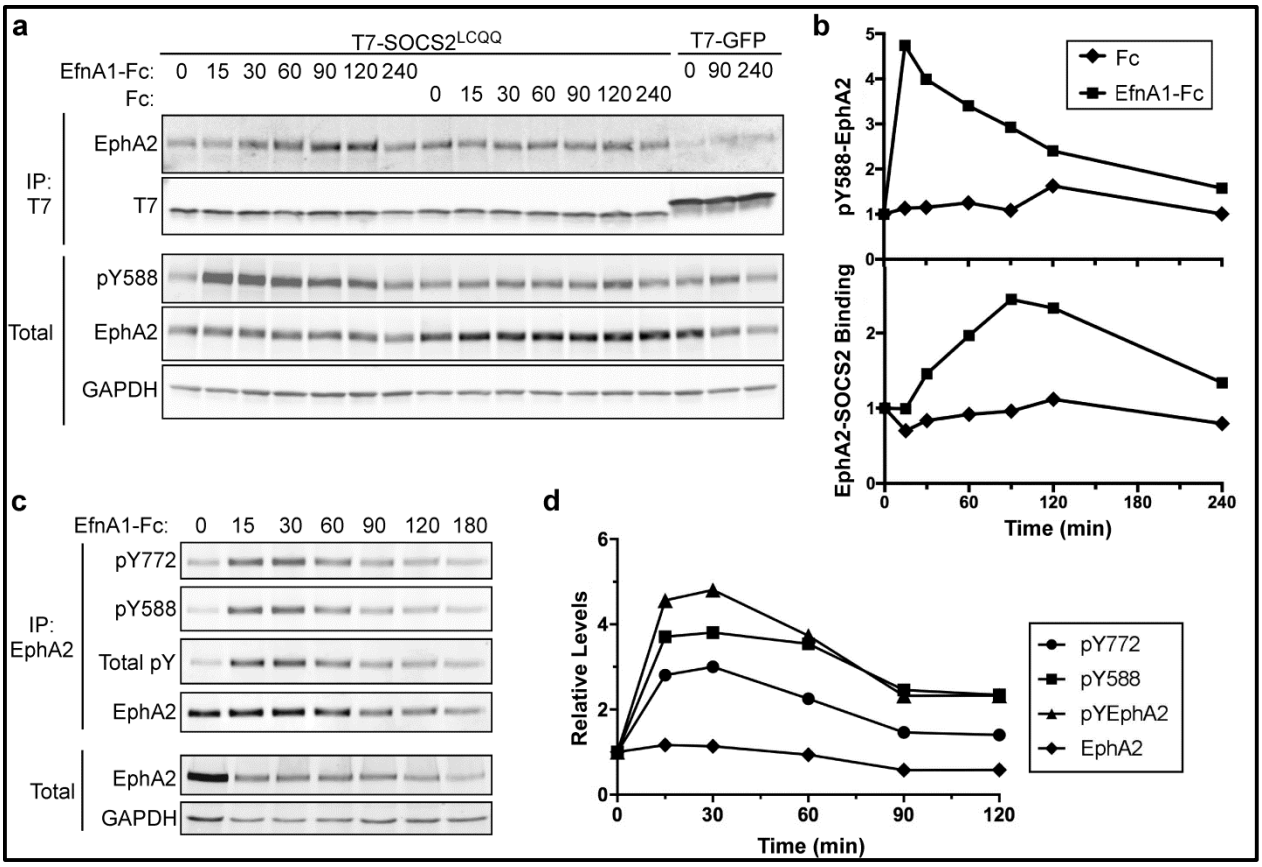

FIGURE 3.4 EPHA2 ACTIVATION BY EFNA1 STIMULATES SOCS2-EPHA2 BINDING AFTER A DELAY

(a) EfnA1 stimulates EphA2 binding to SOCS2 and the binding kinetics lag behind EphA2 phosphorylation. HeLa cells were transiently transfected with T7- SOCS2^{LCQQ} or T7-GFP. Twenty-four hours after transfection the cells were starved in DMEM 0.5% BSA 10 mM HEPES for 4 hr. EfnA1-Fc or Fc (1 µg/mL) was added to cells, cells were then lysed at the indicated time, immunoprecipitated with antibody to T7 and then anti-mouse IgG Sepharose beads. The whole cell extract represents 6% of the lysate used for the pull down. (b) pY588-EphA2-peaks 15 min after EfnA-Fc addition and binding peaks 120 min after EfnA-Fc addition. Western blot images from Fig. 5a were analyzed using the ImageQuantTL software. Samples were normalized to time zero. (c) pY-EphA2, pY771, pY588 EphA2 display similar phosphorylation dynamics. HeLa cells were starved in DMEM 0.5% BSA 10 mM HEPES for 4 hr followed by 1 µg/mL EprinA1-Fc stimulation. Cells were lysed at the indicated time-points, immunoprecipitated with antibody to EphA2 and A/G agarose beads. The whole cell extract represents 12% of the lysate used for the pull down. (d) Quantification of EphA2 phosphorylation after EfnA1-Fc stimulation. Western blot images from the immunoprecipitation were analyzed using the ImageQuantTL software and normalized to time zero.

We tested whether SOCS association paralleled EphA2 phosphorylation by immunoblotting. Unfortunately, a phosphoepitope antibody to pY772 bound a co-migrating protein; however, an antibody to the major juxtamembrane autophosphorylation site, pY588 was specific (Supplementary Fig. S5). Addition of EfnA1-Fc but not Fc stimulated pY588-EphA2 phosphorylation, with maximal phosphorylation 15-30 min after stimulation (Figure 3.4a, b). Together this suggested that EfnA1 stimulates EphA2-SOCS2 association, but binding is delayed relative to EphA2 autophosphorylation at pY588.

We considered that EphA2-SOCS2 binding might be delayed because phosphorylation of the SOCS binding site, Y772, may also be delayed. The pY772 antibody is fairly specific for phosphorylation at Y772 when it is used on EphA2 immunoprecipitates (Supplementary Fig S5). Therefore, we immunoprecipitated EphA2 at various times after EfnA1-Fc stimulation and probed immunoblots with antibodies to pY772, pY588 and total phosphotyrosine (Figure 3.4c). Phosphorylation of all sites peaked around 15-30 min (Figure 3.4d). Taken together, these results indicate that SOCS2 binding is increasing at the same time as pY772 phosphorylation is decreasing. This was surprising, and suggested additional regulation of EphA2-SOCS2 interaction.

3.2.4 *SOCS2 associates with internalized EphA2*

Efn's activate Eph's at the cell surface and then induce receptor internalization (*292*). We wondered whether the delayed binding of SOCS2 to EphA2 reflects a dependence on EphA2 internalization. We followed EphA2 internalization using MDA-MB-231 cells, which have high levels of EphA2 and low levels of EfnA1 (Supplementary Fig. S6 a). Flag-HA-SOCS2^{LCQQ} was stably expressed in these cells. To inhibit internalization and synchronize receptor traffic, cells were pre-incubated with EfnA1-Fc in the cold for 1 hr. Under these conditions, EphA2 was mostly on the plasma membrane and Flag-HA-SOCS2^{LCQQ} was diffusely distributed in the cytoplasm (Figure 3.5a). Unbound EfnA1-Fc was then washed off and the cells were rapidly warmed to 37°C to induce internalization. EphA2 rapidly translocated into intracellular vesicles, where it co-localized extensively with SOCS2 (Figure 3.5a). Co-localization was maximal 30 to 120 min after warming (Figure 3.5b). Immunoblotting showed that the receptor becomes

phosphorylated during the pre-incubation with EfnA1-Fc at 4°C and is progressively dephosphorylated after warming (Supplementary Fig. S6 b). These results suggest that SOCS2 does not bind to active EphA2 at the plasma membrane and only associates with EphA2 after internalization, when EphA2 phosphorylation is declining.

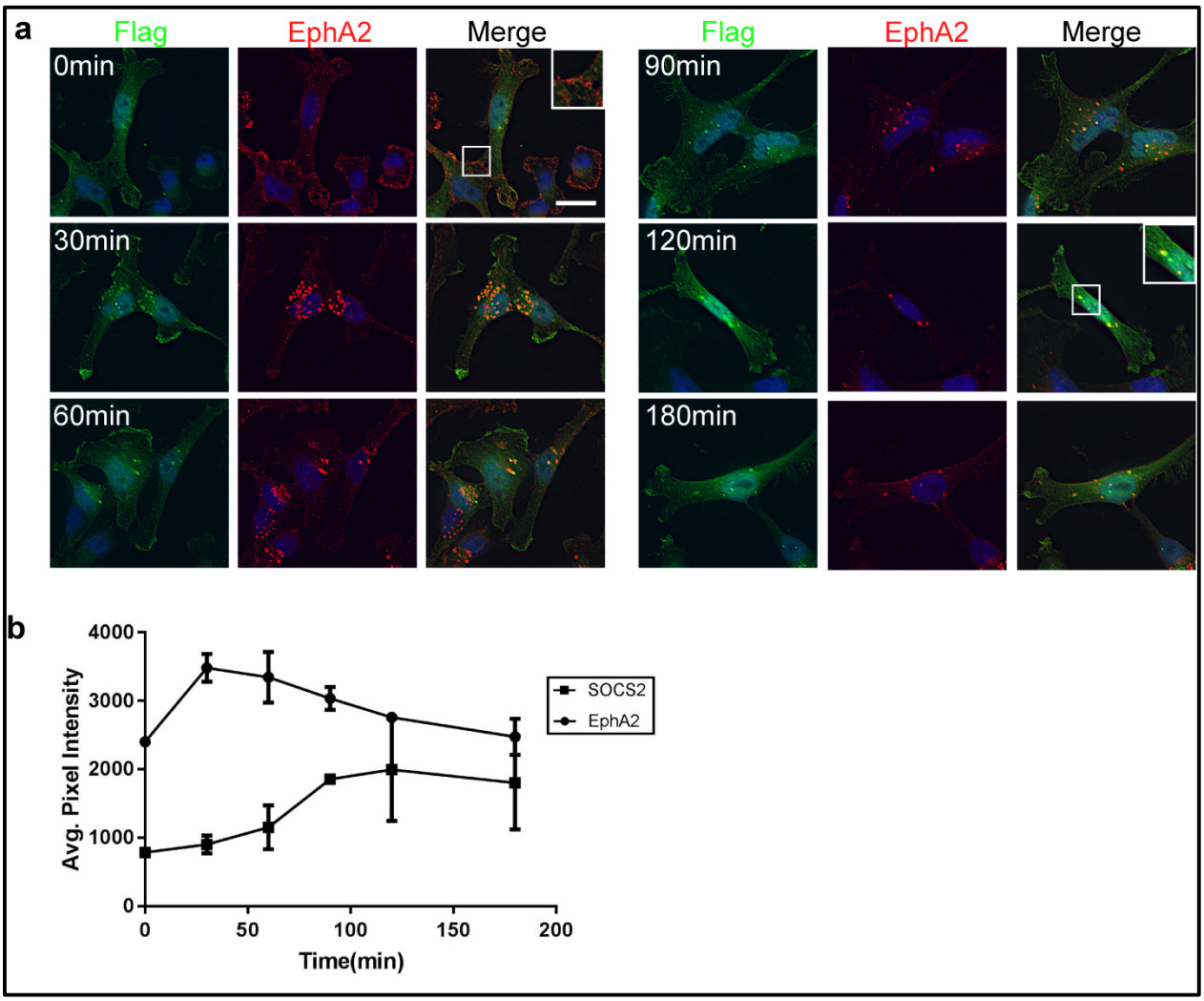

FIGURE 3.5 SOCS2 ASSOCIATES WITH INTERNALIZED EPHA2

(a) EfnA1 stimulates EphA2 internalization and association of SOCS2^{LCQQ} with endosomes containing EphA2. Flag-HA-SOCS2^{LCQQ} was stably expressed in MDA-MB-231 cells. Cells were starved in DMEM 0.5% BSA 10 mM HEPES for 4 hr followed by a 1 hr incubation with EfnA1-Fc (1 µg/mL) on ice. The ligand was washed off and the cells were placed at 37 °C for the indicated amount of time before being fixed. Fixed and permeabilized cells were stained with anti-Flag M2, anti-EphA2 and appropriate secondary antibodies. Images are a single Z-section. Exposure and brightness/contrast are the same for all pictures. Scale bar: 20 µm. (b) EphA2-SOCS2 co-localization is maximal 120 min after EfnA1-Fc addition. EphA2 vesicles were identified using the find object function in the Volocity Software. The intensities of

EphA2 (circles) and SOCS2 (square) in these vesicles were measured. Points are mean and standard error of the mean of two biological independent experiments.

We next tested whether SOCS2 relocalization required EphA2 activation and the SOCS2 SH2 domain. SOCS2 did not localize to endosomes in cells stimulated with Fc, suggesting that EphA2 activation is required for relocalization (Figure 3.6a, Flag-HA-SOCS2^{LCQQ} + Fc). Relocalization did not require CRL5 binding (compare Flag-HA-SOCS2^{WT} and Flag-HA-SOCS2^{LCQQ}, Figure 3.6a). However, SH2 domain mutant Flag-HA-SOCS2^{R73K} did not re-localize, suggesting that SH2 domain-phosphotyrosine interaction is involved (Figure 3.6a). The vesicles that contain EphA2 at 120 min also contain EfnA1-Fc, suggesting that the ligand has not been degraded (Supplementary Fig. S7). The SOCS2/EphA2/EfnA1-Fc vesicles are surrounded by the endosomal markers EEA1 and LAMP1 (Figure 3.6b and c). This suggests that EphA2 receptor and EfnA1-Fc ligand are internalized and remain together, and the receptor traffics through the endosomal system where it associates with SOCS2. The presence of both EEA1 and LAMP1 on SOCS2/EphA2/EfnA1-Fc vesicles was surprising because they mark early and late endosomes, respectively (*33, 293*). However, EphA2 is degraded slowly after EfnA1-Fc stimulation, (*52, 287, 294*) so these endosomes may be still maturing from early endosomes into a multi-vesicular body. Altogether, these results suggest that EfnA1-Fc stimulation induces EphA2 phosphorylation and internalization, and SOCS2 only binds to autophosphorylated EphA2 after internalization to endosomes.

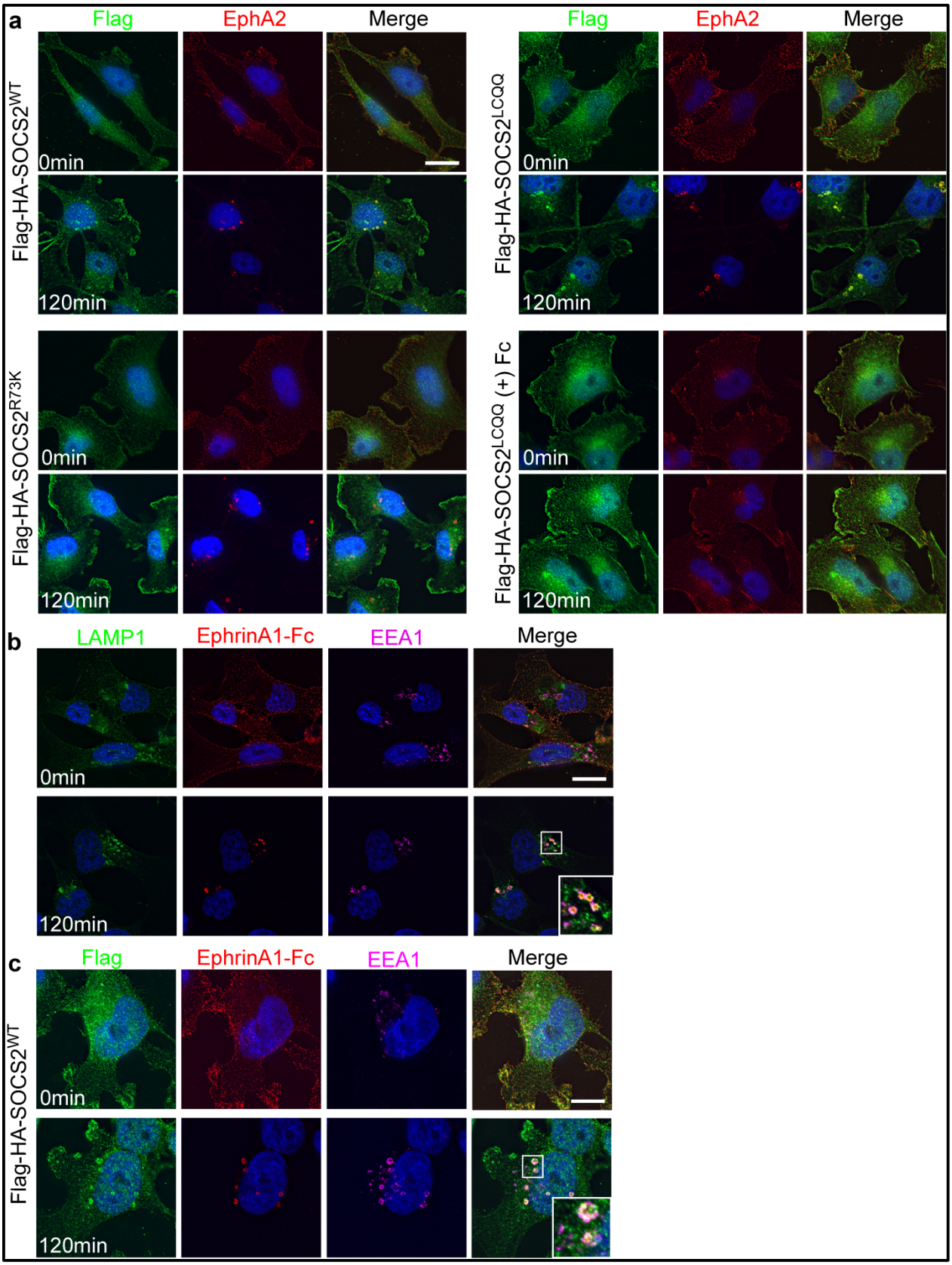
a
Flag
EphA2
Merge
Flag-HA-SOCS2WT
Flag-HA-SOCS2LCQQ
Flag-HA-SOCS2R73K
Flag-HA-SOCS2LCQQ (+) Fc
0min
120min
b
LAMP1
EphrinA1-Fc
EEA1
Merge
c
Flag
EphrinA1-Fc
EEA1
Merge
Flag-HA-SOCS2WT

FIGURE 3.6 REQUIREMENT FOR SOCS2-EPHA2 CO-LOCALIZATION

(a) SOCS2-EphA2 co-localization on endosomes requires EfnA1 stimulation and SOCS2-EphA2 interaction, but not SOCS2-CRL5 interaction. Flag-HA-SOCS2^{WT} and Flag-HA-SOCS2^{LCQQ} but not Flag-HA-SOCS2^{R73K} form puncta 120 min after stimulation with EfnA1-Fc but not Fc. The Flag-HA-SOCS2 puncta co-localize with EfnA1-Fc. The indicated Flag-HA-SOCS2 constructs were stably integrated into MDA-MB-231 cells. Cells were starved in DMEM 0.5% BSA 10 mM HEPES for 4 hr followed by a 1 hr incubation with EfnA1-Fc or Fc (1 μg/mL) on ice. The ligand was washed off and the cells were placed at 37 °C for the indicated times and then fixed. Fixed and permeabilized cells were stained with anti-Flag M2, anti-EphA2 and appropriate secondary antibodies. Scale bar: 25 μm. (b) Endosomes that contain EfnA1-Fc are associated with LAMP1 and EEA1. Cells were starved and stimulated as in (a). Fixed and permeabilized cells were stained with anti-LAMP1, anti-Fc, anti-EEA1. Scale bar: 15 μm. (c) SOCS2 associates with EEA1-positive endosomes that contain EfnA1-Fc. Cells were starved and stimulated as in (a). Fixed and permeabilized cells were stained with anti-Flag M2, anti-Fc, anti-EEA1. Scale bar: 15 μm. In all cases, images are maximum intensity projections of 3 Z-sections. The scaled intensity is unequal in some images to allow for visualization. See methods for details.

3.2.5 *SOCS2 overexpression induces EfnA1 expression and down regulates EphA2*

The delayed binding of SOCS2 to EphA2 at late endosomes led us to hypothesize that CRL5^{SOCS2} may catalyze EphA2 ubiquitylation after it has been internalized, providing a signal for incorporation into intraluminal vesicles and targeting for lysosomal degradation. To test whether SOCS2 regulates EphA2 degradation, we measured endogenous EphA2 levels in cells co-overexpressing SOCS2 and ElgB/C, which stabilizes SOCS2 (*94*). Over-expressed SOCS2^{WT} decreased EphA2 protein but not RNA, suggesting that degradation may be increased (Figure 3.7a). To test whether SOCS2-induced EphA2 down-regulation involved CRL5, we over-expressed SOCS2^{LCQQ}, which does not interact with CRL5. This mutant was less effective than SOCS2^{WT} in down-regulating EphA2 (Figure 3.7a), but it was also under-expressed relative to SOCS2^{WT}, presumably because SOCS2^{LCQQ} is not stabilized by ElgB/C (*167*). As an alternative approach, we tested whether SOCS2^{WT} would induce EphA2 down-regulation in Cul5-depleted cells. EphA2 levels declined when SOCS2^{WT} was expressed even when Cul5 was absent (Figure 3.7b). This suggests that SOCS2 targets EphA2 for degradation independent of CRL5.

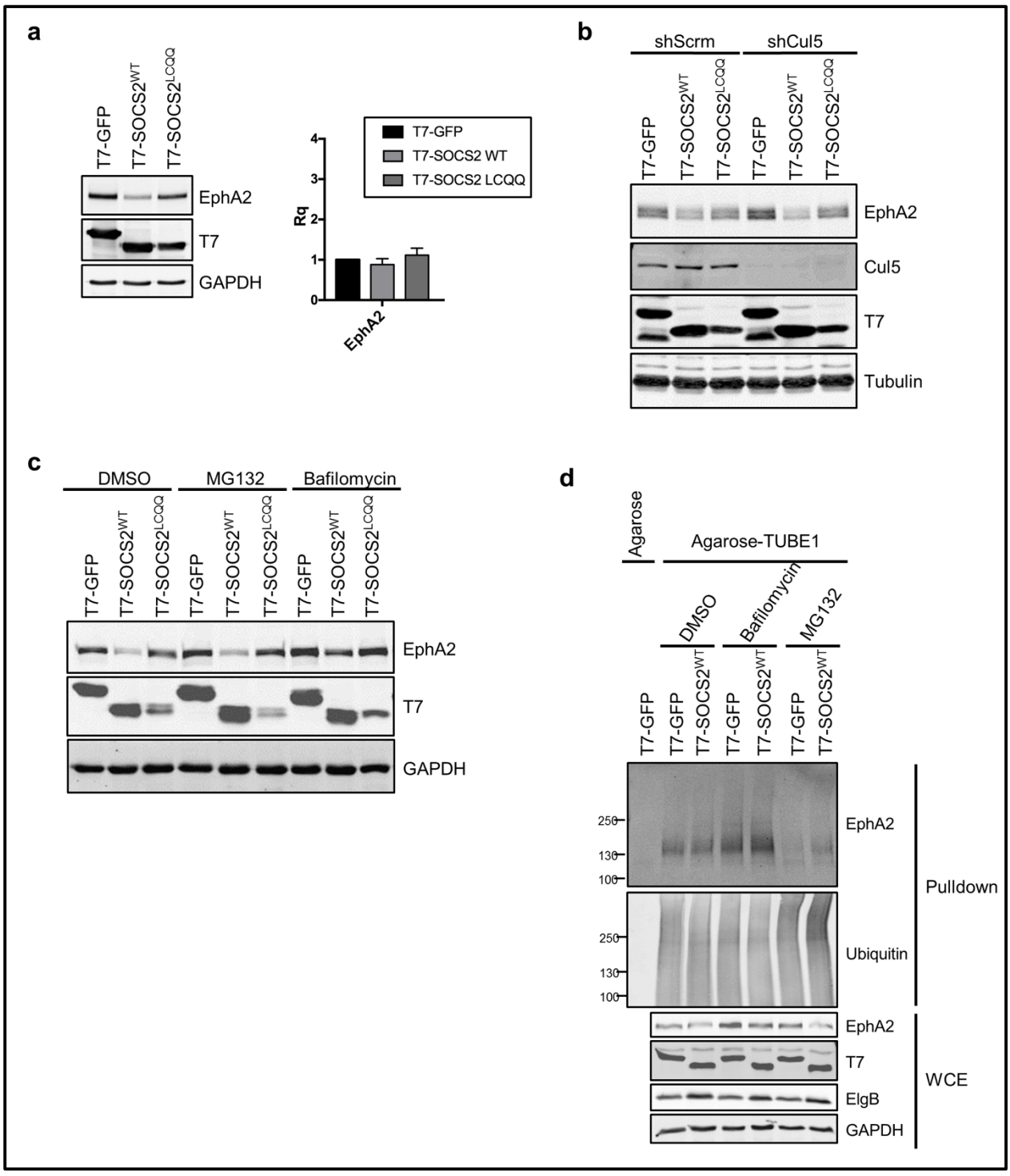

FIGURE 3.7 SOCS2^{WT} OVER-EXPRESSION DOWN-REGULATES EPHA2 VIA THE LYSOSOME

(a) SOCS2^{WT} but not SOCS2^{LCQQ} overexpression decreases EphA2 protein level. HeLa cells were transiently transfected with ElgB/C and either T7-GFP, T7-SOCS2^{WT}, or T7-SOCS2^{LCQQ}. Total protein or RNA was harvested from the cells 48 hours after transfection. Proteins were analyzed by Western blotting. RNA was quantified using the

ΔΔCt method with SYBR Green qPCR. Bars are mean and standard deviation of three independent experiments. (b) SOCS2 over-expression stimulates EphA2 down-regulation independent of CRL5. Control or Cul5-depleted HeLa cells were transiently transfected with ElgB/C and either T7-GFP, T7-SOCS2^{WT}, or T7-SOCS2^{LCQQ}. Forty-eight hours after transfection cell lysate was harvested and analyzed by Western blotting. (c) Lysosomal but not proteasomal inhibitors block the SOCS2-induced decrease in EphA2. HeLa cells were transiently transfected with ElgB/C and either T7-GFP, T7-SOCS2^{WT}, or T7-SOCS2^{LCQQ}. Forty-eight hours after transfection, DMSO, Bafilomycin or MG132 was added to the cells for a further 24 hr before lysis and analysis by Western blotting. (d) SOCS2 overexpression stimulates EphA2 ubiquitylation, that is further increased by lysosome, but not proteasome, inhibitors. HeLa cells were transiently transfected with ElgB/C and either T7-GFP, T7-SOCS2^{WT}, or T7-SOCS2^{LCQQ}. Forty-eight hours after transfection, DMSO, Bafilomycin or MG132 was added to the cells for 4 hr before lysis. Lysates were incubated with agarose or agarose-TUBE1 beads and ubiquitylated proteins were analyzed by Western blotting. The whole cell extract represents 2% of the lysate used for streptavidin pull down.

To understand the mechanism by which SOCS2 down-regulates EphA2, we tested whether SOCS2-induced EphA2 down-regulation is inhibited by proteasomal or lysosomal inhibitors, MG132 and Bafilomycin, respectively. EphA2 levels increased when the lysosome but not proteasome was inhibited, in control cells and cells over-expressing SOCS2, suggesting that SOCS2 increases the basal rate of lysosomal degradation of EphA2 (Figure 3.7c). To determine if SOCS2 stimulates EphA2 ubiquitylation, we isolated ubiquitylated proteins using Tandem Ubiquitin Binding Entities (TUBEs) (*295*). Total protein ubiquitylation was not affected by lysosomal or proteasomal inhibitors or SOCS2 over-expression, so any differences in EphA2 abundance in the pulldowns can be attributed to changes in EphA2 ubiquitylation state (Figure 3.7d). EphA2 ubiquitylation was increased by Bafilomycin, consistent with destruction of ubiquitylated EphA2 by the lysosome. EphA2 ubiquitylation increased further when SOCS2^{WT} was over-expressed, despite a decrease in total EphA2 levels (Figure 3.7d). Curiously, EphA2 ubiquitylation was reduced by MG132, potentially because MG132 depletes the free ubiquitin pool available for K63-linked ubiquitylation or multi-monoubiquitylation of proteins destined for lysosomal degradation (*23, 296*). These results suggest two things: first, that EphA2 is constitutively ubiquitylated and degraded by the lysosome, and second, that SOCS2^{WT} overexpression stimulates muti-monoubiquitylation or polyubiquitylation and lysosomal degradation of EphA2.

SOCS2 may induce EphA2 turnover by a variety of indirect mechanisms. One possibility is that SOCS2 might increase production of EfnA1, thereby stimulating EphA2 lysosomal degradation. To assay EfnA1 gene expression, we measured EfnA1 mRNA levels in control and SOCS2 over-expressing cells. Remarkably, EfnA1 mRNA was strongly induced by SOCS2 over-expression (Figure 3.8a). This suggests that SOCS2 may down-regulate EphA2 indirectly, by inducing EfnA1 and stimulating EphA2 lysosomal degradation. To check if EfnA1 is required for SOCS2-induced EphA2 down-regulation, we knocked down EfnA1 in control and SOCS2-expressing cells. Indeed, the EphA2 protein to RNA ratio was negatively correlated with the level of EfnA1 expression (Figure 3.8b-d). Taken together, these results are consistent with a model in which SOCS2 over-expression induces EfnA1 gene expression, and autocrine stimulation by EfnA1 increases ubiquitylation and lysosomal turnover of EphA2, potentially by $CRL5^{SOCS2}$-independent mechanisms.

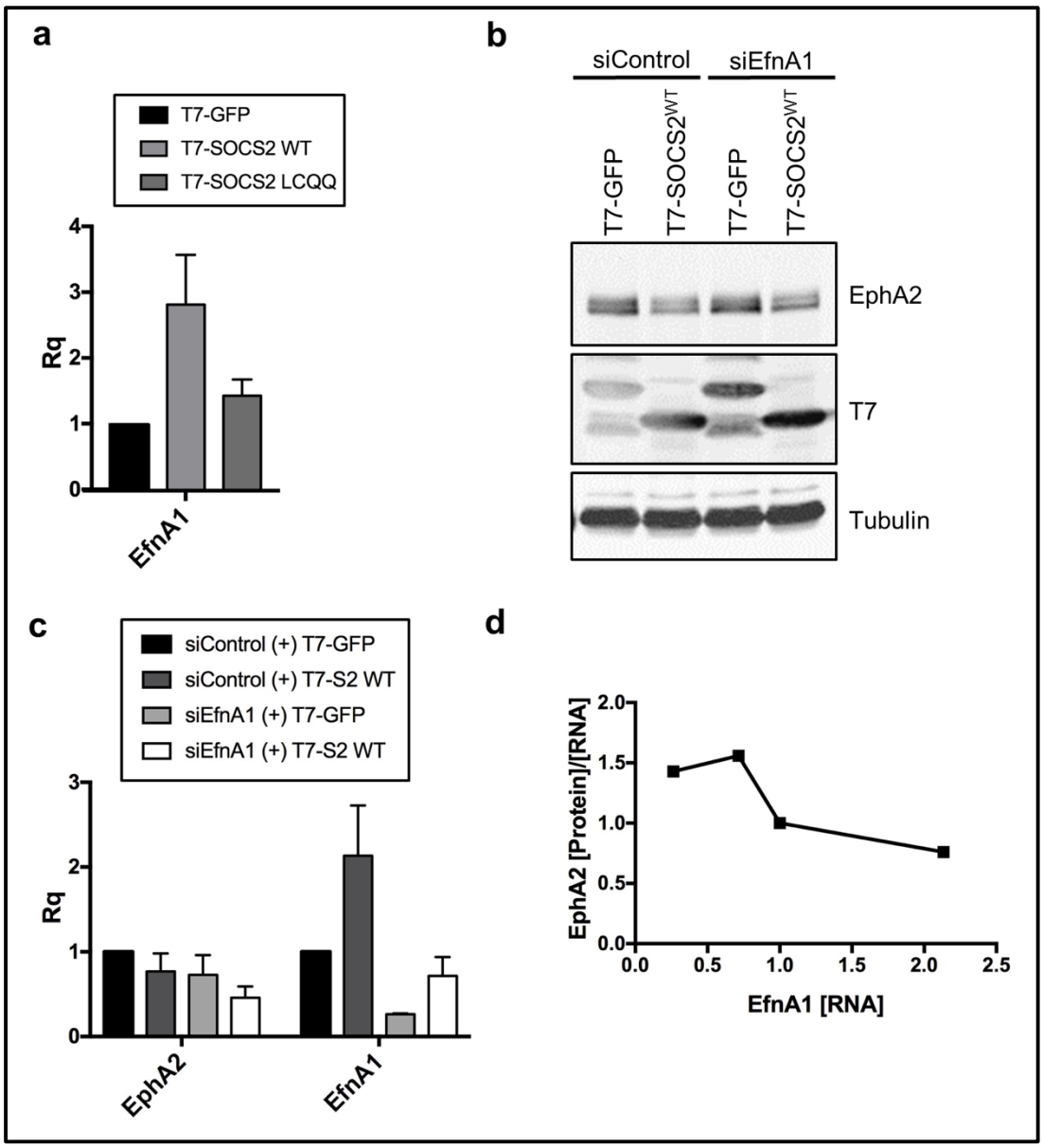

FIGURE 3.8 ENDOGENOUS ENFA1 PROMOTES TURNOVER OF EPHA2

(a) SOCS2^{WT} but not SOCS2^{LCQQ} overexpression induces EfnA1 expression. HeLa cells were transiently transfected with ElgB/C and either T7-GFP, T7-SOCS2^{WT}, or T7-SOCS2^{LCQQ}. Total protein or RNA was harvested from the cells 48 hours after transfection. Proteins were analyzed by Western blotting. RNA was quantified using the ΔΔCt method with SYBR Green qPCR. Bars are mean and standard deviation of three independent experiments. These are the same RNA samples analyzed in Fig. 7a. (b–d) EfnA1-depletion inhibits EphA2 down-regulation in cells overexpressing SOCS2^{WT}. HeLa cells were transfected with the indicated siRNA, allowed to recover for 36 hours, then transfected again with the same siRNA. One day later, the cells were transfected with ElgB/C and either T7-GFP or T7-SOCS2^{WT}. Forty-eight hours later, total protein or RNA was harvested. (b) Protein was analyzed by Western blotting. (c) RNA was quantified using SYBR Green qPCR and the ΔΔCt method. Bars are mean and standard

deviation of two biological independent experiments. (d) EphA2 protein to RNA ratio is inversely correlated with the amount of EfnA1 RNA.

3.3 DISCUSSION

SOCS proteins inhibit phosphotyrosine signaling in immune cells by several mechanisms, including directly inhibiting tyrosine kinases, masking phosphorylation sites, and recruiting CRL5 to ubiquitylate and ultimately degrade phosphorylated targets (*297*). To gain insights into SOCS functions in non-immune cells, we sought new SOCS binding proteins by performing the first large scale affinity enrichment proteomics screens of SH2 domain-containing SOCS proteins. We detected 48 proteins that interacted with SOCS2 and 74 proteins that interacted with SOCS6. We found known interaction partners, including proteins involved in ubiquitylation or the proteasome, the CRL5 complex, and RNA polymerase II. One unresolved mystery is how SOCS2 and SOCS6 bind to proteins such as RNA pol II, that have their own substrate receptors (*274*). Of the new SOCS2/6-interacting proteins detected, only a few were annotated as tyrosine kinase substrates and few were clearly signaling proteins. Notably, both SOCS2 and 6 interacted with a variety of transmembrane proteins and vesicle traffic proteins, perhaps indicating a role for SOCS proteins in protein traffic.

We chose a set of SOCS2-interacting proteins previously reported to be tyrosine phosphorylated for functional validation. These proteins (Ezrin, Crk, IRS4, EphA2 and β-catenin) were confirmed to interact with SOCS2 and not SOCS6 in another cell type. Interactions were diminished when the SOCS2 SH2 domain was inactivated, suggesting that the interaction is mediated by phosphotyrosine. However, many of the other proteins we detected are not known to be tyrosine phosphorylated. Binding of these proteins may involve the divergent N-terminal regions of SOCS2 and SOCS6. SOCS6 in particular has a very long N-terminus (384 amino acids). Some of the non-phosphorylated proteins identified in our screen may bind to the N-termini of SOCS2 and SOCS6 and further study of the interactions will help elucidate the function of this region. The novel hits that we identified may help define additional biological roles for SOCS proteins in epithelial cell biology.

We focused on EphA2 as a representative of a group of tyrosine-phosphorylated proteins that interact with SOCS2 and each other (according to the STRING database), suggesting SOCS2 SH2-phosphotyrosine interactions. Indeed, EphA2-SOCS2 binding requires the SOCS2 SH2 domain, EphA2 autophosphorylation in the kinase domain, and two kinase domain tyrosine residues, Y772 and Y729. Y772 is the activation loop tyrosine - a well-known EphA2 autophosphorylation site. This region is disordered when EphA2 is active and may be accessible to the SOCS2 SH2 domain (*227, 228*). Y729 was once identified as an autophosphorylation site (*291*) but this may not be the case (*298*). It is possible that Y729 plays a structural role in binding SOCS2. The results suggest that phosphorylation of Y772 by EphA2 creates a binding site for SOCS2, with contribution from Y729.

SOCS2 binding to EphA2 was stimulated by the EphA2 ligand EfnA1, suggesting it may be physiologically important. Curiously, however, EphA2-SOCS2 interaction did not parallel EphA2 phosphorylation. Rather, EphA2-SOCS2 binding lagged behind EphA2 phosphorylation by 30-60 min. Delayed binding of RTKs to SOCS proteins has been observed before. SOCS2 binds to IGF-IR 40 min after IGF-I stimulation (*154*), which is 20 min after phosphorylation has peaked (*299*). Kit ligand activates Kit phosphorylation at 5 min, but SOCS6 binding to Kit is maximal 30-60 min later (*162*). This suggests that other factors may regulate RTK-SOCS binding in cells. For example, a SOCS protein may be unable to bind an RTK soon after activation due to masking of the binding site by other molecules. Alternatively, there may be delayed activation, recruitment or induction of other factors that are needed to stabilize the RTK-SOCS interaction. In the case of SOCS2 and EphA2, we found that delayed binding may reflect a requirement for ligand-stimulated EphA2 internalization. SOCS2 and EphA2 did not co-localize significantly at the cell surface, but co-localized on endosomes after EfnA1-Fc stimulation. These endosomes persisted for up to 2 hours and contained EfnA1-Fc and EphA2 together with EEA1 and LAMP1, markers for early and late endosomes. This suggests that SOCS2-EphA2 association may be blocked at the plasma membrane or stimulated on endosomes. If the latter, then SOCS2 binding to EphA2 may be stabilized by secondary interactions between SOCS2 and endosomal membranes, perhaps through binding interactions we detected with endosomal proteins such as the vacuolar ATPase and SCAMP3. There may also be avidity effects: EphA2 is much more concentrated on endosomal membranes after

internalization than on the plasma membrane, and the increased density of EphA2 in endosomes may decrease the SOCS2 dissociation rate and increase the effective avidity.

EphA2 undergoes constitutive endocytosis and rapid recycling back to the surface regardless of ligand stimulation (*300*). This constitutively internalized EphA2 may be spontaneously activated at the surface, perhaps by crowding, and is dephosphorylated in Rab11-positive endosomes before recycling back to the surface (*52, 300*). When ligand is added, some of the internalized EphA2 is diverted to the lysosome (*48*). We found that inhibiting the lysosome but not the proteasome increased ubiquitylation of EphA2 and the total level of EphA2, suggesting that a portion of EphA2 is constitutively targeted to the lysosome for degradation. Since HeLa cells express endogenous EfnA1, this constitutive turnover may be due to autocrine activation of EphA2 by EfnA1 made in the same cell or neighboring cells. When SOCS2 was over-expressed, endogenous EfnA1 production increased, as did the ubiquitylation and lysosomal degradation of EphA2. Indeed, SOCS2-induced down-regulation of EphA2 required EfnA1. Moreover, the SOCS2-stimulated degradation of EphA2 was Cul5-independent. This suggests that the effect of over-expressed SOCS2 on EphA2 is quite indirect, involving induction of EfnA1 and increased EfnA1-induced internalization and degradation of EphA2.

EphA2 has been reported to bind to two additional E3 ubiquitin ligases: Cbl and UBE4A-SLAP. Cbl binds to activated EphA2 and Cbl over-expression increases ubiquitylation and degradation of over-expressed EphA2 (*52, 245, 246*). The adaptor protein Src-like adaptor protein (SLAP) binds to Y594 in the EphA2 juxtamembrane region, which then recruits to the E3 Ub ligase UBE4A (*249*). UBE4A-SLAP has been shown to ubiquitylate EphA2 in cells and in vitro, and knockdown of SLAP or of UBE4A slightly increased total EphA2 protein in colorectal cancer cell lines. Cbl or SLAP-UBE4A may be responsible for the increased turnover of EphA2 in SOCS2-overexpressing cells.

Ligand activation of other RTKs stimulates binding to various E3s, including Cbl, as well as SOCS proteins. For example, insulin stimulates INSR-SOCS1,3,6; Flt ligand stimulates Flt3-SOCS1,2,6; EGF stimulates EGFR-SOCS2,3,4,5,6; and SCF stimulates Kit-SOCS1,4,6 (*78, 130, 149, 152, 153, 155, 158-160, 162, 163, 301, 302*). However, all of these SOCS-RTK interactions

have been shown using exogenous expression of the SOCS protein and the biological/mechanistic links between SOCS and RTKs have been elucidated through SOCS overexpression studies. Additionally, none of these studies checked mRNA expression of the RTK or their associated ligand(s). Our results suggest that SOCS overexpression may result in indirect effects on RTK ligand expression and this can provide a biological/mechanistic link between SOCS and RTKs. If SOCS overexpression increases ligand expression for other RTKs, then the indirect effects of increased ligand expression will need to be separated from the direct effect of SOCS-CRL5 down regulating the RTK protein. The key experiment will be to perform loss of function studies on these SOCS-RTK interactions to confirm conclusions made with exogenously expressed SOCS. Either way there is a need for more studies on RTK-SOCS interactions to confirm the mechanism and biological roles of these interactions.

Chapter 4. INCREASED EGFR LIGAND PRODUCTION IN CUL5-DEPLETED CELLS PROMOTES GROWTH IN EGF-FREE MEDIA

4.1 INTRODUCTION

The epidermal growth factor receptor (EGFR/ErbB) family of receptor tyrosine kinases consists of four family members: ErbB1/EGFR, ErbB2/Her2, ERBB3/Her3 and ERBB4/Her4. The ErbB family members are single pass transmembrane receptors that possess intrinsic kinase activity, with the exception of ErbB3 that has no tyrosine kinase activity. Similar to other RTKs, the ErbB receptors hetero and homodimerize upon ligand binding, this leads to transphosphorylation of the receptor in the kinase activation loop, activation of the kinase, phosphorylation of the cytoplasmic side of the receptor and binding/activation of downstream signaling pathways (*304-306*).

There are thirteen known ErbB family ligands: epidermal growth factor (EGF), transforming growth factor (TGF-α), Heparin-binding EGF-like growth factor (HB-EGF), amphiregulin (AREG), betacellulin (BTC), epigen (EPGN), epiregulin (EREG), neuroregulin-1 (NRG-1), neuroregulin-2 (NRG-2), neuroregulin-3 (NRG-3), and neuroregulin-4 (NRG-4). The most well studied ErbB family member, EGFR, has been shown to bind to seven of these ligands: EGF, TGF-α, AREG, BTC, HB-EGF, EREG and EPGN (*307*). The Her2 receptor cannot bind to any of these ligands. However, EGFR can form EGFR/Her2 heterodimers when it binds to some of these ligands (*308*).

Upon ligand binding, EGFR is autophosphorylated tyrosine 845 in the kinase activation loop (Y845). This then leads to autophosphorylation at Y1045, Y1068, Y1086, Y1148 and Y1173 on the receptor (*306*). Each of these sites recruits downstream signaling molecules. The main signaling pathways activated in response to EGFR ligand binding are the mitogen-activated protein kinase (MAPK), phosphatidylinositol 3-kinase (PI3K)-AKT, STAT and Src pathways (*308*).

EGFR activity is negatively regulated somewhat through PTP-catalyzed dephosphorylation but phosphate is rapidly re-added as long as the kinase is active. Instead, most EGFR down-regulation is through the internalization of EGFR into endosomes inside of the cell (*309*). The fate of early endosomes containing an EGFR-ligand pair is controlled by the relative affinity of the ligand to the receptor. The pH on the inside of the endosome decreases as the early endosome matures into a late endosome. If the ligand dissociates after a relatively mild change in pH, early on during endosome maturation, then EGFR is diverted to the fast recycling pathway where the receptor is trafficked back to the plasma membrane. Recycled receptors can bind to and be activated by another ligand. However, ligand-receptor pairs that remain bound as the endosome matures and the pH drops are targeted to the late endosome and eventually to the lysosome for degradation. Sustained kinase activity during late endosome trafficking creates binding sites for E3 ubiquitin ligases that are needed to sustain ubiquitylation for recognition by the ESCRT complex that will pinch the receptor off into the multivesicular body (*42, 44, 310*).

MCF10A cells are normal breast epithelial cells that are commonly used to analyze epithelial transformation (*311-313*). Due to their normal phenotype MCF10A cells require EGF, Insulin, and hydrocortisone in the media to grow in culture. Many transformation assays make use of a EGF-free media (full growth media without EGF and low serum), because untransformed MCF10A cells cannot proliferate under these conditions (*313*). Our lab recently found that Cul5-depleted cells can grow in EGF-free media, suggesting that Cul5 acts a tumor suppressor in MCF10A cells to prevent their growth-factor independent proliferation (*143*). To better understand this growth-factor independence, we investigated the role of the EGFR in this phenotype.

4.2 RESULTS

To test if EGFR was required for the increased growth of the Cul5-depleted cells in EGF-free media, we depleted EGFR with siRNA. EGFR-depletion caused the Cul5-depeleted cells to grow at the same rate as control cells, suggesting EGFR was required for their growth in EGF-free media (Figure 4.1a). Because EGFR is kinase we next tested if EGFR kinase activity was also required for the increased growth of the Cul5-depleted cells. Cells were grown in the presence of

the EGFR specific kinase inhibitor, AG1478 (*314, 315*). The growth of the control cells was unaffected by the presence of AG1478, but the Cul5-depleted cells grew at the same rate as control cells (Figure 4.1b). This indicated that the kinase activity of EGFR was required for the growth of the Cul5-depleted cells.

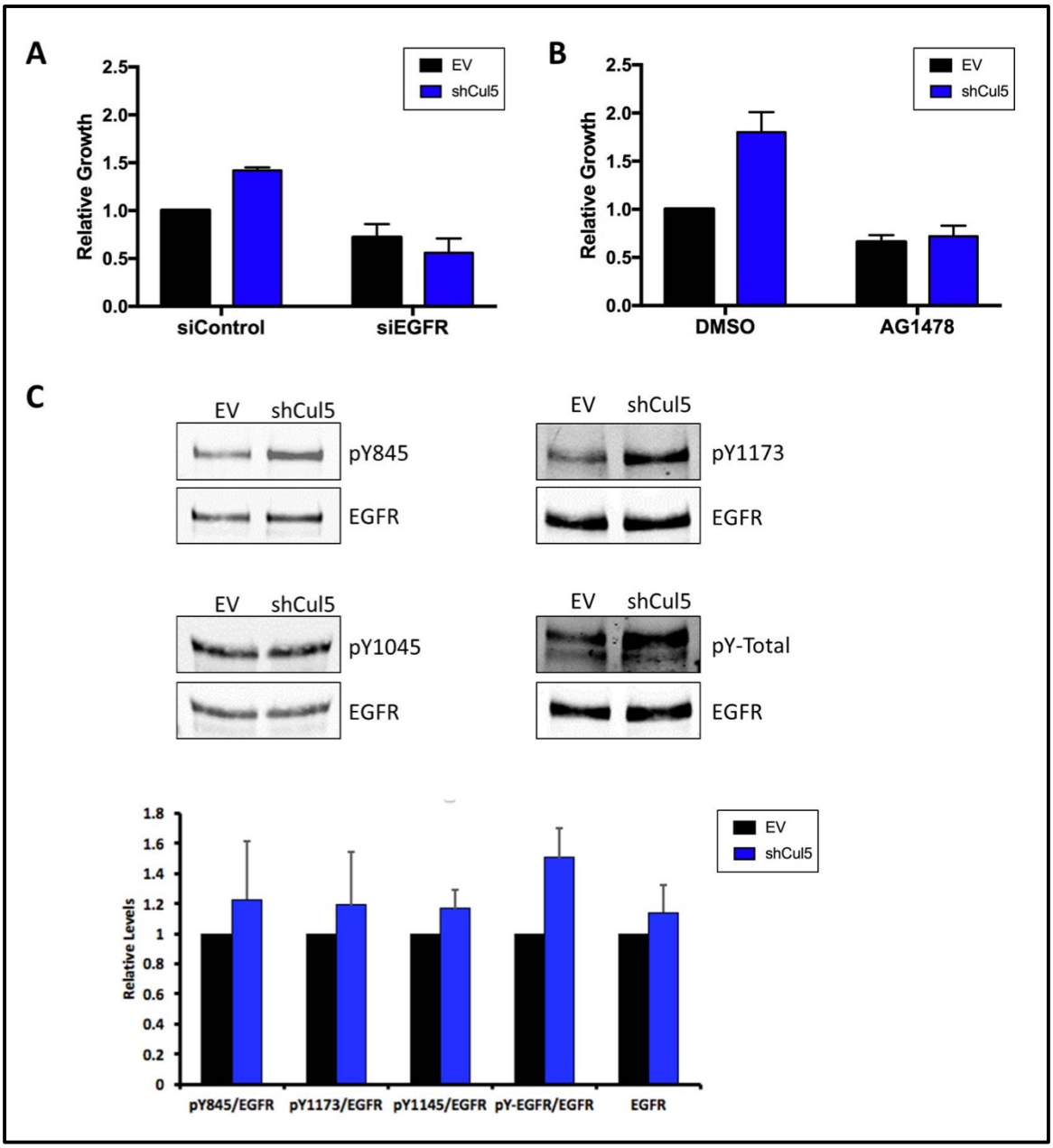

FIGURE 4.1 EGFR KINASE ACTIVITY IS REQUIRED FOR EGF-INDEPENDENT GROWTH OF CUL5-DEPLETED CELLS

(a) EGFR is required for EGF-independent growth of Cul5-depleted cells. MCF10A cells were reverse transfected with the indicated siRNA overnight in complete growth media. The next day the media was removed and replaced with EGF-free media. One

plate was fixed when the media was removed and the other was fixed 72 hours later. Plates were stained with crystal violet. Bars are mean and SEM of the 72 hour to zero hour crystal violet stain, normalized to the control condition. (b) EGFR kinase activity is required for EGF-independent growth of Cul5-depleted cells. MCF10A cells were plated in complete growth media and allowed to sit down overnight. The next day the media was removed and replaced with EGF-free media containing the indicated drug. One plate was fixed when the media was removed and the other was fixed 72 hours later. Plates were stained with crystal violet. Bars are mean and SEM of the 72 hour to zero hour crystal violet stain, normalized to the control condition. (c) Cul5-depleted cells grown in EGF-free media for 48 hours have increased EGFR phosphorylation. The indicated MCF10A cells were grown to sub-confluence and then switched to EGF-free media. 48 hours after the media change the cells were harvested, EGFR was immunoprecipitated and analyzed using Western blotting. The Western blotting from the biological triplicates were quantified using ImageQuantTLV2005. Bars are mean and SD.

Since many SOCS proteins have been shown to bind to EGFR and SOCS overexpression increases EGFR ubiquitylation and degradation (*76, 140, 152, 155, 159, 160, 163*), we wondered whether EGFR levels or phosphorylation are altered in Cul5-deficient cells. Indeed, one of our early mass spectrometry screens showed an increase in one EGFR phosphotyrosine peptide in Cul5-deficient cells (*143*). To validate this observation, control and Cul5-depleted cells were harvested after 48 hours in EGF-free media and EGFR was immunoprecipitated. The immunoprecipitates were probed for the autophosphorylation sites: pY845, pY1173, pY1045 and total tyrosine phosphorylation. The amount of total EGFR pulled down was the same in the control and Cul5-depleted cells. However, Cul5-depleted cells had a large increase in pY845, pY1773 and total pY and a slight increase in pY1145 (Figure 4.1c). This indicated one of two things: either degradation of phospho-EGFR was diminished upon Cul5-depletion or EGFR autophosphorylation was increased in Cul5-depleted cells, perhaps through increased kinase activity of EGFR.

One of the increased phosphotyrosine residues, Y845, is located in the kinase activation loop of EGFR. Phosphorylation of Y845 stabilizes the kinase domain activation loop leading to an active kinase (*316*). Src kinase, in addition to EGFR kinase, can phosphorylate Y845 (*317, 318*) and we previously found Src kinase activity is increased in Cul5-depleted cells grown in full growth media (*143*). This raises the possibility that increased EGFR kinase activity/phosphorylation may be caused by Src. To determine whether increased EGFR phosphorylation in Cul5-depleted cells

needed EGFR kinase activity, we used two inhibitors: Lapatinib, an EGFR/Her2 dual kinase inhibitor, and AG1478, a EGFR inhibitor (*314, 315, 319-321*). MCF10A control and Cul5-depleted cells were incubated in EGF-free media for 48 hours in the presence of these inhibitors and either harvested or stimulated with EGF for 5 min to check the activity of the inhibitors. Both inhibitors prevented EGFR phosphorylation after acute EGF stimulation, confirming that they inhibit autophosphorylation (Figure 4.2 right). In the EGF-free media Lapatinib and AG1478 both inhibited the increase pY845 phosphorylation seen in the Cul5-depleted cells (Figure 4.2). These results suggested that Cul5 depletion stimulates EGFR pY845 autophosphorylation due either to increased EGFR kinase activity or decreased degradation of pY-EGFR.

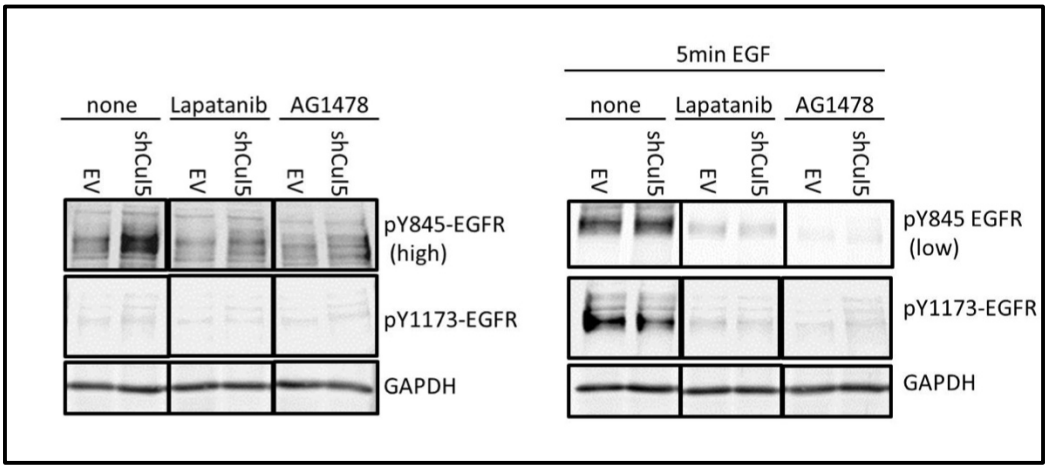

FIGURE 4.2 EGFR IS ACTIVATED BY AUTOPHOSPHORYLATION IN CUL5-DEPLETED CELLS

Increased EGFR phosphorylation in Cul5-depleted cells requires EGFR kinase activity. The indicated MCF10A cells were grown to sub-confluence and then switched to EGF-free media with the indicated inhibitors. 48 hours after the media change the cells were treated with 50 nM of EGF for 5 min before harvest. Cells were then analyzed using Western blotting.

To differentiate between these two possibilities, we analyzed pY-EGFR levels at different time points after moving the cells to EGF-free media. If the increased phosphorylation at 48 hours was due to decreased degradation of pY-EGFR then the amount of pY-EGFR should not change over time. When the cells are in EGF-containing media, total EGFR is low (Figure 4.3a, Time 0). This is presumably due to EGF-induced phosphorylation of EGFR that leads to lysosomal degradation of the receptor (*322*). When the cells are moved to EGF-free media, total EGFR levels begin to increase and come to a new equilibrium due to the decreased degradation of pY-

EGFR. Total EGFR levels in control and Cul5-depleted cells increase at the same rate (Figure 4.3b). Phosphorylation of Y845 is high when the cells are in full growth media (0 hour) and dips to barely detectable levels after 16 hours in EGF-free media. In the control cells pY845 levels remain low over the next 72 hours in EGF-free media. However, pY845 levels in the Cul5-depleted cells start to rise over the next 56 hours and eventually are at the same level as observed in full growth media (Figure 4.3a, b). This result indicated that activation of EGFR kinase in Cul5-depleted cells occurred gradually over time in EGF-free media.

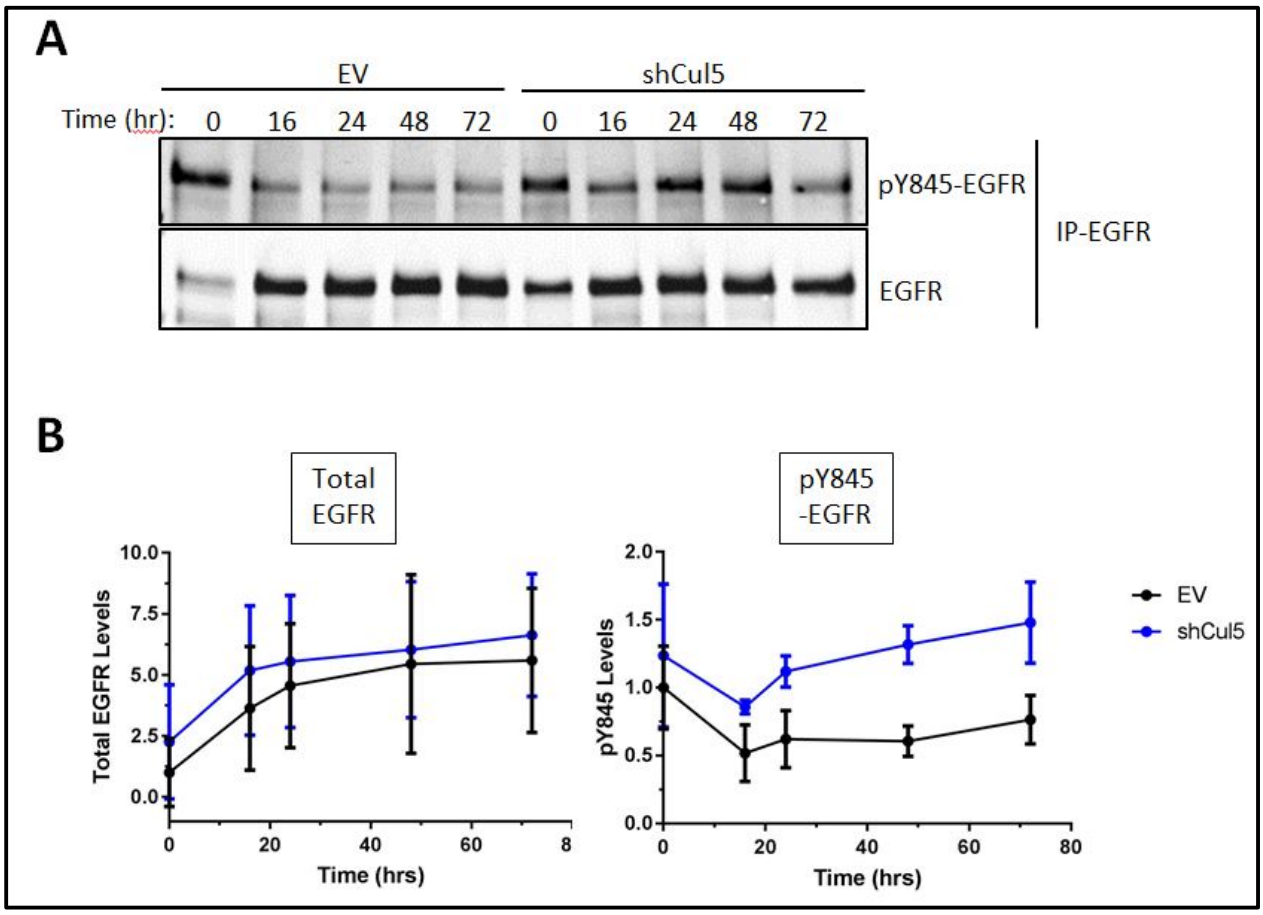

FIGURE 4.3 EGFR ACTIVITY INCREASES OVER TIME IN EGF-FREE MEDIA

(a) EGFR activity decreases, and receptor levels rebound, upon EGF withdrawal, but EGFR activity then increases over time in Cul5-deficient cells. The indicated MCF10A cells were grown to sub-confluence and switched to EGF-free media. The cells were harvested at the indicated times, EGFR was immunoprecipitated and then analyzed by Western blotting. (b) Quantification of biological triplicate Western blots in panel A. The Western blotting from the biological triplicates panel A were quantified using ImageQuantTLV2005. Points are mean and SD of biological triplicates.

Previous reports have shown that MCF10A cells expressing an oncogene are able to make EGFR ligands in EGF-free media, that can then activate EGFR in an autocrine manner (*323*). This combined with the gradual increase in pY-EGFR in Cul5-depleted cells led us to hypothesize that one or multiple EGFR ligand(s) are accumulating in the EGF-free media of Cul5-depleted cells over time. Increased expression of EGFR ligand(s) could activate the EGFR kinase, which in turn could activate the transcription of these ligand(s) resulting in a positive feedback loop. This could cause a gradual increase in extracellular ligand abundance and activation of EGFR kinase activity over time. To test this model, we tested whether the EGFR ligand-binding domain is required for the growth of Cul5-depleted cells. A growth assay was performed in the presence of anti-EGFR antibody that had been reported to block the ligand-binding site of EGFR (*324*). Cul5-depleted cells grown in the presence of this antibody had a similar growth rate to control MCF10A cells (Figure 4.4a). This indicated that EGFR ligand binding was required for and contributed to the increased growth of Cul5-depleted cells. However, antibody binding to the extracellular domain of EGFR can induce receptor degradation via the lysosome (*322*). If the antibody we used induced EGFR degradation in the Cul5-depleted cells, then the decrease in growth could have been caused by EGFR-depletion rather than lack of ligand binding. Indeed, the antibody induced EGFR degradation, although the reduction in EGFR level seems unlikely to fully account for the decreased growth rate (Figure 4.4b).

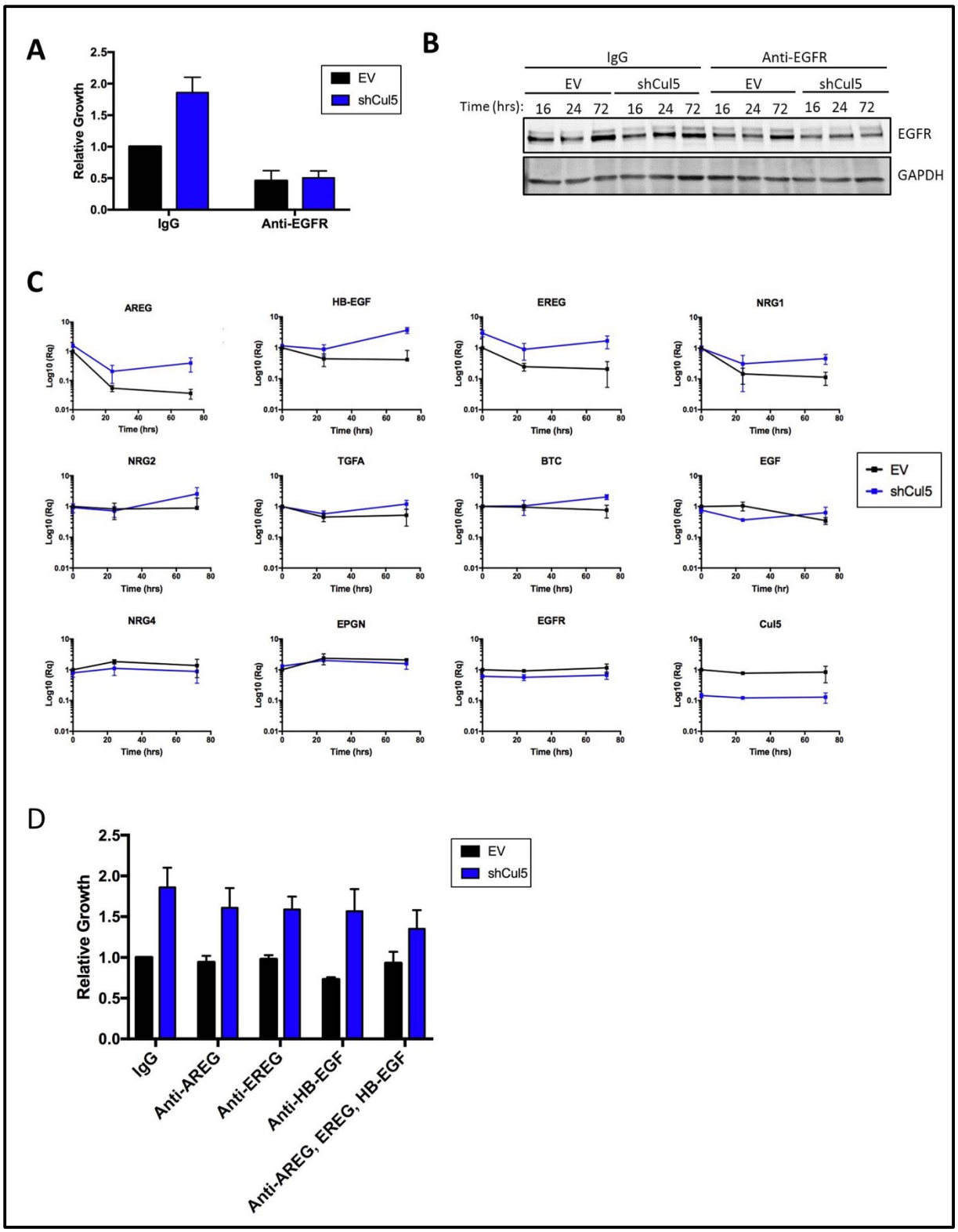

FIGURE 4.4 EGFR LIGANDS ACCUMULATE IN EGF-FREE MEDIA AND BIND TO EGFR

(a) EGFR antagonist antibody inhibits growth of Cul5-depleted cells. MCF10A cells were plated in complete growth media and allowed to sit down overnight. The next day the media was removed and replaced with heat inactivated EGF-free media containing anti-EGFR (528) antibody. One plate was fixed when the media was removed and the other was fixed 72 hours later. Plates were then stained with crystal violet. Bars are mean and SEM. (b)EGFR antagonist antibody does not induce EGFR degradation. The indicated MCF10A cells were grown to sub-confluence and switched to EGF-free media with either IgG or anti-EGFR (528) antibody. Cells were harvested at the indicated times after the media change and analyzed using Western blotting. (c) Expression of AREG, HB-EGF and EREG is regulated by Cul5. The indicated MCF10A cells were grown to sub-confluence and switched to EGF-free media. RNA was harvested at the indicated time points after the media change using the RNeasy kit. cDNA was then synthesized and the indicated genes were analyzed using SYBR qPCR. Points are mean and SD of biological triplicates. (d) Ligand sequestering antibodies against AREG, EREG, HB-EGF slightly inhibit the growth of Cul5-depleted cells in EGF-free media. MCF10A cells were plated in complete growth media and allowed to sit down overnight. The next day the media was removed and replaced with heat inactivated EGF-free media containing the indicated antibodies. One plate was fixed when the media was removed and the other was fixed 72 hours later. Plates were then stained with crystal violet. Bars are mean and SEM.

Next, we checked whether mRNA expression of ErbB family ligands was changed in Cul5-depleted cells. RNA was harvested from control and Cul5-depleted MCF10A cells at various time points after transfer to EGF-free media. mRNA abundance of ErbB ligands, Cul5 and EGFR was measured using reverse transcription and quantitative PCR. One of our control genes, EGFR, had equal and constant mRNA levels throughout the time in EGF-free media. The other control gene, Cul5, showed Cul5-depleted cells have 10% Cul5 mRNA compared to control cells and this difference remains constant throughout the assay (Figure 4.4c). This indicates that the assay was working and there were no large fluctuations in loading or other technical errors. Expression of the ErbB family ligands was variously altered in Cul5-deficient cells. NRG4, EPGN and EGF were equally expressed in control and Cul5-depleted cells throughout the 72 hours. NRG2, TGFA and BTC were expressed at similar levels at time 0 and expression remained constant in control cells and increased slightly in Cul5-deficient cells. AREG, HB-EGF, ERG and NRG1 expression declined in control cells but increased in Cul5-deficient cells. AREG and EREG expression was higher in Cul5-depleted cells even at time 0, ie, in the presence of EGF (Figure 4.4c). It appears that transcription of many ErbB family ligands are being modestly or strongly induced in the Cul5-depleted cells over time in EGF-free media, potentially leading to EGFR activation.

Next, we wanted to determine if these ligands were being translated, secreted and binding to EGFR, causing the gradual increase in pY-EGFR observed over time in EGF-free media. AREG, EREG and HB-EGF were the EGFR ligands with the largest increase in mRNA abundance in Cul5-depleted cells. Ligand-neutralizing antibodies against these three ligands were added individually or in combination to the media during the growth assay. These antibodies have been shown to prevent the ligand from binding to EGFR (*325-327*). When each of these antibodies was incubated individually they had little to no effect on the growth of Cul5-depleted cells. However, when all three of the ligand-blocking antibodies were added at the same time, growth of Cul5-depleted cells was inhibited, although the change was not significant. This suggested that these ligands were being translated and binding to EGFR contributing to the increased growth of these cells. We may have gotten a significant decrease in Cul5-depleted cell growth if TGF-α and BTC antibodies were also included in the mix.

These results suggest that Cul5 indirectly inhibits EGFR, perhaps by inhibiting production of endogenous EGFR ligands, and EGFR contributes to the growth of Cul5-depleted cells in EGF-free media. It is possible that Cul5 directly regulates a pathway induces EGFR ligand expression and is downstream of EGFR. MAPK activates some transcription factors downstream of EGFR (*306*), so we tested whether MAPK activity is required for EGF-independent growth and EGFR ligand expression in Cul5-deficient cells.

To determine if MAPK signaling was required for the growth of Cul5-depleted cells we grew cells in the presence of the MAPK inhibitor U0126 (*328*). U0126 inhibited the increased EGF-independent growth of Cul5-depleted cells, suggesting that Cul5 inhibits MAPK signaling (Figure 4.5a). Next, we measured AREG, EREG, HB-EGF expression in control and Cul5-depleted cells treated with or without U0126. AREG and HB-EGF mRNA abundance in Cul5-depleted cells did not change in the presence of the U0126 inhibitor. However, EREG induction in presence of EGF-free media was inhibited by U0126 (Figure 4.5b). This suggested that the induction/sustained high levels of EREG in Cul5-depleted cells is induced by MAPK.

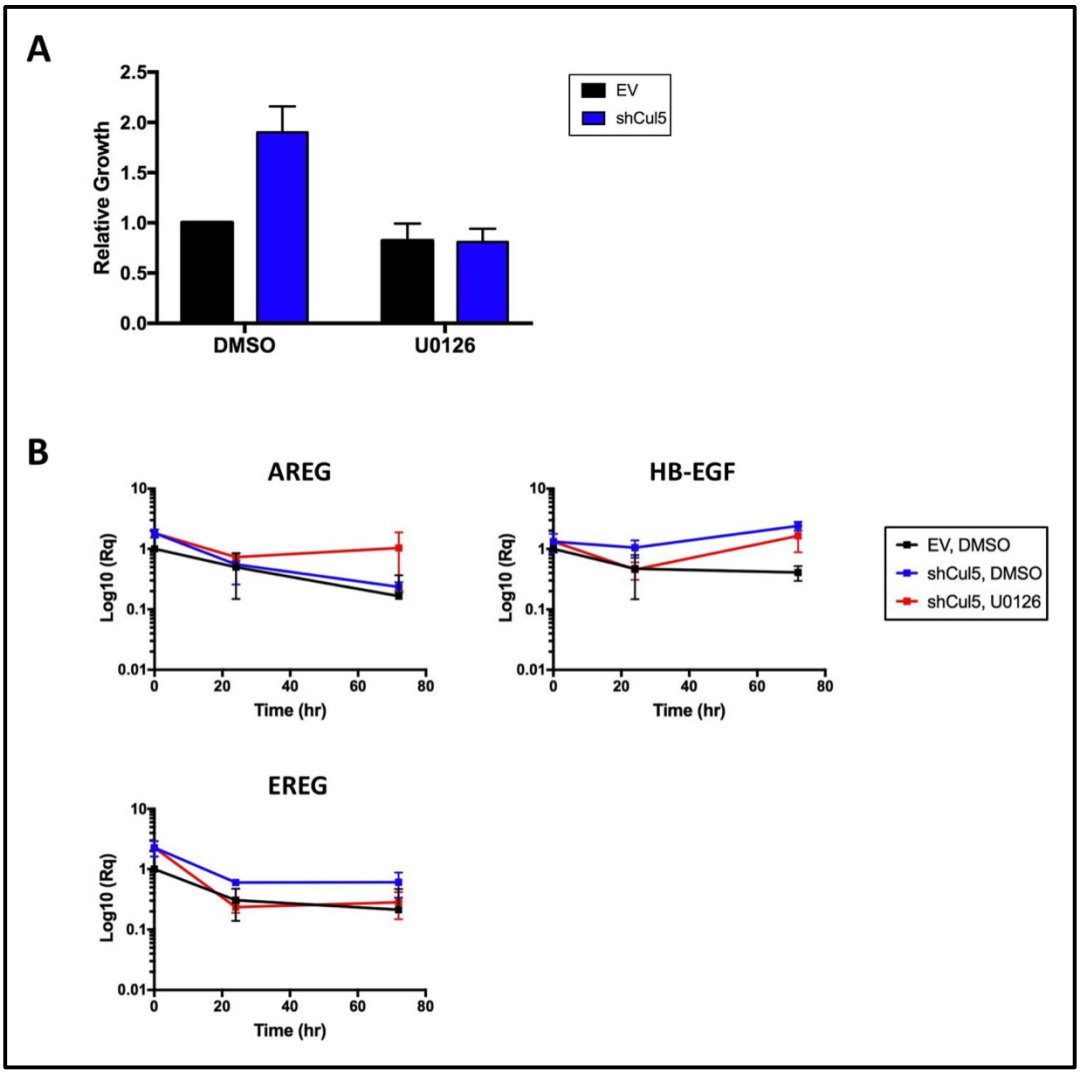

FIGURE 4.5 MAPK ACTIVITY IS REQUIRED FOR THE INDUCTION OF EREG IN CUL5-DEPLETED CELLS

(a) MAPK activity is required for the increased growth of Cul5-depleted cells in EGF-free media. MCF10A cells were plated in complete growth media and allowed to sit down overnight. The next day the media was removed and replaced with EGF-free media containing the indicated drug. One plate was fixed when the media was removed and the other was fixed 72 hours later. Plates were then stained with crystal violet. Bars are mean and SEM. (b) MAPK activity is required for the induction EREG, but not AREG or HB-EGF. The indicated MCF10A cells were grown to sub-confluence and then switched into EGF-free media with the indicated drugs. RNA was harvested at the indicated time points after the media change using the RNeasy kit. cDNA was then synthesized and the indicated genes were analyzed using SYBR qPCR. Points are mean and SD of biological triplicates.

4.3 DISCUSSION

We sought to elucidate the role of EGFR in the growth of Cul5-depleted cells. We found that Cul5-depleted cells require EGFR kinase activity to grow in EGF-free media and displayed an increase EGFR autophosphorylation and total pY-EGFR in EGF-free media. The increased EGFR autophosphorylation required EGFR kinase activity and increased gradually after the cells were transferred to EGF-free media. The Cul5-depleted cells had increased transcription of three EGFR ligands (AREG, HB-EGF and EREG) after 72 hours in EGF-free media. The EGFR ligand binding domain was required for the growth of Cul5-depleted cells and ligand sequestration slightly inhibited growth. MAPK was required for the increased expression of EREG but not AREG or HB-EGF, and was required for EGF-independent growth.

Our data suggest that Cul5 removal induces transcription of genes for EGFR ligands, which are then translated and secreted, activating the EGFR and cell proliferation. Because EGF withdrawal decreases ligand gene expression in control cells, EGF may normally induce ligand expression, as reported for HB-EGF (*329*). In this case, removal of Cul5 may induce expression of EGFR ligands, which activate the EGFR and in turn activate more ligand expression. Interestingly, AREG and EREG induce EGFR recycling rather than degradation and lead to continuous signaling through repeated rounds of receptor activation (*44*). By inducing these ligands, Cul5 depletion may keep EGFR signaling high in EGF-free media.

While we did not directly show EGFR kinase activity was required for the higher transcription of AREG, HB-EGF and EREG in Cul5-depleted cells, the requirement of EGFR kinase activity for the growth and increased pY845-EGFR phosphorylation suggests EGFR kinase activity may be required for increased ligand expression as well. The requirement of MAPK for EREG transcription provides further evidence for this model. In future work, we should test if EGFR activity is required to induce endogenous ligands. In addition, we were unable to fully inhibit EGF-independent growth of Cul5-deficient cells by adding neutralizing antibodies to AREG, HB-EGF and EREG. It is possible that these antibodies are not very potent, or that autocrine EGFR activation occurs within the secretory pathway. An alternative would be to knockdown all three ligands simultaneously.

The protein(s) that are directly regulated by Cul5 and increase ligand expression still need to be identified. An approach we could take to identify these factors would be a targeted siRNA screen. If EGFR is shown to be required for ligand induction, the screen could target transcription factors downstream of EGFR. If EGFR is not required for ligand induction then the screen could be against transcription factors known to bind the promoter region of these ligands. Any transcription factor identified in this screen could then could then be used to work up the signaling pathway to identify the direct substrate. Hopefully this targeted approach would identify the signaling proteins that are directly regulated by Cul5.

Chapter 5. CONCLUSIONS & FUTURE DIRECTIONS

The previous chapters report the results of a screen for phosphotyrosine proteins whose abundance is regulated by Cul5 and a screen for SOCS2- and 6-binding partners. I provide detailed investigation of some candidate CRL5 substrates, with an emphasis on RTKs, specifically the INSR/IGF-IR, EphA2 and EGFR. The main conclusion is that $CRL5^{SOCS}$ can indirectly affect RTK levels or activity and it remains unclear whether $CRL5^{SOCS}$ is directly involved in ubiquitylation and degradation of RTKs.

Many independent labs have discovered SOCS-RTK interactions but their functions have not been shown in a convincing manner. Some RTKs have even been shown to bind multiple SOCS proteins. There are papers that have shown changes in steady state receptor levels or activity, and suggested that $CRL5^{SOCS}$ is regulating RTK ubiquitylation and degradation. However, the work in this dissertation shows CRL5 regulates many processes that can indirectly alter the steady-state abundance, phosphorylation, and ubiquitylation of RTKs; without the appropriate controls, one may incorrectly conclude that CRL5/SOCS regulate RTK abundance, phosphorylation, and ubiquitylation directly. We found that CRL5 depletion and SOCS overexpression can increase RTK ligand mRNA expression for both the EphA2 and EGFR receptors. Increased ligand expression can give one of two phenotypes depending on whether the ligand targets the RTK to the recycling pathway or the lysosome. If the receptor recycles, RTK phosphorylation but not steady state abundance may be altered, as for the EGFR when Cul5 expression was inhibited. On the other hand, if ligand induces RTK degradation, RTK steady state abundance may decrease, as we found for EphA2 when SOCS2 was over-expressed. In both situations $CRL5^{SOCS}$ may only be regulating ligand expression and only indirectly regulating the RTK. Our results suggest that the literature on RTK CRL5 biology should be analyzed with care. My results suggest that a SOCS-RTK paper must include the appropriate controls, such as: measurement of RTK and ligand mRNA abundance, direct SOCS binding and in vitro ubiquitylation.

5.1 SOCS & CRL5 REGULATION OF RTK UBIQUITYLATION AND DEGRADATION

Most of the work completed in this dissertation started with the hypothesis that $CRL5^{SOCS}$ regulates IGF-IR, EphA2 or EGFR ubiquitylation and degradation. We tested this hypothesis in steady-state conditions (normal growing cells) and after acute stimulation of the RTK with its most preferred ligand. In data not shown we observed no change in the degradation kinetics of EphA2 after acute EfnA1-Fc stimulation in Cul5- and SOCS2-depleted cells compared to a control cell line. However, many other things can activate RTK ubiquitylation that we were unable to test due to time constraints. Our hypothesis may very well still be valid, under different stimulation conditions or in a different cellular context.

One possibility is that we were using the incorrect ligand to stimulate EphA2. The exogenous EfnA1-Fc ligand induced relatively slow EphA2 degradation ($t_{1/2}$ 280min). The slow degradation of EphA2 is most likely because only 50% of EfnA1-Fc remains bound to EphA2 at pH 5.5 and higher (*48*); the pH of the late endosome/MVB is between pH 5-6 (*330*). Perhaps EphA2 has a long half-life after EfnA1-Fc stimulation because 50% EphA2 is routed to the slow recycling pathway after EfnA1-Fc dissociation in the late endosome/MVB. If this is true, then only 30-40% of total EphA2 was being targeted to the lysosome after our acute EfnA1-Fc stimulation. The large amount of recycling EphA2 may mask any changes in degradation kinetics induced by $CRL5^{SOCS2}$. Four other EfnA ligands can bind to EphA2, presumably with different binding affinities (*236*). Perhaps another EfnA ligand will more potently route EphA2 to the lysosome. If this is true, measuring EphA2 half-life in control and Cul5/SOCS2-depleted cells after acute stimulation with a different EfnA ligand may show a more robust phenotype.

Another possibility is that Cul5 or SOCS2 depletion would affect EphA2 degradation if EfnA1 was presented on a cell membrane. In a normal cellular context, Eph-Efn receptor-ligand pairs are endocytosed from one cell to the next in a mechanism called trans-endocytosis. The Efn ligands are bound to Eph's on the membranes of adjacent cells. Trans-endocytosis is Rac-mediated endocytosis of plasma membrane from the adjacent cell into the endocytic cells. Trans-endocytosis can go into either the Eph- or Efn-expressing cell (*232, 331*). Maybe activation of Rac and other signals needed to pinch off the adjacent EfnA membrane would cause synergistic

signaling and additional SOCS-EphA2 interactions that must work together to produce more potent EphA2 degradation. Indeed, our results showed that increased expression of endogenous EfnA1, in SOCS2 overexpressing cells, potently downregulated EphA2 protein via the lysosome. Perhaps we should have analyzed the effect of Cul5 or SOCS2 depletion on receptor traffic in cells overexpressing EfnA1, rather than using recombinant EfnA1-Fc.

Another option is that EfnA1-Fc was the correct stimulus, but we were testing the effect of depleting SOCS2 and Cul5 depletion in the wrong cells or environment. We used exogenous SOCS2 to detect an association with endogenous EphA2. MCF10A, HeLa and MDA-MB-231 cells were used for all of our EphA2 degradation experiments, but SOCS2 expression is relatively low in these cells (data not shown). Unfortunately, we were unable to determine if endogenous SOCS2 bound to endogenous EphA2 due to technical difficulties. We do not know if endogenous SOCS2 can bind to and potentially regulate EphA2. Cytokine receptor or RTK activation activates transcription of SOCS proteins; for example, SOCS1-3, CisH mRNA expression is not detectable until cytokine stimulation in immune cells, SOCS2 is induced in cells expressing constitutively active FLT3, and SOCS6 increases 5-fold after insulin stimulation (*142, 332-335*). We did not check to see if EfnA1-Fc stimulation induced SOCS2 mRNA expression in our cell lines. If high levels of SOCS2 expression are required for a functional effect on EphA2, and there was no induction of SOCS2 or not enough endogenous SOCS2 in the cell lines analyzed, then our hypothesis may have been correct, but we would have needed to analyze the function in a cell line or context that had higher SOCS2 expression.

One way we could induce SOCS2 expression is through the simultaneous or sequential exposure to cytokine(s) and EfnA1-Fc. Cells in the organism are not exposed to one cytokine or growth factor in isolation. Many times, they are exposed to multiple ligands at the same time or sequentially. To recapitulate this in a cell line we could stimulate control, Cul5- and SOCS2-depleted cells with a cytokine or growth factor that has been shown to increase SOCS2 levels and is commonly seen at the same time as EfnA1 in the body. Simultaneous stimulation of cell lines would induce SOCS2 expression and stimulate EphA2 activation, giving us a simple reductionist system to study SOCS2 regulation of EphA2. A more physiological method would

be to analyze the function of EphA2-SOCS2 in a developmental context where both the proteins are highly expressed and required.

There are many developmental contexts that require EphA2, however only a few of these have been shown to have high SOCS2 as well. Mammary gland development in preparation for lactation is one developmental system where SOCS2 and EphA2 are both expressed at high levels. SOCS2 expression in the mammary gland has been shown to increase after pregnancy and during lactation when the breast is undergoing branching and morphogenesis (*110*). EphA2 expressed in the terminal end buds of the mammary gland ductal network where it plays a role in development (*336*). It would be interesting to see if removal of SOCS2 has an effect on EphA2 levels or downstream pathway activation in this developmental context. EphA2, IGF-IR, and EGFR have been shown to play a role in many developmental pathways. It may be more useful to study SOCS regulation of these RTKs in their relevant developmental contexts rather than in tissue culture cells.

Finally, $CRL5^{SOCS2}$ may also regulate lysosomal targeting of EphA2 through non-ligand mediated methods. The virus KSHV binds to integrins and EphA2, which stimulates macropinocytosis-based entry of the virus and the associated receptors into the cells. The virus does this through the activation and assembly of many putative and confirmed SOCS-binding partners (FAK, Cas, Crk, PI3K) on the cytoplasmic side of the receptor (*248, 337*). Multiple SOCS proteins will be bound to a KSHV-EphA2 early endosome, potentially at the same time. Perhaps this would lead to synergistic ubiquitylation of the RTK or associated proteins that would help target the virus-containing early endosomes to the late endosome/lysosome. Many other viruses use EphA2 and EGFR for entry into the cell. The signal coordination initiated by virus binding to these RTKs may very well be regulated by SOCS or Cul5. Recently, researchers showed that SOCS5 knockout lung tissue and primary cells infected with influenza have increased levels of EGFR, and this increases influenza infection (*140*). It is unclear at this time if the increase is due to inhibition of $CRL5^{SOCS5}$ ubiquitylation and degradation of EGFR, but it very well may be. Virus-containing endosomes often have multiple RTKs and receptors clustered together that can potentially cross-talk with one another. EphA2 can be activated through cross-talk with other receptors, such as E-Cadherin (*338*). Activation through this

ligand-independent mechanism would most likely stimulate Y772 phosphorylation and presumably SOCS2 binding as well. Maybe cross-talk with another receptor could target EphA2 to the lysosome more potently.

5.2 Functions independent of RTK Ubiquitylation and Degradation

SOCS proteins and Cul5 may be brought to RTKs to serve a function independent of endocytosis and degradation. In our studies and other RTK SOCS binding studies, researchers did not determine if the interaction between a SOCS protein and RTK is direct. All of the observed SOCS-RTK and Cul5-RTK binding interactions could be mediated through a signaling molecule bound directly to the RTK. If this is the case, Cul5 and SOCS proteins may not regulate any RTK function, instead, they are binding and regulating one of the many downstream signaling proteins directly bound to the receptor. A quick scan of the cytosolic proteins known to bind to SOCS proteins reveals many well-known RTK binding partners (see Table 1.2). It is possible that these cytosolic proteins are the direct binders of SOCS proteins and the RTKs just appear to interact. In future work, it will be important to understand if the SOCS-RTK binding is direct or indirect to help elucidate the true function of these interactions.

If the interaction between a SOCS and RTK is direct, then there may be degradation-independent functions of SOCS-RTK binding. SOCS proteins could be competing with downstream signaling proteins for pY binding sites on the receptor like has been shown for some STAT-cytokine receptor interactions. For EphA2 specifically, the pY772 binding site is in the activation loop. This tyrosine has no reported binding partners in the literature, so we were unable to test this hypothesis without a screen. Another possibility is that SOCS2 binding to the activation loop tyrosine could block substrate access to the active site of the kinase domain, or protect the site from dephosphorylation. Kinase inhibition could occur through ubiquitylation as well. $CRL5^{SOCS2}$ binding could inactivate EphA2 by ubiquitylating residues in the active site. Indeed, ubiquitylation of EphA protein has been detected near the activation loop (*339*). In data not shown we checked pY588 or pY772 levels in SOCS2-depleted cells after acute EfnA1-Fc stimulation and did not observe a difference in the autophosphorylation of EphA2. However, the

low SOCS2 expression in the three cell lines used could have been the reason for this negative result.

Perhaps, SOCS binding plays a role in trafficking to a location other than the lysosome. EGFR has been shown to traffic from endosomes to other organelles in the cell, such as the nucleus, mitochondria, and Golgi (*340*). We found SOCS2 and SOCS6 bound to membrane proteins from a variety of different organelles in the cell, including the nucleus, mitochondria, and Golgi. Maybe SOCS proteins traffic RTK-containing endosomes to other organelles in the cell by acting as a bridge. The SOCS protein could be simply acting as a scaffold linking the endosome to organelle proteins.

5.3 SOCS-RTK-STAT FUNCTIONS

SOCS proteins are most well known for their regulation of STAT functions (*334*). Many RTKs can bind to and activate STATs (*341, 342*). Perhaps the entire function of SOCS-RTK binding is to regulate STAT activity through competition for STAT binding sites on an RTK, STAT ubiquitylation, or by increasing the local concentration of the SOCS proteins, so it can bind to a STAT as soon as it is released from the receptor and before it can form a dimer with another activated STAT.

EphA2 has not been shown to bind to STATs in the literature. However, there is a putative STAT SH2 binding site in the C-terminus of SOCS2 and SOCS2 has been shown to be phosphorylated after acute growth factor stimulation (*7, 153*). If EphA2 activation stimulates phosphorylation of SOCS2 at this putative STAT binding site, then STAT recruitment to EphA2 and possibly activation would be delayed until SOCS2 binds at the early endosome. The RTK MET must be trafficked to a perinuclear compartment before it can bind and activate STATs. The delayed activation of STATs provides stronger STAT activation because of the short distance the STAT needs to travel the nucleus to activate transcription (*343*). Constitutively active FLT3 potently activates STAT5 when it is in the ER (*344*). If EphA2 activation of a STAT must occur near the nucleus, then pY-SOCS2 recruitment of a STAT may be how this occurs.

Chapter 6. MATERIALS AND METHODS

6.1 PLASMIDS

pCAG-T7-mCul5 K799R, pCAG-T7-mSOCS1, pCAG-T7-mSOCS2, pCAG-T7-mSOCS3, pCAG-T7-mSOCS4, pCAG-T7-mSOCS5, pCAG-T7-mSOCS6, pCAG-T7-mSOCS7 and pCAG-T7-mCisH constructs have been previously described (*143, 145*). The LC-QQ mutants were made using PfuTurbo DNA Polymerase (Agilent Technologies) to perform site directed mutagenesis and the following primers: mSOCS1 LC-QQ, mSOCS2 LC-QQ and mSOCS6 LC-QQ (Table 6.1). The pCAG-ElgC-T2A-ElgB were described earlier (*145*).

Table 6.1 SOCS Cloning & SDM Primers

PRIMER	SEQUENCE
hSOCS2 R73K Fwd	5'-GGCACCAGAAGGAACTTTCTTGATTAAAGATAGCTCGCATT-3'
hSOCS2 R73K Rev	5'-AATGCGAGCTATCTTTAATCAAGAAAGTTCCTTCTGGTGCC-3'
hSOCS2 LCQQ Fwd	5'-TCAGCACCATCTCAGCAGCATCTCCAAAGGCTCACCATT-3'
hSOCS2 LCQQ Rev	5'-AATGGTGAGCCTTTGGAGATGCTGCTGAGATGGTGCTGA-3'
attB1 hSOCS2	5'-GGGGACAAGTTTGTACAAAAAAGCAGGCTTCATGACCCTGCGGTGCCTT-3'
attB2 hSOCS2	5'-GGGGACCACTTTGTACAAGAAAGCTGGGTTTCATACCTGGAATTTATATTCTTCC-3'
mSOCS2 R73K Fwd	5'-GAATGCGAACTATCTTTAATCAAGAAAGTTCCTTCTGGAGCC-3'
mSOCS2 R73K Rev	5'-GGCTCCAGAAGGAACTTTCTTGATTAAAGATAGTTCGCATTC-3'
mSOCS1 LCQQ Fwd	5'-GCC GCA GCA GGA GCT GCA GCG CCA GCG CAT CGT G-3'
mSOCS1 LCQQ Rev	5'-GCT GGC GCT GCA GCT CCT GCT GCG GCC GCA CGC G-3'
mSOCS2 LCQQ Fwd	5'-CAGCACCCACTCAGCAGCATTTCCAGCGACTCGCCATTAAC-3'
mSOCS2 LCQQ Rev	5'-CGAGTCGCTGGAAATGCTGCTGAGTGGGTGCTGATGTATAC-3'
mSOCS3 LCQQ Fwd	5'-GCC ACC CAG CAG CAT CTT CAG CGG AAG ACT GTC AAC GG-3'
mSOCS3 LCQQ Rev	5'-AGT CTT CCG CTG AAG ATG CTG CTG GGT GGC CAC GTT GG-3'
mSOCS4 LCQQ Fwd	5'-ACC GTT CTC TGA ATA TGC TGC TGG GAA AAG GGG AAC GTC C-3'
mSOCS4 LCQQ Rev	5'-ACC GTT CTC TGA ATA TGC TGC TGG GAA AAG GGG AAC GTC C-3'
mSOCS5 LCQQ Fwd	5'-CTT TCA GCC AGC AGT ATA TCC AGC GCG CAG TGA TCT GC-3'
mSOCS5 LCQQ Rev	5'-CTG CGC GCT GGA TAT ACT GCT GGC TGA AAG GGA AAG TTC-3'
mSOCS6 LCQQ Fwd	5'-GCTCGCAGCAGTACCTGCAGCGCTTTGTTATCCGTCAG-3'
mSOCS6 LCQQ Rev	5'-TAACAAAGCCGTGCAGGTACTGCTGCGAGCGCAAATGC-3'
mSOCS7 LCQQ Fwd	5'-TCAGCAATGTCAAGTCCCAACAGCATCTTCAAAGATTCCGGATCCGGCAGCT-3'
mSOCS7 LCQQ Rev	5'-AGCTGCCGGATCCGGAATCTTTGAAGATGCTGTTGGGACTTGACATTGCTGA-3'
mCISH LCQQ Fwd	5'-AGT GCC CGC AGC CAA CAA CAT CTG CAG CGG CTA GTC ATC-3'
mCISH LCQQ Rev	5'-GAT GAC TAG CCG CTG CAG ATG TTG TTG GCT GCG GGC ACT-3'

The pMXpuroII and pMXpuroII-shCul5 constructs were previously described (*143*).

pHAGE-Flag-HA-hSOCS2^{WT}, pHAGE-Flag-HA-hSOCS2^{LCQQ}, pHAGE-Flag-HA-hSOCS4^{WT}, pHAGE-Flag-HA-hSOCS5^{WT} and pHAGE-Flag-HA-hSOCS6^{WT} plasmids were made as follows. hSOCS2 was PCR amplified using Phusion taq polymerase (Thermo Fisher Scientific)

from MCF10A cDNA by Sashcha Straight. The hSOCS2 PCR product was then PCR amplified using PfuTurbo (Agilent Technology) with flanking attB sties. The attBhSOCS2 PCR product was moved it into the pDONR221 vector using a BP reaction (Thermo Fisher Scientific).

The pDONR221-hSOCS2^{LCQQ} was made using PfuTurbo DNA Polymerase (Agilent Technologies) to perform site directed mutagenesis using the following primers: hSOCS2 LC-QQ (Table 6.1). pLX304-hSOCS4, pLX304-hSOCS5, pLX304-hSOCS6 were obtained from the human ORFome (*345*) and moved it into the pDONR221 vector using a BP reaction (Thermo Fisher Scientific). The pDONR221-hSOCS2^{WT}, pDONR221-hSOCS2^{LCQQ}, pDONR221-hSOCS4^{WT}, pDONR221-hSOCS5^{WT}, and pDONR221-hSOCS6^{WT} were moved into the Gateway destination vector pHAGE-N-Flag-HA-IRES-PURO, a kind gift from Wade Harper (*182*), using a LR reaction (Thermo Fisher Scientific). The pHAGE-Flag-HA-hSOCS2 R73K was made by mutating pHAGE-Flag-HA-hSOCS2 WT using PfuTurbo DNA Polymerase (Agilent Technologies) to perform site directed mutagenesis using the following primers: hSOCS2 R73K (Table 6.1).

The pcDNA3.1-Myc-BirA-mSOCS2 and pcDNA3.1-Myc-BriA-mSOCS6 vectors were made as follows. The pcDNA3.1-Myc-BirA was purchased through Addgene (35700). The T7-mSOCS2 and T7-mSOCS6 were PCR amplified with 5' EcoRI and 3' KplI flanking sites from pCAG-T7-mSOCS2 and mSOCS6 using PfuTurbo (Agilent Technology). The PCR products were then subcloned into pcDNA3.1-Myc-BirA vector downstream of BirA.

The pcDNA5-Myc-BirA FRT/TO, pcDNA5-Myc-BirA-T7-mSOCS2 FRT/TO and pcDNA5-Myc-BirA-T7-mSOCS6 FRT/TO vectors were made as follows. The pcDNA5/FRT/TO vector (V6520202) was purchased from Thermo Fisher Scientific. A unique NheI site was introduced into the polylinker of the pcDNA5/FRT/TO vector. The Myc-BirA, Myc-BirA-T7-mSOCS2 and Myc-BirA-T7-mSOCS6 were PCR amplified with 5'-EcoRV and 3'-SpeI primers using Herculase II Fusion polymerase (Agilent) using the appropriate pcDNA3.1-Myc-BirA vector as a template. The PCR product was cut with EcoRV and SpeI and ligated into the altered pcDNA5/FRT/TO vector between EcoRV and NheI.

The pcDNA5-N-3xFlag-hSOCS2 FRT/TO and pcDNA5-N-3xFlag-mSOCS6 FRT/TO plasmids were made as follows. The mSOCS6 WT was PCR amplified with flanking attB sties from pCAG-T7-mSOCS6 using PfuTurbo (Agilent Technology) and moved into the pDONR221 vector using a BP reaction (Thermo Fisher Scientific). The destination vector pDEST-5'-TripleFlag pcDNA5 FRT TO with stop codon was a kind gift from Anne-Claude Gingras. The pDONR221-hSOCS2 and pDONR221-mSOCS6 were moved into pDEST-5'-TripleFlag pcDNA5 FRT TO using a LR reaction (Thermo Fisher Scientific).

pLKO.1-nontarget small hairpin RNA (shRNA) control vector (SHC002), pLKO.1-shSOCS2 vector (TRCN0000057058) and pLKO.1-shEphA2 vector (TRCN0000006403) were purchased from (Sigma Aldrich).

The Igk–Myc hEphA2 WT, hEphA2-ΔKD (aa 1–606 and 906–976), and hEphA2-ΔSAM (aa 1–886) were a kind gift from Hironori Katoh (*346*). Igk–Myc hEphA2-ΔJM (aa 1-565 and 613-975) was made using PfuTurbo DNA Polymerase (Agilent Technologies) and the following primers: hEphA2 ΔJM (Table 6.2). The Igk–Myc EphA2 single amino acid mutants were made using PfuTurbo DNA Polymerase (Agilent Technologies) and the primers listed in (Table 6.2).

Table 6.2 EphA2 SDM Primers

PRIMER	SEQUENCE
hEphA2_Y588F_Fwd	5'-TGG GGG TCC ACG AAT GTC TTC AGG GGC-3'
hEphA2_Y588F_Rev	5'-GCC CCT GAA GAC ATT CGT GGA CCC CCA-3'
hEphA2_Y594F_Fwd	5'-GTT GGG GTC CTC AAA TGT GTG GGG GTC CA-3'
hEphA2_Y594F_Rev	5'-TGG ACC CCC ACA CAT TTG AGG ACC CCA AC-3'
hEphA2_K464M_Fwd	5'-CCG GTG GCC ATC ATG ACG CTG AAA GCC-3'
hEphA2_K464M_Rev	5'-GGC TTT CAG CGT CAT GAT GGC CAC CGG-3'
Y685F_hEphA2_Fwd	5'-CAT CAT GGG CTT GAA TTT GGA GAT GAC GCC CTC T-3'
Y685F_hEphA2_Rev	5'-AGA GGG CGT CAT CTC CAA ATT CAA GCC CAT GAT G-3'
Y652F_hEphA2_R	5'-GCT GCT TCT CTG TGA AGC CGG CTT TCA GC-3'
Y652F_hEphA2_F	5'-GCT GAA AGC CGG CTT CAC AGA GAA GCA GC-3'
Y729F_hEphA2_F	5'-GTT GGC CAG GAA CTT CAT GCC AGC TGC GAT-3'
Y729F_hEphA2_R	5'-ATC GCA GCT GGC ATG AAG TTC CTG GCC AAC-3'
Y847F_hEphA2_Rev	5'-CAT GAG CTG GAA GAT GGC GGA GGG GC-3'
Y847F_hEphA2_Fwd	5'-GCC CCT CCG CCA TCT TCC AGC TCA TG-3'
Y818F_hEphA2_Fwd	5'-GAC AAC TCC CAG AAG GGC CGC TCG C-3'
Y818F_hEphA2_Rev	5'-GCG AGC GGC CCT TCT GGG AGT TGT C-3'
hEphA2_Y772F_Fwd	5'-CCG AGG CCA CCT TCA CCA CCA GTG G-3'
hEphA2_Y772F_Rev	5'-CCA CTG GTG GTG AAG GTG GCC TCG G-3'
hEphA2_Y735F_Fwd	5'-AGT ACC TGG CCA ACA TGA ACT TTG TGC ACC GTG-3'
hEphA2_Y735F_Rev	5'-CAC GGT GCA CAA AGT TCA TGT TGG CCA GGT ACT-3'
hEphA2_Y628F_Fwd	5'-CTT CAG CAT GCC CTT GAA CAC CTC CCC AAA CTC-3'
hEphA2_Y628F_Rev	5'-GAG TTT GGG GAG GTG TTC AAG GGC ATG CTG AAG-3'
hEphA2_Y694F_Fwd	5'-GGG CCC CAT TCT CCA TGA ACT CAG TGA TGA TCA TC-3'
hEphA2_Y694F_Rev	5'-GAT GAT CAT CAC TGA GTT CAT GGA GAA TGG GGC CC-3'
hEphA2_Y791F_Fwd	5'-GAA CTT CCG GAA GGA AAT GGC CTC CGG G-3'
hEphA2_Y791F_Rev	5'-CCC GGA GGC CAT TTC CTT CCG GAA GTT C-3'
hEphA2_Y813F_Fwd	5'-CGC TCG CCA AAG GTC ATC ACC TCC CAC-3'
hEphA2_Y813F_Rev	5'-GTG GGA GGT GAT GAC CTT TGG CGA GCG-3'
hEphA2_dJM_Fwd	5'-CAGCGTGCCCGCGTCACTCGGCAG-3'
hEphA2_dJM_Rev	5'-CTGCCGAGTGACGCGGGCACGCTG-3'

pEF-BOS-FLAG-mSOCS2 WT, mSOCS2 ΔNT, and mSOCS2 ΔSB were a kind gift from Amilcar Flores-Morales(*94*). The pEF-BOS-FLAG-mSOCS2 R73K was made using PfuTurbo DNA Polymerase (Agilent Technologies) and the following primers: mSOCS2 R73K (Table 6.1).

The pCAG-Flpe was purchased from Addgene (#13787). pOG44 was a kind gift from Anne-Claude Gingras.

The pCMV-dsRed-IRES-GFP-DEST, pCMV-dsRed-IRES-GFP-d1, pCMV-dsRed-IRES-GFP-d4, pCMV-dsRed-IRES-GFP-d24 and pCMV-dsRed-IRES-GFP-PolR2A plasmids were a kind gift from Sherry Yen (*174*).

The pCMV-dsRed-IRES-GFP-Cas WT was made as follows. Cas was PCR amplified using PfuTurbo (Agilent Technology) with flanking attB sties from pCAG-T7-Cas described previously (*171*). The attBCas PCR product was moved it into the pDONR221 vector using a BP reaction (Thermo Fisher Scientific). A LR reaction (Thermo Fisher Scientific) was performed to move Cas into the pCMV-dsRed-IRES-GFP-DEST vector.

6.2 CELL LINES

Flp-IN T-Rex 293 cells were purchased (Thermo Fisher Scientific) and grown in DMEM 10% FBS, 100 µg/mL Zeocin, 15 µg/mL Blasticidin. The Flp-IN T-Rex 293 cells were transfected with a corresponding FRT/TO vector and either pCAG-Flpe or pOG44 to flp in the gene of interest. The transfected cells were then selected in DMEM 10% Tet-Free FBS, 150 µg/mL Hygromycin B, 15 µg/mL Blasticidin and grown in this media from then on.

MCF10A cells were cultured in DMEM/F12 (Thermo Fisher Scientific) supplemented with 5% horse serum (Thermo Fisher Scientific), 20 ng/ml EGF (Thermo Fisher Scientific), 0.5 µg/ml hydrocortisone (Sigma-Aldrich, St. Louis, MO), 0.1 µg/ml cholera toxin (EMD Millipore, Billerica, MA), 10 µg/ml insulin, and penicillin/streptomycin both at 100 U/mL (Thermo Fisher Scientific). MCF10A cells stably expressing pMXpuroII empty vector or pMXpuroII-shCul5 have been previously described (*143*), they were grown in the presence of 2 µg/ml puromycin. The MCF10A cells stably expressing pLKO.1 shSOCS2 RNA were made as follows. Recombinant lentiviruses were packaged using HEK 293T cells, and infection carried out by standard protocols. After selection with 2 µg/ml puromycin cells were maintained in the presence of antibiotic.

HeLa, 293T, and MDA-MB-231 cells were cultured in DMEM supplemented with 10% FBS and penicillin/streptomycin both at 100 U/ml. Recombinant lentiviruses containing pLKO.1-shScrm,

shSOCS2, or shEphA2 were packaged using HEK 293T cells, and infections were carried out by standard protocols. After selection with 10µg/ml puromycin cells were maintained in the presence of antibiotic. Recombinant retroviruses containing pMXpuroII-shCul5 were packaged using HEK 293T cells, and infections were carried out by standard protocols. The cells were then selected and grown in 10µg/mL puromycin.

Cul5 CRISPR knockout MCF10A cells were made as follows. Double stranded DNA templates for in vitro transcription of guide RNAs were created by annealing and extending synthetic oligonucleotides (T7 promoter and *CUL5*-specific target sequence: TAATACGACTCACTATAggtgcatgcagtctgtctttGTTTTAGAGCTAGAA, guide RNA scaffold: AAAAGCACCGACTCGGTGCCACTTTTTCAAGTTGATAACGGACTAGCCTTATTTTAA CTTGCTATTTCTAGCTCTAAAAC) using Q5 DNA polymerase (NEB M0491). Guide RNAs were transcribed using the T7 HiScribe kit (NEB E2040) and purified by phenol-chloroform extraction and isopropanol precipitation. MCF10A cells at passage 13 from ATCC were plated in 12 well plates in standard growth media at ~50% confluence the day before transfection. Cells were transfected with 1µg Cas9 mRNA (5meC, Ψ, Trilink bio L6125) and 1 µg sgRNA using the Ribojuice mRNA transfection kit (EMD Millipore TR1013). Single cell clones were isolated by serial limiting dilution in 96 well plates, expanded into 24 well plates, and screened by Western blot using an antibody to cullin 5 (Abcam, ab184177). Genomic DNA was isolated using the QuickExtract™ DNA Extraction Solution (EpiBio QE09050) and the targeted region of *CUL5* was amplified by PCR using Immomix Red DNA polymerase (Bioline 25022) and the primers (forward: atgtgaggcaattacaagcgt, reverse: ctgtgtggactgatgtgtagcc). PCR products were cloned using the pGEM-T easy kit (Promega A1360). Twelve clones were sequenced and showed an equal distribution of two alleles with either a 2 or 20 bp deletion immediately 5' to the protospacer adjacent motif. Both deletions were predicted to produce early stop codons (W53Gfs*2 and D46Lfs*3 respectively).

The Flag-HA-SOCS2 MDA-MB-231 cells used to visualize SOCS2 localization were made as follows. Recombinant lentiviruses containing pHAGE-Flag-HA-hSOCS2^{WT}, pHAGE-Flag-HA-hSOCS2^{R73K} and pHAGE-Flag-HA-hSOCS2$^{LC\text{-}QQ}$ were packaged using HEK 293T cells, and

infections of MDA-MB-231 cells were carried out by standard protocols. After selection with 5 μg/ml puromycin cells were maintained in the presence of antibiotic.

The Flag-HA-SOCS 2, 4, 5, 6 MCF10A cell lines used for PAC proteomics were made as follows. Recombinant lentiviruses containing pHAGE-Flag-HA-hSOCS2^{WT}, pHAGE-Flag-HA-hSOCS4^{WT}, pHAGE-Flag-HA-hSOCS5^{WT}, and pHAGE-Flag-HA-hSOCS6^{WT} were packaged using HEK 293T cells, and infections of MCF10A cells were carried out by standard protocols. After selection with 2 μg/ml puromycin cells were maintained in the presence of antibiotic

The GPS cell lines were made as follows. Recombinant lentiviruses containing pCMV-dsRed-IRES-GFP-Cas, pCMV-dsRed-IRES-d1GFP, pCMV-dsRed-IRES-d4GFP, pCMV-dsRed-IRES-d24GFP and pCMV-dsRed-IRES-GFP-PolR2A were packaged using HEK 293T cells, and infections were carried out by standard protocols. After selection with 1 μg/ml puromycin cells were maintained in the presence of antibiotic.

6.3 Reagents and Antibodies

The following chemicals and recombinant proteins were used: AG1478 and Lapatinib (Cell Signaling Technology, Beverly, MA) SU6656 (EMD Millipore) U0126 and Sodium orthovanadate (Sigma-Aldrich, St Louis, MO) EfnA1-Fc (R&D Systems) and MLN4924 (Active Biochem).

The following antibodies were used: mouse anti-paxillin, mouse anti-EEA1, rabbit anti-Crk (BD Biosciences, San Jose, CA), rabbit anti-ElgB, mouse anti-IRS4, rabbit anti-Cas, rabbit anti-FAK, rabbit anti-GAPDH, rabbit anti-Cul5, mouse anti-Myc (9E10), IGF-IRα (G-5), mouse anti-EGFR (528), rabbit anti-p-EGFR (Tyr 845) and mouse anti-tubulin (Santa Cruz Biotechnology, Inc., Santa Cruz, CA), mouse anti-vinculin, rabbit anti-β-catenin, mouse anti-Flag (M2) (Sigma-Aldrich), mouse anti-EphA2 (8B6), rabbit anti-EphA2 (D4A2), and rabbit anti-EphA2 (pY588), rabbit anti-EphA2 (pY772), rabbit anti-EEA1, rabbit anti-Phospho-EGF Receptor (Tyr1045), rabbit anti-Phospho-EGF Receptor (Tyr1173), rabbit anti-IGF-I Receptor β (D23H3), rabbit anti-

Ezrin and rabbit anti-phospho-IGF-I Receptor β (Tyr 1135) (Cell Signaling Technology, Beverly, MA); mouse anti-T7 (EMD Millipore), mouse anti-HA (HA.11) (BioLegend, Dedham, MA) and rabbit anti-HA and rabbit anti-BCAR3 (Bethyl, Montgomery, TX) goat anti-human IgG Fc (Jackson ImmunoResearch Inc.) Insulin Receptor beta (Novusbio, Littleton, CO) mouse anti-EGFR AB-12 (Thermo Scientific) goat anti-human HB-EGF, goat anti-human amphiregulin, goat anti-human Epiregulin, (R&D Systems). 4G10 was made in house from the 4G10 hybridoma.

6.4 siRNA Sequences

The sequence of the siRNAs used in this dissertation are listed in Table 6.3.

Table 6.3 siRNA Sequences

siRNA	Target Sequence	Source
Control siRNA	5'-AATTCTCCGAACGTGTCACGT-3'	Qiagen
EphA2 siRNA Pool	5'-CAGCGCCAAGTAAACAGGGTA-3' 5'-AAGCGCCTGTTCACCAAGATT-3' 5'-AAGGAAGTGGTACTGCTGGAC-3' 5'-CGAGGTGATGAAAGCCATCAA-3'	Qiagen
SOCS2 siRNA Pool	5'-AACGGCACTGTTCACCTTTAT-3' 5'-CGCATTCAGACTACCTACTAA-3' 5'-CCAACTAATCTTCGAATCGAA-3' 5'-AAGAGGTAGCTAGGTGTTTAA-3'	Qiagen
Cul5 siRNA Pool	5'-GACACGACGTCTTATATTA-3' 5'-CGTCTAATCTGTTAAAGAA-3' 5'-GATGATACGGCTTTGCTAA-3' 5'-GTTCAACTACGAATACTAA-3'	GE Dharmacon
SOCS1 siRNA Pool	5'-TACCCAGTATCTTTGCACAAA-3' 5'-TAAAGTCAGTTTAGGTAATAA-3' 5'-TAGGATGGTAGCACACAACCA-3' 5'-CTGGTTGTTGTAGCAGCTTAA-3'	Qiagen
EGFR siRNA Pool	5'- CCCATCCAATTTATCAAGGAA-3' 5'- AAGCTCACGCAGTTGGGCACT-3' 5'- TACGAATATTAAACACTTCAA-3' 5'- ATAGGTATTGGTGAATTTAAA-3'	Qiagen
siCul5-586	5'-GGCAUACUUGGAUUCAACATT-3'	Thermo
siCul5-587	5'-CCCUCGUAUUUACAACAAATT-3'	Thermo
siCul5-588	5'-GGAAUAGUUCAACUACGAATT-3'	Thermo

6.5 PROLIFERATION ASSAY

MCF10A cells were plated at 2,000 cells/well in a 96 well plate. Immediately after plating 60µmol of pooled siRNA was transfected in using Lipofectamine2000. Sixteen hours following the siRNA transfection one plate was fixed with formalin for a zero-time point. The media was removed from the second plate and assay medium (DMEM/F12, 2% horse serum, 0 ng/ml EGF, 0.5 µg/mL hydrocortisone, 100 ng/mL cholera toxin, 10 µg/mL Insulin) was added to the cells. Cells with assay media were left in the incubator for 72 hours. At the end of the 72 hours the plate was fixed, each time point was stained with Crystal Violet, solubilized, measured and the fold increase in cell number was calculated.

6.6 QPCR OF RNA ABUNDANCE

RNA was extracted using the Qiagen RNeasy Mini kit. cDNA was synthesized using the iScript kit (BioRad). The abundance of the cDNA was measured by qPCR using the iTaq Universal SYBR Green Supermix kit (BioRad), and run on the 7900HT Real Time PCR System or QuantStudio 5 Real Time (qPCR) System using the SDS software or QuantStudio respectively (Applied Biosystems). The primers used are listed in Table 6.4.

Table 6.4 qPCR Primers

PRIMER	Sequence
EPHA2 FORWARD	5'-CTGGTCTGCAAGGTGTCTGA-3'
EPHA2 REVERSE	5'-TTGGACAACTCCCAGTAGGG-3'
EFNA1 FORWARD	5'-CACACCGTCTTCTGGAACAG-3'
EFNA1 REVERSE	5'-CTCATGCTCCACCAGGTACA-3'
CUL5 FORWARD	5'-TTTTATGCGCCCGATTGTTTTG-3'
CUL5 REVERSE	5'-TTGCTGGGCCTTTATCATCCC-3'
SOCS2 FORWARD	5'-CAGATGTGCAAGGATAAGCGG-3'
SOCS2 REVERSE	5'-GCGGTTTGGTCAGATAAAGGTG-3'
GAPDH FORWARD	5'-CAGCCTCAAGATCATCAGCA-3'
GAPDH REVERSE	5'-TGTGGTCATGAGTCCTTCCA-3'
EGF FORWARD	5'-GCC AAG CAG TCT GTG ATT GA-3'
EGF REVERSE	5'-CTG ATG GCA TAG CCC AAT CT-3'
HB-EGF FORWARD	5'-GGC AGA TCT GGA CCT TTT GA-3'
HB-EGF REVERSE	5'-CCC CTT GCC TTT CTT CTT TC-3'
BTC FORWARD	5'-TGG GAA TTC CAC CAG AAG TC-3'
BTC REVERSE	5'-CCT TTC CGC TTT GAT TGT GT-3'
EREG FORWARD	5'-CGT GTG GCT CAA GTG TCA AT-3'
EREG REVERSE	5'-AGT GTT CAC ATC GGA CAC CA-3'
EPGN FORWARD	5'-TGA CAG CAC TGA CCG AAG AG-3'
EPGN REVERSE	5'-ATC TTC CAG GCA AAG GTG TG-3'
TGF-α FORWARD	5'-TCG CTC TGG GTA TTG TGT TG-3'
TGF-α REVERSE	5'-GGG AAT CTG GGC AGT CAT TA-3'
NRG2 FORWARD	5'-TTC CTA CCG TTG GTT CAA GG-3'
NRG2 REVERSE	5'-TCC TCC ACC TTC ACC TTG TT-3'
NRG4 FORWARD	5'-GGT CCC AGT CAC AAG TCG TT-3'
NRG4 REVERSE	5'-GAG CCT GGG AGA AAA ACC TC-3'
NRG1 FORWARD	5'-TAC ATC CAC CAC TGG GAC AA-3'
NRG1 REVERSE	5'-ACT CCC CTC CAT TCA CAC AG-3'
INSR FORWARD	5'-TGCCAGTGATGTGTTTCCAT-3'
INSR REVERSE	5'-TGAGGAACTCAATCCGCTCT-3'
IGF-IR FORWARD	5'-ATG CTG ACC TCT GTT ACC TCT-3'
IGF-IR REVERSE	5'-GGCTTATTCCCCACAATGTAGTT-3'

6.7 DNA TRANSFECTIONS, CELL LYSIS, WESTERN ANALYSIS

HeLa cells were plated at 80% confluence in either a 6cm or 6-well plates. A DNA/Lipofectamine 2000 (Thermo Fisher Scientific) mixture, made according to manufacture

protocol, was added to the cells immediately after plating and left on the cells for 4hrs. Around 24 or 48hrs later cells were washed two times in phosphate-buffered saline (PBS) and lysed in X-100 buffer (1% X-100, 150mM NaCl, 10mM HEPES (pH 7.4), 2mM EDTA, 50mM NaF) with fresh protease inhibitors (10µg/mL Aprotinin, 10µg/mL Leupeptin, 1mM Sodium Vanadate, 1mM PMSF).

Proteins were resolved by SDS-PAGE using a 30:1 acrylamide:bisacrylamide ratio and subsequently transferred onto nitrocellulose membrane. The membrane was blocked in Odyssey Blocking Buffer (PBS) (LI-COR Biosciences-U.S.) for phosphotyrosine antibodies or 5% non-fat dry milk in Tris-buffered saline with 0.1% Tween (all other antibodies), probed first with the indicated primary, followed by either IRDye 680RD goat anti-mouse or IRDye 800CW goat anti-rabbit conjugated secondary antibodies and visualized using the Odyssey Infrared Imaging System (LI-COR Biosciences-U.S.).

6.8 FLOW CYTOMETRY

293T cells stably expressing GPS constructs were transfected with the indicated constructs using Lipofectamine2000. Twenty-four hours after transfection the cells were then treated with the indicated drugs for the indicated amount of time. Cells were then trypsinized, spun down, washed and re-suspended in PBS.

Cells were analyzed on a Becton Dickinson LSRII machine. Ratio scaling was used in Diva software (BD Bioscience) to get a GFP/dsRed ratio. Plots were made using FlowJo software (FLOWJO, LLC).

6.9 IMMUNOPRECIPITATION

Immunoprecipitation of T7, EphA2, EGFR, Myc tagged proteins was performed as described in (*143*). The Flag immunoprecipitation was performed as previously described with the following changes: anti-Flag M2 magnetic beads (Sigma-Aldrich) were used instead of antibody and AG beads. Unless otherwise noted all immunoprecipitations were stimulated with 1 mM pervanadate for 30 min prior to cell lysis. Immunoprecipitation from cells stimulated with EfnA1-Fc (R&D

Systems) or hIgG1 Fc (Life Technologies) had the following changes. T7-tagged SOCS2 or GFP proteins were transfected into HeLa cells using Lipofectamine2000. Twenty-four hours after transfection, cells were washed twice with PBS and starved in DMEM 0.5% BSA overnight. The following day cells were stimulated with either 1 µg/mL EfnA1-Fc or Fc for the corresponding amount of time, lysed on ice in cold X-100 buffer containing fresh protease inhibitors, followed by centrifugation for 15 minutes at 14,000 g. Lysates were rotated with mouse anti-T7 antibody for 2 hours at 4◦C. Anti-mouse IgG Sepharose Bead Conjugate (Cell Signaling Technology) was added to the lysate and antibody mix for 1 hour at 4◦C. After centrifugation, the protein–antibody–bead complex was washed three times in lysis buffer, re-suspended in Laemmli buffer, then resolved by SDS-PAGE.

6.10 IMMUNOFLUORESCENCE

MDA-MB-231 cells were plated on 12 mm glass coverslips, coated with 1 mg/mL poly-L-lysine (Sigma Aldrich) in borate buffer (40 mM boric acid, 19 mM sodium tetraborate, pH 8.5) for 24 hr. Cells were washed twice with PBS and starved in DMEM, 0.5% BSA, 10 mM HEPES for 4 hr. The cells were then moved onto wet ice, washed one time in ice cold PBS followed by the addition of DMEM 0.5% BSA, 10 mM HEPES containing 1 µg/mL EphrinA1-Fc or 1 µg/mL Fc. The plate was incubated with the ligand on wet ice at 4°C for 1 hr. At the end of the hour the coverslips were washed three times with ice cold PBS, followed by the addition of 37°C DMEM 0.5% BSA, 10 mM HEPES. The coverslips were moved to a water bath in an incubator. Cells were fixed in 4% PFA in PBS at 4°C for 30 minutes at each corresponding time point. Cells were then permeabilized with 0.1% Triton X-100 in PBS for 5 min at 25°C, washed in PBS and blocked for 1 hr in 5% normal goat serum or 5% BSA in PBS before primary antibody was added for either for 1 hr at 25°C or overnight at 4°C. Coverslips were rinsed in PBS before the addition of Alexa Fluor 488-, Alexa Fluor 568- or Alexa Fluor 647-conjugated secondary antibodies, diluted (1:1,000), for 1 h at 25°C. After several PBS rinses, coverslips were mounted in ProLong Gold with DAPI solution. For the stainings containing the anti-hFc antibody, a two-step staining protocol was followed to prevent cross reactivity with the rabbit primary. Briefly, cells were blocked, incubated with anti-hFc, Alexa Fluor 568- secondary, blocked, incubated with rabbit and mouse primary antibodies and finally with Alexa Fluor 488- and Alexa Fluor 647-conjugated secondary antibodies.

6.11 IMAGING AND IMAGE ANALYSIS

Fixed cells were visualized using a 40x, 60x or 100× numerical aperture (NA) 1.4 oil objective on a DeltaVision IX70 microscope (Olympus). Images were recorded using fixed camera settings (IX- HLSH100; Olympus). Images were acquired and deconvolved using softWoRx (Applied Precision, Issaquah, WA), and all exposure times were equal within an experiment. Deconvolved images from single plane in the cells or maximum intensity *z*-projections were used in the figures. Image scaling was equal for all images in a panel with the following exceptions Figure 3.6a 488 channel upper contrast, 594 upper contrast; Figure 3.6b 488 channel upper contrast, 594 upper contrast; Figure 3.6c 488 upper and lower contrast and 594 upper contrast. Figures were assembled using Canvas (ACD Systems) software.

To quantify co-localization between EphA2 and Flag-HA-SOCS2^{LCQQ} entire z-sections were moved into Volocity software (PerkinElmer) and EphA2 vesicles were identified using the find object function with these settings (Intensity=1750-Max and Size>0.2 μm). The mean EphA2 and Flag intensity in these objects are reported on the graphs.

6.12 QUANTITATIVE PHOSPHOTYROSINE MASS SPECTROMETRY

6.12.1 *Reduction, Alkylation, and Tryptic Digestion*

Cells were lysed in 8 M urea (Sigma) and were quantified using BCA assay (Pierce). Proteins were reduced with 10 mM dithiothreitol (Sigma) for 1 hour at 56^{o}C and then alkylated with 55 mM iodoacetamide (Sigma) for 1 hour at 25^{o}C in the dark. Proteins were then digested with modified trypsin (Promega) at an enzyme/substrate ratio of 1:50 in 100 mM ammonium acetate, pH 8.9 at 25^{o}C overnight. Trypsin activity was halted by addition of acetic acid (99.9%, Sigma) to a final concentration of 5%. After desalting using a C18 Sep-Pak Plus cartridge (Waters), peptides were lyophilized and store at -80^{o}C.

6.12.2 *TMT labeling*

Peptide labeling with TMT 6plex (Thermo) was performed per manufacturer's instructions. Lyophilized samples were dissolved in 70 µL ethanol and 30 µL of 500 mM triethylammonium bicarbonate, pH 8.5, and the TMT reagent was dissolved in 30 µL of anhydrous acetonitrile. The solution containing peptides and TMT reagent was vortexed and incubated at room temperature for 1 hour. Samples labeled with the six different isotopic TMT reagents were combined and concentrated to completion in a vacuum centrifuge.

6.12.3 *Phosphopeptide enrichment*

For immunoprecipitation, protein G agarose (60 µL, Millipore) was incubated with anti-phosphotyrosine antibodies (12 µg 4G10 (Millipore), 12 µg PT66 (Sigma), and 12 µg PY100 (CST)) in 400 µL of IP buffer (100 mM Tris, 100 mM NaCl, and 1% Nonidet P-40, pH 7.4) for 8 hours at 4^{o}C with rotation. The antibody conjugated protein G was washed with 400 µL of IP buffer. The TMT labeled peptides were dissolved in 400 µL IP buffer and the pH was adjusted to 7.4. The TMT labeled peptides were then incubated with the antibody conjugated protein G overnight at 4^{o}C with rotation. The agarose was washed with 400 µL IP buffer followed by four rinses with 400 µL rinse buffer (100 mM Tris, pH 7.4). Peptides were eluted with 70 µL of 100 mM glycine, pH 2 for 30 minutes at 25^{o}C. Offline immobilized metal affinity chromatography (IMAC) was used to further enrich for phosphotyrosine peptides (*347*).

6.12.4 *LC-MS/MS*

Peptides were loaded on a precolumn and separated by reverse phase HPLC using an EASY-nLC1000 (Thermo) over a 140 minute gradient before nanoelectrospray using a QExactive Plus mass spectrometer (Thermo). The mass spectrometer was operated in a data-dependent mode. The parameters for the full scan MS were: resolution of 70,000 across 350-2000 *m/z*, AGC 3e^{6}, and maximum IT 50 ms. The full MS scan was followed by MS/MS for the top 10 precursor ions in each cycle with a NCE of 34 and dynamic exclusion of 30 s. Raw mass spectral data files (.raw) were searched using Proteome Discoverer (Thermo) and Mascot version 2.4.1 (Matrix Science). Mascot search parameters were: 10 ppm mass tolerance for precursor ions; 15 mmu for fragment ion mass tolerance; 2 missed cleavages of trypsin; fixed modification were carbamidomethylation of cysteine and TMT 6plex modification of lysines and peptide N-termini;

variable modifications were methionine oxidation, tyrosine phosphorylation, and serine/threonine phosphorylation. TMT quantification was obtained using Proteome Discoverer and isotopically corrected per manufacturer's instructions, and were normalized to the mean relative protein quantification ratios obtained from a total protein analysis. For the total protein analysis, 0.2% of the supernatant from the phosphotyrosine peptide immunoprecipitation was analyzed via LC-MS/MS. This analysis serves as a loading control as it gives quantitation for the most abundant non-phosphorylated peptides. Mascot peptide identifications, phosphorylation site assignments, and quantification were verified manually with the assistance of CAMV(*190*). The validated data was analyzed in excel using a one sided two-sample equal variance T-Test.

6.13 BirA and Triple Flag Affinity Purification Mass Spectrometry

6.13.1 *Triple Flag Affinity Purification*

For the FLAG pull-downs, 2x150 cm^2 dishes of 3xFLAG, 3xFlag-SOCS2 or 3xFLAG-SOCS6 293 T-REx cells were grown to 80% confluence then treated with 75 μM vanadate, 1 μM MLN4924, 1 μg/mL Doxycycline for 24 hr. They were then washed twice in 20 mL PBS, scraped into PBS, pooled and collected by centrifugation at 5,000x*g* for 5 min at 4°C. Cell pellets were snap frozen in dry ice and stored at −80 °C until lysis. The cell pellet was weighed and 1:4 pellet weight/lysis buffer (by volume) was added. Lysis buffer consisted of 50 mM HEPES-KOH (pH 8.0), 100 mM KCl, 2 mM EDTA, 0.1% Nonidet P-40, 10% glycerol, 1 mM PMSF, 1 mM DTT and 1x protease inhibitor mixture tablet (Sigma-Aldrich). Upon addition of lysis buffer, cells were incubated in a 37°C water bath with continuous agitation until the pellet melted, then transferred to dry ice for 10 min, subjected to one additional freeze-thaw cycle, and centrifuged at 16,000×*g* for 20 min at 4°C. Supernatant was transferred to a fresh conical tube and 25 μL of a 50% slurry FLAG-M2 magnetic beads (Sigma-Aldrich) were added. The mixture was incubated for 2 hr at 4°C with end-over-end rotation. Beads were pelleted by centrifugation at 100 × *g* for 1 min, magnetized, supernatant was removed and transferred with 1 mL of lysis buffer to a fresh centrifuge tube. Beads were washed three times with 1mL rinsing buffer (20 mM Tris-HCl pH 8.0, 2 mM $CaCl_2$). After the last wash, the beads were pelleted at 500xg for 1 min and all the liquid was removed. The beads were re-suspended in 20 mM Tris-

HCl pH 8.0 with 500 ng trypsin (T6567, Sigma-Aldrich) and incubated with end over end rotation at 37°C for 4hr. The supernatant was then removed and the beads were re-suspended in 20 mM Tris-HCl pH 8.0 with 500 ng trypsin and incubated overnight at 37°C. Following the overnight trypsin digestion, the supernatant was removed, combined, formic acid was added to the peptides to 2% final concentration and then the peptides were stored at -20°C before analysis.

6.13.2 *BirA Affinity Purification*

For the BirA pull downs, 4x150 cm^2 dishes of Myc-BirA, Myc-BirA-T7-SOCS2 or Myc-BirA-T7-SOCS6 293 T-REx cells were grown to 80% confluence then treated with 75 µM vanadate, 1 µM MLN4924, 1 µg/mL Doxycycline and 2 mM Biotin for 24 hr. At the end of the 24 hr they were washed twice in 20mL PBS, scraped into PBS, pooled and collected by centrifugation at 5,000xg for 5 min at 4°C. Cell pellets were snap frozen in dry ice and stored at −80°C until lysis. Pellets were lysed in 2 mL of RIPA lysis buffer (50 mM Tris-HCl pH 7.5, 150 mM NaCl, 1 mM EDTA, 1 mM EGTA, 1% NP-40, 0.1% SDS, 10 mM NaF, 250 µM vanadate,1x cOmplete mini EDTA-free protease inhibitor cocktail (Sigma-Aldrich), 250 U Benzonase Nuclease (Santa Cruz Biotechnology)) at 4°C for 1 hr with agitation, then sonicated (10 sec on and 3 sec off a total of three times at 35% power) to disrupt visible aggregates. The lysate was centrifuged at 21000×g for 30 min. Clarified supernatants were incubated with 30 µL packed, pre-equilibrated streptavidin-Sepharose high performance beads (GE) with end over end agitation at 4°C for 3 hr. Beads were collected by centrifugation 400xg 1 min, supernatant was removed and transferred with 1 mL of RIPA lysis buffer to a fresh centrifuge tube. Beads were washed one more time with RIPA, two times with 1 mL TAP buffer (50 mM HEPES-KOH pH 8.0, 100 mM KCl, 10% glycerol, 2 mM EDTA, 0.1% NP-40) and washed three times with 50 mM ammonium bicarbonate pH 8.0. After the last wash the beads were pelleted at 500xg for 1 min and all the liquid was removed. The beads were re-suspended in 50 mM ammonium bicarbonate pH 8.0 with 1 µg trypsin (T6567, Sigma-Aldrich) and incubated at 37°C with end over end agitation overnight. The supernatant containing the tryptic peptides was collected and lyophilized. The next morning 500 ng of trypsin was added to the beads and incubated at 37°C for two more hours. The supernatant was removed from the beads, the beads were washed two times with mass spec grade water. The washes and supernatant were combined and lyophilized in the speed

vac. The lyophilized peptides were cleaned using ZipTip™ C18 (Millipore Corporation) before the MS analysis.

6.13.3 *LC-MS/MS*

LC-MS/MS analysis was performed with an Easy-nLC 1000 (Thermo Scientific) coupled to an Orbitrap Elite mass spectrometer (Thermo Scientific). The LC system configured in a vented format (*348*) consisted of a fused-silica nanospray needle (PicoTip™ emitter, 75 µm ID, New Objective) packed in-house with Magic C18 AQ 100Å reverse-phase media (Michrom Bioresources Inc.) (25 cm), and a trap (IntegraFrit™ Capillary, 100 µm ID, New Objective) containing Magic C18 AQ 200Å (2 cm). The peptide sample was diluted in 10 µL of 2% acetonitrile and 0.1% formic acid in water and 8 µL was loaded onto the column and separated using a two-mobile-phase system consisting of 0.1% formic acid in water (A) and 0.1% acetic acid in acetonitrile (B). A 90 minute gradient from 7% to 35% acetonitrile in 0.1% formic acid at a flow rate of 400 nL/minute was used for chromatographic separations. The mass spectrometer was operated in a data-dependent MS/MS mode over the m/z range of 400-1800. The mass resolution was set at 240,000. For each cycle, the 20 most abundant ions with +2 and +3 charges states from the scan were selected for MS/MS analysis using 35% normalized collision energy. Selected ions were dynamically excluded for 15 seconds.

6.13.4 *Max Quant Data Search*

The MaxQuant peptide identification and label-free quantification was performed as previously described with the following parameters (*349*). The UniProt Reviewed 9606 human proteome and the contaminats.fasta were used for searching. Variable modifications: Oxidation (M), Acetyl (Protein N-term), and Biotinylated (K). Fixed Modifications Carbamidomethyl (C). Enzyme Trypsin with 2 maximum missed cleavages. Peptide false discovery rate 0.01. Minimum peptide length 7 and maximum peptide mass 4600. Minimum delta score for unmodified peptides 0 and minimum score for unmodified peptides 0. Minimum delta score for modified peptides 6 and minimum score for modified peptides 40.

6.13.5 *Data Filtration*

The average of the top three peptide intensities were used to estimate protein abundance in each biological replicate. The three biological replicate were then run through the SAINTq software with the default settings (*263*). *Bona Fide* Flag interacting proteins had a SAINT score >0.666, corresponding to a Bayesian false discovery rate <7.7%. *Bona Fide* BirA interacting proteins had a SAINT score >0.675, corresponding to a Bayesian false discovery rate <10%.

The top interactions were then imported into Cytoscape and the STRING database was used to determine the interactions between the *Bona Fide* interacting proteins.

APPENDIX

Supplement Figure 1-Cullin5 is depleted in cell Lines used in the quantitative phosphotyrosine mass spectrometry experiment

The three MCF10A biological replicates used in the quantitative phosphotyrosine mass spectrometry experiment were lysed and Cullin5 depletions was checked using Western blotting.

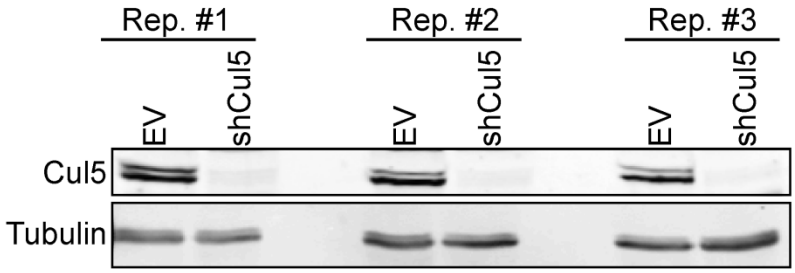

Supplement Figure 2-Ezrin, EphA2, Crk, IRS4, β-Catenin, and CRL5 are strongly biotinylated by BirA-SOCS2.

HeLa cells were transiently transfected with either Myc-BirA, Myc-BirA-SOCS6WT, Myc-BirA-SOCS2WT or Myc-BirA-SOCS2R73K. Twenty-four hours after transfection the cells were stimulated with 75 μM sodium orthovandate, 2 mM Biotin and 1 μM MLN4924 (where indicated) for twenty-four hours. Following the stimulation, the cells were lysed and biotinylated proteins were pulled out using streptavidin agarose beads. The whole cell extract represents 2% of the lysate used for the pull down.

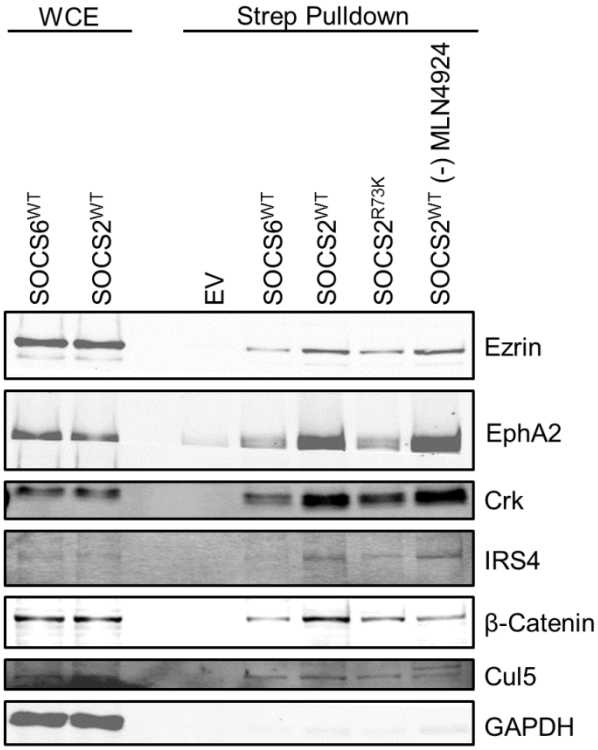

Supplement Figure 3- Myc-EphA2K646M is not autophosphorylated in shControl or shEphA2 HeLa cells.

HeLa shScrm or shEphA2 cells were transiently transfected with either Myc-EphA2^{WT} or Myc-EphA2^{K646M}. Twenty-four hours after transfection the cells were stimulated with 1 mM pervanadate for 30 min, lysed, immunoprecipitated with antibody to Myc and protein A/G beads. The whole cell extract represents 15% of the lysate used for the pull down.

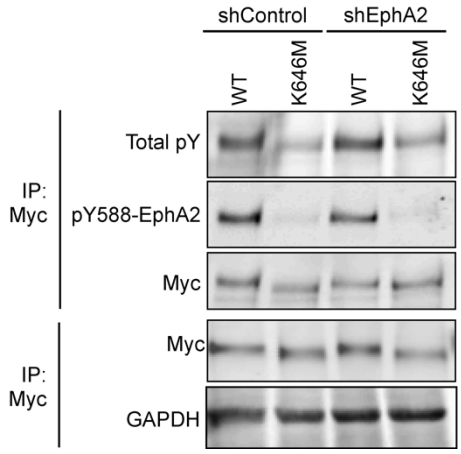

Supplement Figure 4-Single YF mutations in the EphA2 kinase domain do not disrupt binding between EphA2 and SOCS2.

(a) Cartoon crystal structure of the EphA2 kinase domain (PDB: 1MQB), with every tyrosine displayed in green. (b, c) Eleven single tyrosine to phenylalanine point mutants in Myc-EphA2 can all bind to T7-SOCS2^{LCQQ}. HeLa cells were transiently transfected with T7-SOCS2^{LCQQ} and the indicated Myc-EphA2 construct. Twenty-four hours after transfection the cells were stimulated with 1 mM pervanadate for 30 min, lysed and immunoprecipitated with antibody to T7 and protein A/G beads. (d) The Myc-EphA2 Y729F, Y772F and Y729/772F mutants are all phosphorylated in 293T cells. 293T cells were transiently transfected with the indicated Myc-EphA2 construct. Twenty-four hours after transfection the cells were stimulated with 1 mM pervanadate for 30 min, lysed and immunoprecipitated with antibody to Myc and protein A/G beads. The whole cell extract represents the following percent of the lysate used for the pull down: panel a 10%, panel c 5% and panel d 7.5%.

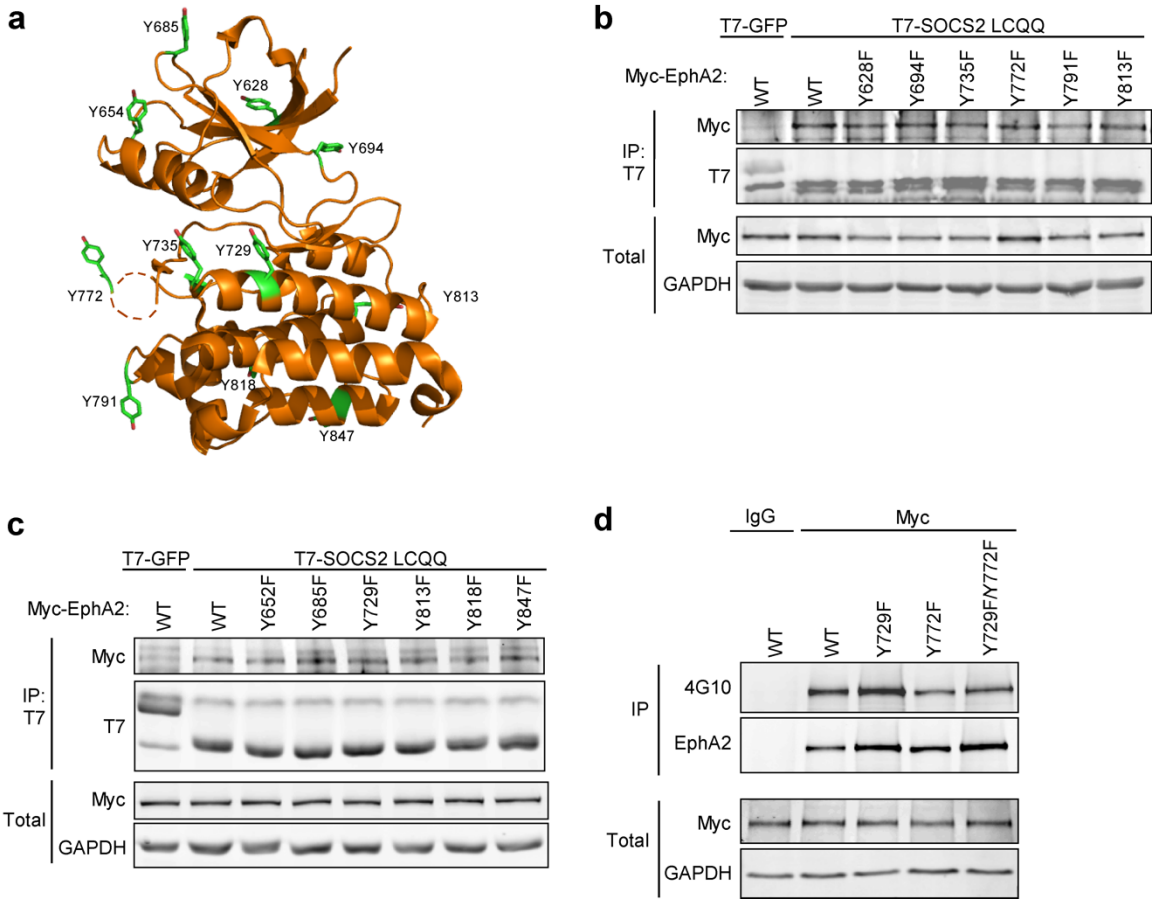

Supplement Figure 5-EphA2 pY588 antibody is specific but the pY771 antibody picks up background bands.

(a) Analysis of the specificity of pY588 and pY772 EphA2 antibodies in whole cell extract. HeLa shScrm or shEphA2 cells were starved in DMEM 0.5% BSA 10 mM HEPES for 16 hrs then stimulated with 1 µg/mL EprinA1-Fc or left un-stimulated for 5 min. The cells were lysed and analyzed with the indicated antibodies. (b) The pY588 and pY772-EphA2 antibodies are specific for their site when EphA2 is immunoprecipitated. HeLa cells were transiently transfected with the indicated Myc-EphA2 constructs. Twenty-four hours after transfection the cells were stimulated with 1 mM pervanadate for 30 min, lysed and immunoprecipitated with antibody to Myc and protein A/G beads.

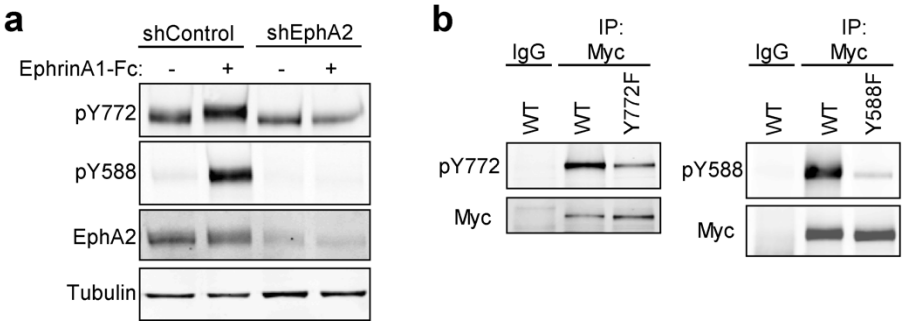

Supplement Figure 6-EphA2 and EfnA1 expression levels in different cell lines, and stimulation of EphA2 phosphorylation by EfnA1-Fc at 0°C

(a) MDA-MD-231 cells have high EphA2 and low EfnA1 RNA compared to MCF10A and HeLa cells. RNA was harvested from un-stimulated HeLa, MCF10A and MDA-MB-231 cells. A SYBR green qPCR was performed on the cDNA from each of these cells lines and gene expression was calculated using the ΔΔCt method. Bars are mean and standard deviation of three biological independent experiments. (b) EfnA1 stimulates EphA2 phosphorylation at 0°C. MDA-MB-231cells were starved in DMEM, 0.5% BSA, 10 mM HEPES for 4 hr followed by a 1 hr incubation with EfnA1-Fc or Fc (1 µg/mL) on ice. The ligand was washed off and the cells were placed at 37°C for the indicated times. Cells were lysed and immunoprecipitated with antibody to EphA2 and protein A/G beads.

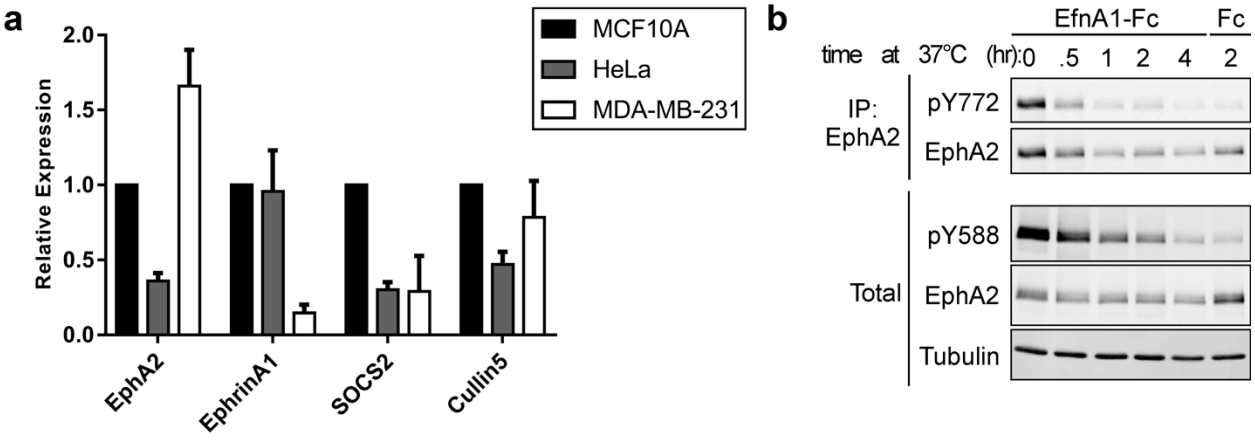

Supplement Figure 7-EphA2 and EfnA1-Fc co-localize.

MDA-MB-231 cells were starved in DMEM 0.5% BSA 10 mM HEPES for 4 hrs followed by a 1 hr incubation with EfnA1-Fc (1 µg/mL) on ice. The ligand was washed off the cells and the cells were moved to 37°C for the indicated amount of time before fixation. Fixed and permeabilized cells were stained with anti-EphA2, anti-Fc and appropriate secondary antibodies. Images are maximum intensity projections of three Z-sections. The EphA2 and EfnA1 brightness/contrast is unequal in some images to allow for easy visualization. Scale bar: 15 µm.

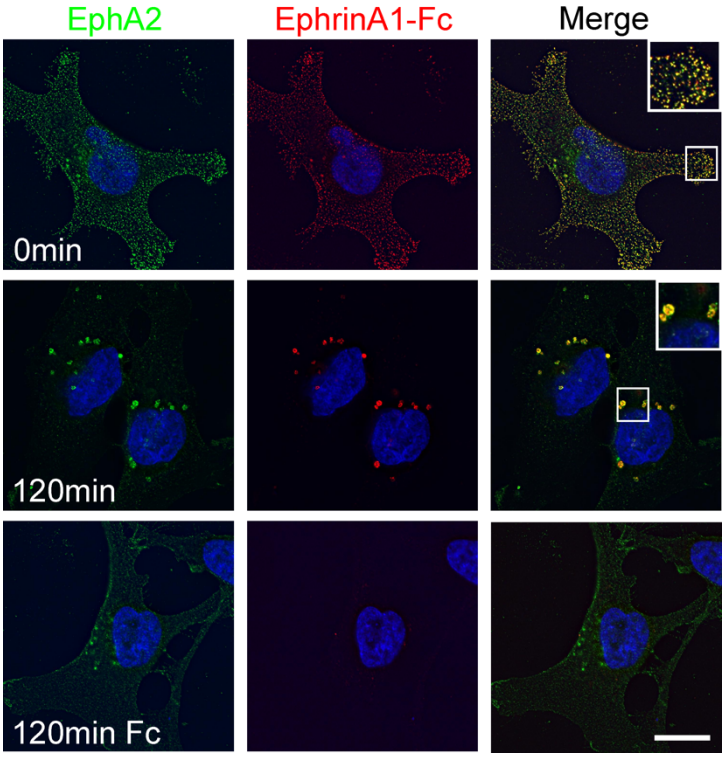

REFERENCES

1. U. K. Friedrich Marks, Karin Müller-Decker, *Cellular Signal Processing: An Introduction to the Molecular Mechanisms of Signal Transduction*. (Garland Science, Taylor and Francis Group, LLC, New York, NY, 2009).
2. S. R. Hubbard, J. H. Till, Protein tyrosine kinase structure and function. *Annual review of biochemistry* **69**, 373-398 (2000).
3. G. Manning, D. B. Whyte, R. Martinez, T. Hunter, S. Sudarsanam, The protein kinase complement of the human genome. *Science (New York, N.Y.)* **298**, 1912-1934 (2002).
4. D. L. Wheeler, Y. Yarden, SpringerLink (Online service). pp. XVII, 878 p. 100 illus., 879 illus. in color.
5. M. A. Lemmon, J. Schlessinger, Cell signaling by receptor tyrosine kinases. *Cell* **141**, 1117-1134 (2010).
6. Z. Lu, T. Hunter, Degradation of activated protein kinases by ubiquitination. *Annual review of biochemistry* **78**, 435-475 (2009).
7. B. A. Liu, B. W. Engelmann, P. D. Nash, The language of SH2 domain interactions defines phosphotyrosine-mediated signal transduction. *FEBS letters* **586**, 2597-2605 (2012).
8. J. Schlessinger, M. A. Lemmon, SH2 and PTB domains in tyrosine kinase signaling. *Science's STKE : signal transduction knowledge environment* **2003**, RE12 (2003).
9. J. A. Wells, A. A. Kossiakoff, Cell biology. New tricks for an old dimer. *Science (New York, N.Y.)* **344**, 703-704 (2014).
10. J. S. Rawlings, K. M. Rosler, D. A. Harrison, The JAK/STAT signaling pathway. *Journal of cell science* **117**, 1281-1283 (2004).
11. G. S. Martin, The hunting of the Src. *Nature reviews. Molecular cell biology* **2**, 467-475 (2001).
12. S. M. Thomas, J. S. Brugge, Cellular functions regulated by Src family kinases. *Annual review of cell and developmental biology* **13**, 513-609 (1997).
13. C. Wu, Focal adhesion: a focal point in current cell biology and molecular medicine. *Cell adhesion & migration* **1**, 13-18 (2007).
14. W. J. Hendriks, A. Elson, S. Harroch, A. W. Stoker, Protein tyrosine phosphatases: functional inferences from mouse models and human diseases. *The FEBS journal* **275**, 816-830 (2008).
15. C. M. Pickart, Back to the future with ubiquitin. *Cell* **116**, 181-190 (2004).
16. M. B. Metzger, V. A. Hristova, A. M. Weissman, HECT and RING finger families of E3 ubiquitin ligases at a glance. *Journal of cell science* **125**, 531-537 (2012).
17. K. N. Swatek, D. Komander, Ubiquitin modifications. *Cell research* **26**, 399-422 (2016).
18. L. K. Goh, A. Sorkin, Endocytosis of receptor tyrosine kinases. *Cold Spring Harbor perspectives in biology* **5**, a017459 (2013).
19. Y. Zwang, Y. Yarden, Systems biology of growth factor-induced receptor endocytosis. *Traffic (Copenhagen, Denmark)* **10**, 349-363 (2009).
20. S. Mayor, R. E. Pagano, Pathways of clathrin-independent endocytosis. *Nature reviews. Molecular cell biology* **8**, 603-612 (2007).
21. E. Boucrot *et al.*, Endophilin marks and controls a clathrin-independent endocytic pathway. *Nature* **517**, 460-465 (2015).
22. M. D. Marmor, Y. Yarden, Role of protein ubiquitylation in regulating endocytosis of receptor tyrosine kinases. *Oncogene* **23**, 2057-2070 (2004).
23. J. S. Bonifacino, L. M. Traub, Signals for sorting of transmembrane proteins to endosomes and lysosomes. *Annual review of biochemistry* **72**, 395-447 (2003).
24. L. M. Traub, Tickets to ride: selecting cargo for clathrin-regulated internalization. *Nature reviews. Molecular cell biology* **10**, 583-596 (2009).
25. J. M. Backer *et al.*, The insulin receptor juxtamembrane region contains two independent tyrosine/beta-turn internalization signals. *The Journal of cell biology* **118**, 831-839 (1992).
26. C. R. Haft, R. D. Klausner, S. I. Taylor, Involvement of dileucine motifs in the internalization and degradation of the insulin receptor. *The Journal of biological chemistry* **269**, 26286-26294 (1994).
27. I. Hamer *et al.*, Dual role of a dileucine motif in insulin receptor endocytosis. *The Journal of biological chemistry* **272**, 21685-21691 (1997).
28. P. Morrison, K. C. Chung, M. R. Rosner, Mutation of Di-leucine residues in the juxtamembrane region alters EGF receptor expression. *Biochemistry* **35**, 14618-14624 (1996).
29. D. Prager, H. L. Li, H. Yamasaki, S. Melmed, Human insulin-like growth factor I receptor internalization. Role of the juxtamembrane domain. *The Journal of biological chemistry* **269**, 11934-11937 (1994).
30. E. Klapisz *et al.*, A ubiquitin-interacting motif (UIM) is essential for Eps15 and Eps15R ubiquitination. *The Journal of biological chemistry* **277**, 30746-30753 (2002).
31. S. Polo *et al.*, A single motif responsible for ubiquitin recognition and monoubiquitination in endocytic proteins. *Nature* **416**, 451-455 (2002).
32. S. Sigismund *et al.*, Clathrin-independent endocytosis of ubiquitinated cargos. *Proceedings of the National Academy of Sciences of the United States of America* **102**, 2760-2765 (2005).
33. R. Villasenor, Y. Kalaidzidis, M. Zerial, Signal processing by the endosomal system. *Current opinion in cell biology* **39**, 53-60 (2016).
34. Z. Liu *et al.*, The ubiquitin-specific protease USP2a prevents endocytosis-mediated EGFR degradation. *Oncogene* **32**, 1660-1669 (2013).
35. D. J. Katzmann, G. Odorizzi, S. D. Emr, Receptor downregulation and multivesicular-body sorting. *Nature reviews. Molecular cell biology* **3**, 893-905 (2002).
36. R. C. Piper, D. J. Katzmann, Biogenesis and function of multivesicular bodies. *Annual review of cell and developmental biology* **23**, 519-547 (2007).
37. B. Mohapatra *et al.*, Protein tyrosine kinase regulation by ubiquitination: critical roles of Cbl-family ubiquitin ligases. *Biochimica et biophysica acta* **1833**, 122-139 (2013).
38. T. Geetha, J. Jiang, M. W. Wooten, Lysine 63 polyubiquitination of the nerve growth factor receptor TrkA directs internalization and signaling. *Molecular cell* **20**, 301-312 (2005).
39. F. Huang, D. Kirkpatrick, X. Jiang, S. Gygi, A. Sorkin, Differential regulation of EGF receptor internalization and degradation by multiubiquitination within the kinase domain. *Molecular cell* **21**, 737-748 (2006).
40. R. Varadan *et al.*, Solution conformation of Lys63-linked di-ubiquitin chain provides clues to functional diversity of polyubiquitin signaling. *The Journal of biological chemistry* **279**, 7055-7063 (2004).

41. J. A. Nathan, H. T. Kim, L. Ting, S. P. Gygi, A. L. Goldberg, Why do cellular proteins linked to K63-polyubiquitin chains not associate with proteasomes? *The EMBO journal* **32**, 552-565 (2013).
42. R. Ebner, R. Derynck, Epidermal growth factor and transforming growth factor-alpha: differential intracellular routing and processing of ligand-receptor complexes. *Cell Regul* **2**, 599-612 (1991).
43. F. Belleudi *et al.*, Keratinocyte growth factor receptor ligands target the receptor to different intracellular pathways. *Traffic (Copenhagen, Denmark)* **8**, 1854-1872 (2007).
44. K. Roepstorff *et al.*, Differential effects of EGFR ligands on endocytic sorting of the receptor. *Traffic (Copenhagen, Denmark)* **10**, 1115-1127 (2009).
45. S. Sigismund *et al.*, Clathrin-mediated internalization is essential for sustained EGFR signaling but dispensable for degradation. *Developmental cell* **15**, 209-219 (2008).
46. A. R. French, G. P. Sudlow, H. S. Wiley, D. A. Lauffenburger, Postendocytic trafficking of epidermal growth factor-receptor complexes is mediated through saturable and specific endosomal interactions. *The Journal of biological chemistry* **269**, 15749-15755 (1994).
47. M. Kazazic *et al.*, EGF-induced activation of the EGF receptor does not trigger mobilization of caveolae. *Traffic (Copenhagen, Denmark)* **7**, 1518-1527 (2006).
48. P. Boissier, J. Chen, U. Huynh-Do, EphA2 signaling following endocytosis: role of Tiam1. *Traffic (Copenhagen, Denmark)* **14**, 1255-1271 (2013).
49. M. Miaczynska, Effects of membrane trafficking on signaling by receptor tyrosine kinases. *Cold Spring Harbor perspectives in biology* **5**, a009035 (2013).
50. A. Morcavallo *et al.*, Insulin and insulin-like growth factor II differentially regulate endocytic sorting and stability of insulin receptor isoform A. *The Journal of biological chemistry* **287**, 11422-11436 (2012).
51. K. Ballmer-Hofer, A. E. Andersson, L. E. Ratcliffe, P. Berger, Neuropilin-1 promotes VEGFR-2 trafficking through Rab11 vesicles thereby specifying signal output. *Blood* **118**, 816-826 (2011).
52. O. Sabet *et al.*, Ubiquitination switches EphA2 vesicular traffic from a continuous safeguard to a finite signalling mode. *Nature communications* **6**, 8047 (2015).
53. M. Baumdick *et al.*, EGF-dependent re-routing of vesicular recycling switches spontaneous phosphorylation suppression to EGFR signaling. *eLife* **4**, (2015).
54. T. Medts *et al.*, Acute ligand-independent Src activation mimics low EGF-induced EGFR surface signalling and redistribution into recycling endosomes. *Experimental cell research* **316**, 3239-3253 (2010).
55. C. R. Lin *et al.*, Protein kinase C phosphorylation at Thr 654 of the unoccupied EGF receptor and EGF binding regulate functional receptor loss by independent mechanisms. *Cell* **44**, 839-848 (1986).
56. Y. Zwang, Y. Yarden, p38 MAP kinase mediates stress-induced internalization of EGFR: implications for cancer chemotherapy. *The EMBO journal* **25**, 4195-4206 (2006).
57. S. Vergarajauregui, A. San Miguel, R. Puertollano, Activation of p38 mitogen-activated protein kinase promotes epidermal growth factor receptor internalization. *Traffic (Copenhagen, Denmark)* **7**, 686-698 (2006).
58. L. Sadowski, I. Pilecka, M. Miaczynska, Signaling from endosomes: location makes a difference. *Experimental cell research* **315**, 1601-1609 (2009).
59. A. Palamidessi *et al.*, Endocytic trafficking of Rac is required for the spatial restriction of signaling in cell migration. *Cell* **134**, 135-147 (2008).
60. C. Joffre *et al.*, A direct role for Met endocytosis in tumorigenesis. *Nature cell biology* **13**, 827-837 (2011).
61. M. H. Schmidt, I. Dikic, The Cbl interactome and its functions. *Nature reviews. Molecular cell biology* **6**, 907-918 (2005).
62. C. B. Thien, W. Y. Langdon, Cbl: many adaptations to regulate protein tyrosine kinases. *Nature reviews. Molecular cell biology* **2**, 294-307 (2001).
63. C. Rubin, G. Gur, Y. Yarden, Negative regulation of receptor tyrosine kinases: unexpected links to c-Cbl and receptor ubiquitylation. *Cell research* **15**, 66-71 (2005).
64. F. Huang, A. Sorkin, Growth factor receptor binding protein 2-mediated recruitment of the RING domain of Cbl to the epidermal growth factor receptor is essential and sufficient to support receptor endocytosis. *Molecular biology of the cell* **16**, 1268-1281 (2005).
65. G. Levkowitz *et al.*, c-Cbl/Sli-1 regulates endocytic sorting and ubiquitination of the epidermal growth factor receptor. *Genes & development* **12**, 3663-3674 (1998).
66. C. B. Thien, F. Walker, W. Y. Langdon, RING finger mutations that abolish c-Cbl-directed polyubiquitination and downregulation of the EGF receptor are insufficient for cell transformation. *Molecular cell* **7**, 355-365 (2001).
67. S. Pennock, Z. Wang, A tale of two Cbls: interplay of c-Cbl and Cbl-b in epidermal growth factor receptor downregulation. *Molecular and cellular biology* **28**, 3020-3037 (2008).
68. L. Duan *et al.*, Cbl-mediated ubiquitinylation is required for lysosomal sorting of epidermal growth factor receptor but is dispensable for endocytosis. *The Journal of biological chemistry* **278**, 28950-28960 (2003).
69. J. V. Abella *et al.*, Met/Hepatocyte growth factor receptor ubiquitination suppresses transformation and is required for Hrs phosphorylation. *Molecular and cellular biology* **25**, 9632-9645 (2005).
70. A. A. de Melker, G. van der Horst, J. Calafat, H. Jansen, J. Borst, c-Cbl ubiquitinates the EGF receptor at the plasma membrane and remains receptor associated throughout the endocytic route. *Journal of cell science* **114**, 2167-2178 (2001).
71. K. Umebayashi, H. Stenmark, T. Yoshimori, Ubc4/5 and c-Cbl continue to ubiquitinate EGF receptor after internalization to facilitate polyubiquitination and degradation. *Molecular biology of the cell* **19**, 3454-3462 (2008).
72. F. D. Myromslien *et al.*, Both clathrin-positive and -negative coats are involved in endosomal sorting of the EGF receptor. *Experimental cell research* **312**, 3036-3048 (2006).
73. M. D. Petroski, R. J. Deshaies, Function and regulation of cullin-RING ubiquitin ligases. *Nature reviews. Molecular cell biology* **6**, 9-20 (2005).
74. J. R. Lydeard, B. A. Schulman, J. W. Harper, Building and remodelling Cullin-RING E3 ubiquitin ligases. *EMBO reports* **14**, 1050-1061 (2013).
75. B. T. Kile *et al.*, The SOCS box: a tale of destruction and degradation. *Trends in biochemical sciences* **27**, 235-241 (2002).

76. A. N. Bullock, M. C. Rodriguez, J. E. Debreczeni, Z. Songyang, S. Knapp, Structure of the SOCS4-ElonginB/C complex reveals a distinct SOCS box interface and the molecular basis for SOCS-dependent EGFR degradation. *Structure (London, England : 1993)* **15**, 1493-1504 (2007).
77. J. J. Babon *et al.*, The structure of SOCS3 reveals the basis of the extended SH2 domain function and identifies an unstructured insertion that regulates stability. *Molecular cell* **22**, 205-216 (2006).
78. F. Zadjali *et al.*, Structural basis for c-KIT inhibition by the suppressor of cytokine signaling 6 (SOCS6) ubiquitin ligase. *The Journal of biological chemistry* **286**, 480-490 (2011).
79. A. N. Bullock, J. E. Debreczeni, A. M. Edwards, M. Sundstrom, S. Knapp, Crystal structure of the SOCS2-elongin C-elongin B complex defines a prototypical SOCS box ubiquitin ligase. *Proceedings of the National Academy of Sciences of the United States of America* **103**, 7637-7642 (2006).
80. E. M. Linossi, J. J. Babon, D. J. Hilton, S. E. Nicholson, Suppression of cytokine signaling: the SOCS perspective. *Cytokine & growth factor reviews* **24**, 241-248 (2013).
81. Z. P. Feng *et al.*, The N-terminal domains of SOCS proteins: a conserved region in the disordered N-termini of SOCS4 and 5. *Proteins* **80**, 946-957 (2012).
82. D. J. Hilton, Negative regulators of cytokine signal transduction. *Cellular and molecular life sciences : CMLS* **55**, 1568-1577 (1999).
83. A. Matsumoto *et al.*, CIS, a cytokine inducible SH2 protein, is a target of the JAK-STAT5 pathway and modulates STAT5 activation. *Blood* **89**, 3148-3154 (1997).
84. A. Yoshimura, The CIS family: negative regulators of JAK-STAT signaling. *Cytokine & growth factor reviews* **9**, 197-204 (1998).
85. K. Yamamoto, M. Yamaguchi, N. Miyasaka, O. Miura, SOCS-3 inhibits IL-12-induced STAT4 activation by binding through its SH2 domain to the STAT4 docking site in the IL-12 receptor beta2 subunit. *Biochemical and biophysical research communications* **310**, 1188-1193 (2003).
86. K. Boyle *et al.*, Deletion of the SOCS box of suppressor of cytokine signaling 3 (SOCS3) in embryonic stem cells reveals SOCS box-dependent regulation of JAK but not STAT phosphorylation. *Cellular signalling* **21**, 394-404 (2009).
87. J. J. Babon *et al.*, Suppression of cytokine signaling by SOCS3: characterization of the mode of inhibition and the basis of its specificity. *Immunity* **36**, 239-250 (2012).
88. H. Yasukawa *et al.*, The JAK-binding protein JAB inhibits Janus tyrosine kinase activity through binding in the activation loop. *The EMBO journal* **18**, 1309-1320 (1999).
89. A. Sasaki *et al.*, Cytokine-inducible SH2 protein-3 (CIS3/SOCS3) inhibits Janus tyrosine kinase by binding through the N-terminal kinase inhibitory region as well as SH2 domain. *Genes to cells : devoted to molecular & cellular mechanisms* **4**, 339-351 (1999).
90. S. E. Nicholson *et al.*, Mutational analyses of the SOCS proteins suggest a dual domain requirement but distinct mechanisms for inhibition of LIF and IL-6 signal transduction. *The EMBO journal* **18**, 375-385 (1999).
91. E. M. Linossi *et al.*, Suppressor of Cytokine Signaling (SOCS) 5 utilises distinct domains for regulation of JAK1 and interaction with the adaptor protein Shc-1. *PloS one* **8**, e70536 (2013).
92. D. Ungureanu, P. Saharinen, I. Junttila, D. J. Hilton, O. Silvennoinen, Regulation of Jak2 through the ubiquitin-proteasome pathway involves phosphorylation of Jak2 on Y1007 and interaction with SOCS-1. *Molecular and cellular biology* **22**, 3316-3326 (2002).
93. J. J. Babon, A. Laktyushin, N. J. Kershaw, In vitro ubiquitination of cytokine signaling components. *Methods in molecular biology (Clifton, N.J.)* **967**, 261-271 (2013).
94. M. Vesterlund *et al.*, The SOCS2 ubiquitin ligase complex regulates growth hormone receptor levels. *PloS one* **6**, e25358 (2011).
95. M. J. van den Eijnden, G. J. Strous, Autocrine growth hormone: effects on growth hormone receptor trafficking and signaling. *Molecular endocrinology (Baltimore, Md.)* **21**, 2832-2846 (2007).
96. R. Starr *et al.*, SOCS-1 binding to tyrosine 441 of IFN-gamma receptor subunit 1 contributes to the attenuation of IFN-gamma signaling in vivo. *Journal of immunology (Baltimore, Md. : 1950)* **183**, 4537-4544 (2009).
97. Y. Qing, A. P. Costa-Pereira, D. Watling, G. R. Stark, Role of tyrosine 441 of interferon-gamma receptor subunit 1 in SOCS-1-mediated attenuation of STAT1 activation. *The Journal of biological chemistry* **280**, 1849-1853 (2005).
98. J. E. Fenner *et al.*, Suppressor of cytokine signaling 1 regulates the immune response to infection by a unique inhibition of type I interferon activity. *Nature immunology* **7**, 33-39 (2006).
99. R. A. Piganis *et al.*, Suppressor of cytokine signaling (SOCS) 1 inhibits type I interferon (IFN) signaling via the interferon alpha receptor (IFNAR1)-associated tyrosine kinase Tyk2. *The Journal of biological chemistry* **286**, 33811-33818 (2011).
100. J. C. Marine *et al.*, SOCS1 deficiency causes a lymphocyte-dependent perinatal lethality. *Cell* **98**, 609-616 (1999).
101. M. M. Chong *et al.*, Suppressor of cytokine signaling-1 is a critical regulator of interleukin-7-dependent CD8+ T cell differentiation. *Immunity* **18**, 475-487 (2003).
102. A. L. Cornish *et al.*, Suppressor of cytokine signaling-1 regulates signaling in response to interleukin-2 and other gamma c-dependent cytokines in peripheral T cells. *The Journal of biological chemistry* **278**, 22755-22761 (2003).
103. S. Ilangumaran *et al.*, Suppressor of cytokine signaling 1 attenuates IL-15 receptor signaling in CD8+ thymocytes. *Blood* **102**, 4115-4122 (2003).
104. G. M. Davey *et al.*, SOCS-1 regulates IL-15-driven homeostatic proliferation of antigen-naive CD8 T cells, limiting their autoimmune potential. *The Journal of experimental medicine* **202**, 1099-1108 (2005).
105. Y. Zhan *et al.*, SOCS1 negatively regulates the production of Foxp3+ CD4+ T cells in the thymus. *Immunology and cell biology* **87**, 473-480 (2009).
106. M. M. Chong, D. Metcalf, E. Jamieson, W. S. Alexander, T. W. Kay, Suppressor of cytokine signaling-1 in T cells and macrophages is critical for preventing lethal inflammation. *Blood* **106**, 1668-1675 (2005).
107. C. J. Greenhalgh *et al.*, SOCS2 negatively regulates growth hormone action in vitro and in vivo. *The Journal of clinical investigation* **115**, 397-406 (2005).
108. P. A. Ram, D. J. Waxman, SOCS/CIS protein inhibition of growth hormone-stimulated STAT5 signaling by multiple mechanisms. *The Journal of biological chemistry* **274**, 35553-35561 (1999).
109. A. Pezet, H. Favre, P. A. Kelly, M. Edery, Inhibition and restoration of prolactin signal transduction by suppressors of cytokine signaling. *The Journal of biological chemistry* **274**, 24497-24502 (1999).
110. J. Harris *et al.*, Socs2 and elf5 mediate prolactin-induced mammary gland development. *Molecular endocrinology (Baltimore, Md.)* **20**, 1177-1187 (2006).

111. D. Lavens *et al.*, A complex interaction pattern of CIS and SOCS2 with the leptin receptor. *Journal of cell science* **119**, 2214-2224 (2006).
112. F. M. Ghazawi, E. M. Faller, P. Parmar, A. El-Salfiti, P. A. MacPherson, Suppressor of cytokine signaling (SOCS) proteins are induced by IL-7 and target surface CD127 protein for degradation in human CD8 T cells. *Cellular immunology* **306-307**, 41-52 (2016).
113. S. Eyckerman *et al.*, Design and application of a cytokine-receptor-based interaction trap. *Nature cell biology* **3**, 1114-1119 (2001).
114. A. Wolfler *et al.*, Site-specific ubiquitination determines lysosomal sorting and signal attenuation of the granulocyte colony-stimulating factor receptor. *Traffic (Copenhagen, Denmark)* **10**, 1168-1179 (2009).
115. D. Zhuang, Y. Qiu, S. J. Haque, F. Dong, Tyrosine 729 of the G-CSF receptor controls the duration of receptor signaling: involvement of SOCS3 and SOCS1. *Journal of leukocyte biology* **78**, 1008-1015 (2005).
116. M. I. Irandoust *et al.*, Suppressor of cytokine signaling 3 controls lysosomal routing of G-CSF receptor. *The EMBO journal* **26**, 1782-1793 (2007).
117. S. E. Nicholson *et al.*, Suppressor of cytokine signaling-3 preferentially binds to the SHP-2-binding site on the shared cytokine receptor subunit gp130. *Proceedings of the National Academy of Sciences of the United States of America* **97**, 6493-6498 (2000).
118. R. Lang *et al.*, SOCS3 regulates the plasticity of gp130 signaling. *Nature immunology* **4**, 546-550 (2003).
119. C. Brender *et al.*, Suppressor of cytokine signaling 3 regulates CD8 T-cell proliferation by inhibition of interleukins 6 and 27. *Blood* **110**, 2528-2536 (2007).
120. S. L. Dunn *et al.*, Feedback inhibition of leptin receptor/Jak2 signaling via Tyr1138 of the leptin receptor and suppressor of cytokine signaling 3. *Molecular endocrinology (Baltimore, Md.)* **19**, 925-938 (2005).
121. A. Sasaki *et al.*, CIS3/SOCS-3 suppresses erythropoietin (EPO) signaling by binding the EPO receptor and JAK2. *The Journal of biological chemistry* **275**, 29338-29347 (2000).
122. M. Hortner, U. Nielsch, L. M. Mayr, P. C. Heinrich, S. Haan, A new high affinity binding site for suppressor of cytokine signaling-3 on the erythropoietin receptor. *European journal of biochemistry* **269**, 2516-2526 (2002).
123. Y. Seki *et al.*, Expression of the suppressor of cytokine signaling-5 (SOCS5) negatively regulates IL-4-dependent STAT6 activation and Th2 differentiation. *Proceedings of the National Academy of Sciences of the United States of America* **99**, 13003-13008 (2002).
124. F. Verdier *et al.*, Proteasomes regulate erythropoietin receptor and signal transducer and activator of transcription 5 (STAT5) activation. Possible involvement of the ubiquitinated Cis protein. *The Journal of biological chemistry* **273**, 28185-28190 (1998).
125. A. Yoshimura *et al.*, A novel cytokine-inducible gene CIS encodes an SH2-containing protein that binds to tyrosine-phosphorylated interleukin 3 and erythropoietin receptors. *The EMBO journal* **14**, 2816-2826 (1995).
126. F. Dif, E. Saunier, B. Demeneix, P. A. Kelly, M. Edery, Cytokine-inducible SH2-containing protein suppresses PRL signaling by binding the PRL receptor. *Endocrinology* **142**, 5286-5293 (2001).
127. A. Matsumoto *et al.*, Suppression of STAT5 functions in liver, mammary glands, and T cells in cytokine-inducible SH2-containing protein 1 transgenic mice. *Molecular and cellular biology* **19**, 6396-6407 (1999).
128. M. J. Aman *et al.*, CIS associates with the interleukin-2 receptor beta chain and inhibits interleukin-2-dependent signaling. *The Journal of biological chemistry* **274**, 30266-30272 (1999).
129. Y. B. Choi, M. Son, M. Park, J. Shin, Y. Yun, SOCS-6 negatively regulates T cell activation through targeting p56lck to proteasomal degradation. *The Journal of biological chemistry* **285**, 7271-7280 (2010).
130. P. De Sepulveda *et al.*, Socs1 binds to multiple signalling proteins and suppresses steel factor-dependent proliferation. *The EMBO journal* **18**, 904-915 (1999).
131. N. A. Cacalano, D. Sanden, J. A. Johnston, Tyrosine-phosphorylated SOCS-3 inhibits STAT activation but binds to p120 RasGAP and activates Ras. *Nature cell biology* **3**, 460-465 (2001).
132. P. De Sepulveda, S. Ilangumaran, R. Rottapel, Suppressor of cytokine signaling-1 inhibits VAV function through protein degradation. *The Journal of biological chemistry* **275**, 14005-14008 (2000).
133. K. Ohya *et al.*, SOCS-1/JAB/SSI-1 can bind to and suppress Tec protein-tyrosine kinase. *The Journal of biological chemistry* **272**, 27178-27182 (1997).
134. A. Ryo *et al.*, Regulation of NF-kappaB signaling by Pin1-dependent prolyl isomerization and ubiquitin-mediated proteolysis of p65/RelA. *Molecular cell* **12**, 1413-1426 (2003).
135. L. Rui, M. Yuan, D. Frantz, S. Shoelson, M. F. White, SOCS-1 and SOCS-3 block insulin signaling by ubiquitin-mediated degradation of IRS1 and IRS2. *The Journal of biological chemistry* **277**, 42394-42398 (2002).
136. E. Liu, J. F. Cote, K. Vuori, Negative regulation of FAK signaling by SOCS proteins. *The EMBO journal* **22**, 5036-5046 (2003).
137. S. H. Lee *et al.*, Suppressor of cytokine signaling 2 regulates IL-15-primed human NK cell function via control of phosphorylated Pyk2. *Journal of immunology (Baltimore, Md. : 1950)* **185**, 917-928 (2010).
138. I. Paul *et al.*, The ubiquitin ligase Cullin5SOCS2 regulates NDR1/STK38 stability and NF-kappaB transactivation. *Scientific reports* **7**, 42800 (2017).
139. H. Frobose *et al.*, Suppressor of cytokine Signaling-3 inhibits interleukin-1 signaling by targeting the TRAF-6/TAK1 complex. *Molecular endocrinology (Baltimore, Md.)* **20**, 1587-1596 (2006).
140. L. Kedzierski *et al.*, Suppressor of cytokine signaling (SOCS)5 ameliorates influenza infection via inhibition of EGFR signaling. *eLife* **6**, (2017).
141. D. L. Krebs *et al.*, SOCS-6 binds to insulin receptor substrate 4, and mice lacking the SOCS-6 gene exhibit mild growth retardation. *Molecular and cellular biology* **22**, 4567-4578 (2002).
142. L. Li *et al.*, Insulin induces SOCS-6 expression and its binding to the p85 monomer of phosphoinositide 3-kinase, resulting in improvement in glucose metabolism. *The Journal of biological chemistry* **279**, 34107-34114 (2004).
143. A. Teckchandani *et al.*, Cullin 5 destabilizes Cas to inhibit Src-dependent cell transformation. *Journal of cell science* **127**, 509-520 (2014).
144. A. S. Banks *et al.*, Deletion of SOCS7 leads to enhanced insulin action and enlarged islets of Langerhans. *The Journal of clinical investigation* **115**, 2462-2471 (2005).
145. S. Simo, J. A. Cooper, Rbx2 Regulates Neuronal Migration through Different Cullin 5-RING Ligase Adaptors. *Developmental cell*, (2013).
146. D. C. Palmer *et al.*, Cish actively silences TCR signaling in CD8+ T cells to maintain tumor tolerance. *The Journal of experimental medicine* **212**, 2095-2113 (2015).

147. M. S. Melikova, K. A. Kondratov, E. S. Kornilova, Two different stages of epidermal growth factor (EGF) receptor endocytosis are sensitive to free ubiquitin depletion produced by proteasome inhibitor MG132. *Cell biology international* **30**, 31-43 (2006).
148. R. P. Bourette *et al.*, Suppressor of cytokine signaling 1 interacts with the macrophage colony-stimulating factor receptor and negatively regulates its proliferation signal. *The Journal of biological chemistry* **276**, 22133-22139 (2001).
149. R. A. Mooney *et al.*, Suppressors of cytokine signaling-1 and -6 associate with and inhibit the insulin receptor. A potential mechanism for cytokine-mediated insulin resistance. *The Journal of biological chemistry* **276**, 25889-25893 (2001).
150. Y. Gui *et al.*, Regulation of MET receptor tyrosine kinase signaling by suppressor of cytokine signaling 1 in hepatocellular carcinoma. *Oncogene* **34**, 5718-5728 (2015).
151. T. Ben-Zvi, A. Yayon, A. Gertler, E. Monsonego-Ornan, Suppressors of cytokine signaling (SOCS) 1 and SOCS3 interact with and modulate fibroblast growth factor receptor signaling. *Journal of cell science* **119**, 380-387 (2006).
152. L. Xia *et al.*, Identification of both positive and negative domains within the epidermal growth factor receptor COOH-terminal region for signal transducer and activator of transcription (STAT) activation. *The Journal of biological chemistry* **277**, 30716-30723 (2002).
153. J. U. Kazi, L. Ronnstrand, Suppressor of cytokine signaling 2 (SOCS2) associates with FLT3 and negatively regulates downstream signaling. *Molecular oncology* **7**, 693-703 (2013).
154. B. R. Dey, S. L. Spence, P. Nissley, R. W. Furlanetto, Interaction of human suppressor of cytokine signaling (SOCS)-2 with the insulin-like growth factor-I receptor. *The Journal of biological chemistry* **273**, 24095-24101 (1998).
155. Y. Goldshmit, C. E. Walters, H. J. Scott, C. J. Greenhalgh, A. M. Turnley, SOCS2 induces neurite outgrowth by regulation of epidermal growth factor receptor activation. *The Journal of biological chemistry* **279**, 16349-16355 (2004).
156. R. T. Uren *et al.*, A novel role of suppressor of cytokine signaling-2 in the regulation of TrkA neurotrophin receptor biology. *J Neurochem* **129**, 614-627 (2014).
157. B. R. Dey, R. W. Furlanetto, P. Nissley, Suppressor of cytokine signaling (SOCS)-3 protein interacts with the insulin-like growth factor-I receptor. *Biochemical and biophysical research communications* **278**, 38-43 (2000).
158. B. Emanuelli *et al.*, SOCS-3 is an insulin-induced negative regulator of insulin signaling. *The Journal of biological chemistry* **275**, 15985-15991 (2000).
159. E. Kario *et al.*, Suppressors of cytokine signaling 4 and 5 regulate epidermal growth factor receptor signaling. *The Journal of biological chemistry* **280**, 7038-7048 (2005).
160. S. E. Nicholson *et al.*, Suppressor of cytokine signaling (SOCS)-5 is a potential negative regulator of epidermal growth factor signaling. *Proceedings of the National Academy of Sciences of the United States of America* **102**, 2328-2333 (2005).
161. B. A. Callus, B. Mathey-Prevot, SOCS36E, a novel Drosophila SOCS protein, suppresses JAK/STAT and EGF-R signalling in the imaginal wing disc. *Oncogene* **21**, 4812-4821 (2002).
162. J. Bayle, S. Letard, R. Frank, P. Dubreuil, P. De Sepulveda, Suppressor of cytokine signaling 6 associates with KIT and regulates KIT receptor signaling. *The Journal of biological chemistry* **279**, 12249-12259 (2004).
163. J. U. Kazi *et al.*, Suppressor of cytokine signaling 6 (SOCS6) negatively regulates Flt3 signal transduction through direct binding to phosphorylated tyrosines 591 and 919 of Flt3. *The Journal of biological chemistry* **287**, 36509-36517 (2012).
164. E. M. Linossi, S. E. Nicholson, Kinase inhibition, competitive binding and proteasomal degradation: resolving the molecular function of the suppressor of cytokine signaling (SOCS) proteins. *Immunological reviews* **266**, 123-133 (2015).
165. J. U. Kazi, N. N. Kabir, A. Flores-Morales, L. Ronnstrand, SOCS proteins in regulation of receptor tyrosine kinase signaling. *Cellular and molecular life sciences : CMLS* **71**, 3297-3310 (2014).
166. G. M. Tannahill *et al.*, SOCS2 can enhance interleukin-2 (IL-2) and IL-3 signaling by accelerating SOCS3 degradation. *Molecular and cellular biology* **25**, 9115-9126 (2005).
167. J. Piessevaux *et al.*, Functional cross-modulation between SOCS proteins can stimulate cytokine signaling. *The Journal of biological chemistry* **281**, 32953-32966 (2006).
168. T. E. Adams *et al.*, Growth hormone preferentially induces the rapid, transient expression of SOCS-3, a novel inhibitor of cytokine receptor signaling. *The Journal of biological chemistry* **273**, 1285-1287 (1998).
169. L. Feng, N. S. Allen, S. Simo, J. A. Cooper, Cullin 5 regulates Dab1 protein levels and neuron positioning during cortical development. *Genes & development* **21**, 2717-2730 (2007).
170. S. Simo, Y. Jossin, J. A. Cooper, Cullin 5 regulates cortical layering by modulating the speed and duration of Dab1-dependent neuronal migration. *J Neurosci* **30**, 5668-5676 (2010).
171. A. Teckchandani, J. A. Cooper, The ubiquitin-proteasome system regulates focal adhesions at the leading edge of migrating cells. *eLife* **5**, (2016).
172. E. M. Linossi, S. E. Nicholson, The SOCS box-adapting proteins for ubiquitination and proteasomal degradation. *IUBMB life* **64**, 316-323 (2012).
173. D. L. Krebs, D. J. Hilton, SOCS proteins: negative regulators of cytokine signaling. *Stem cells (Dayton, Ohio)* **19**, 378-387 (2001).
174. H. C. Yen, Q. Xu, D. M. Chou, Z. Zhao, S. J. Elledge, Global protein stability profiling in mammalian cells. *Science (New York, N.Y.)* **322**, 918-923 (2008).
175. H. C. Yen, S. J. Elledge, Identification of SCF ubiquitin ligase substrates by global protein stability profiling. *Science (New York, N.Y.)* **322**, 923-929 (2008).
176. M. J. Emanuele *et al.*, Global identification of modular cullin-RING ligase substrates. *Cell* **147**, 459-474 (2011).
177. H. C. Lin *et al.*, SELENOPROTEINS. CRL2 aids elimination of truncated selenoproteins produced by failed UGA/Sec decoding. *Science (New York, N.Y.)* **349**, 91-95 (2015).
178. G. Xu, J. S. Paige, S. R. Jaffrey, Global analysis of lysine ubiquitination by ubiquitin remnant immunoaffinity profiling. *Nature biotechnology* **28**, 868-873 (2010).
179. S. A. Sarraf *et al.*, Landscape of the PARKIN-dependent ubiquitylome in response to mitochondrial depolarization. *Nature* **496**, 372-376 (2013).
180. K. G. Mark, T. B. Loveless, D. P. Toczyski, Isolation of ubiquitinated substrates by tandem affinity purification of E3 ligase-polyubiquitin-binding domain fusions (ligase traps). *Nat Protoc* **11**, 291-301 (2016).
181. K. G. Mark, M. Simonetta, A. Maiolica, C. A. Seller, D. P. Toczyski, Ubiquitin ligase trapping identifies an SCF(Saf1) pathway targeting unprocessed vacuolar/lysosomal proteins. *Molecular cell* **53**, 148-161 (2014).
182. M. E. Sowa, E. J. Bennett, S. P. Gygi, J. W. Harper, Defining the human deubiquitinating enzyme interaction landscape. *Cell* **138**, 389-403 (2009).

183. M. K. Tan, H. J. Lim, E. J. Bennett, Y. Shi, J. W. Harper, Parallel SCF adaptor capture proteomics reveals a role for SCFFBXL17 in NRF2 activation via BACH1 repressor turnover. *Molecular cell* **52**, 9-24 (2013).
184. M. A. Davis *et al.*, The SCF-Fbw7 ubiquitin ligase degrades MED13 and MED13L and regulates CDK8 module association with Mediator. *Genes & development* **27**, 151-156 (2013).
185. J. C. Weems *et al.*, Assembly of the Elongin A Ubiquitin Ligase Is Regulated by Genotoxic and Other Stresses. *The Journal of biological chemistry* **290**, 15030-15041 (2015).
186. C. Kahana, G. Asher, Y. Shaul, Mechanisms of protein degradation: an odyssey with ODC. *Cell cycle (Georgetown, Tex.)* **4**, 1461-1464 (2005).
187. T. A. Soucy *et al.*, An inhibitor of NEDD8-activating enzyme as a new approach to treat cancer. *Nature* **458**, 732-736 (2009).
188. M. Harreman *et al.*, Distinct ubiquitin ligases act sequentially for RNA polymerase II polyubiquitylation. *Proceedings of the National Academy of Sciences of the United States of America* **106**, 20705-20710 (2009).
189. Y. Zhang, A. Wolf-Yadlin, F. M. White, Quantitative proteomic analysis of phosphotyrosine-mediated cellular signaling networks. *Methods in molecular biology (Clifton, N.J.)* **359**, 203-212 (2007).
190. T. G. Curran, B. D. Bryson, M. Reigelhaupt, H. Johnson, F. M. White, Computer aided manual validation of mass spectrometry-based proteomic data. *Methods* **61**, 219-226 (2013).
191. A. M. Nichols, F. M. White, Manual validation of peptide sequence and sites of tyrosine phosphorylation from MS/MS spectra. *Methods in molecular biology (Clifton, N.J.)* **492**, 143-160 (2009).
192. G. S. Goldberg *et al.*, Src phosphorylates Cas on tyrosine 253 to promote migration of transformed cells. *The Journal of biological chemistry* **278**, 46533-46540 (2003).
193. N. Y. Shin *et al.*, Subsets of the major tyrosine phosphorylation sites in Crk-associated substrate (CAS) are sufficient to promote cell migration. *The Journal of biological chemistry* **279**, 38331-38337 (2004).
194. B. B. Brasher, R. A. Van Etten, c-Abl has high intrinsic tyrosine kinase activity that is stimulated by mutation of the Src homology 3 domain and by autophosphorylation at two distinct regulatory tyrosines. *The Journal of biological chemistry* **275**, 35631-35637 (2000).
195. K. Dorey *et al.*, Phosphorylation and structure-based functional studies reveal a positive and a negative role for the activation loop of the c-Abl tyrosine kinase. *Oncogene* **20**, 8075-8084 (2001).
196. R. Plattner, L. Kadlec, K. A. DeMali, A. Kazlauskas, A. M. Pendergast, c-Abl is activated by growth factors and Src family kinases and has a role in the cellular response to PDGF. *Genes & development* **13**, 2400-2411 (1999).
197. P. T. Lakkakorpi, A. J. Bett, L. Lipfert, G. A. Rodan, L. T. Duong, PYK2 autophosphorylation, but not kinase activity, is necessary for adhesion-induced association with c-Src, osteoclast spreading, and bone resorption. *The Journal of biological chemistry* **278**, 11502-11512 (2003).
198. M. Collins *et al.*, The T cell receptor-mediated phosphorylation of Pyk2 tyrosines 402 and 580 occurs via a distinct mechanism than other receptor systems. *Journal of leukocyte biology* **87**, 691-701 (2010).
199. T. M. Aten *et al.*, Tyrosine phosphorylation of the orphan receptor ESDN/DCBLD2 serves as a scaffold for the signaling adaptor CrkL. *FEBS letters* **587**, 2313-2318 (2013).
200. J. Settleman, C. F. Albright, L. C. Foster, R. A. Weinberg, Association between GTPase activators for Rho and Ras families. *Nature* **359**, 153-154 (1992).
201. R. W. Roof *et al.*, Phosphotyrosine (p-Tyr)-dependent and -independent mechanisms of p190 RhoGAP-p120 RasGAP interaction: Tyr 1105 of p190, a substrate for c-Src, is the sole p-Tyr mediator of complex formation. *Molecular and cellular biology* **18**, 7052-7063 (1998).
202. J. R. Glenney, Jr., B. F. Tack, Amino-terminal sequence of p36 and associated p10: identification of the site of tyrosine phosphorylation and homology with S-100. *Proceedings of the National Academy of Sciences of the United States of America* **82**, 7884-7888 (1985).
203. Y. Shi, K. Alin, S. P. Goff, Abl-interactor-1, a novel SH3 protein binding to the carboxy-terminal portion of the Abl protein, suppresses v-abl transforming activity. *Genes & development* **9**, 2583-2597 (1995).
204. Z. Dai *et al.*, Oncogenic Abl and Src tyrosine kinases elicit the ubiquitin-dependent degradation of target proteins through a Ras-independent pathway. *Genes & development* **12**, 1415-1424 (1998).
205. J. R. Ryu, A. Echarri, R. Li, A. M. Pendergast, Regulation of cell-cell adhesion by Abi/Diaphanous complexes. *Molecular and cellular biology* **29**, 1735-1748 (2009).
206. T. Stradal *et al.*, The Abl interactor proteins localize to sites of actin polymerization at the tips of lamellipodia and filopodia. *Current biology : CB* **11**, 891-895 (2001).
207. B. E. Tanos, A. M. Pendergast, Abi-1 forms an epidermal growth factor-inducible complex with Cbl: role in receptor endocytosis. *Cellular signalling* **19**, 1602-1609 (2007).
208. X. Xiong *et al.*, Allosteric inhibition of the nonMyristoylated c-Abl tyrosine kinase by phosphopeptides derived from Abi1/Hssh3bp1. *Biochimica et biophysica acta* **1783**, 737-747 (2008).
209. A. M. Cross *et al.*, Breast cancer antiestrogen resistance 3-p130Cas interactions promote adhesion disassembly and invasion in breast cancer cells. *Oncogene* **35**, 5850-5859 (2016).
210. C. Hernandez-Sanchez, V. Blakesley, T. Kalebic, L. Helman, D. LeRoith, The role of the tyrosine kinase domain of the insulin-like growth factor-I receptor in intracellular signaling, cellular proliferation, and tumorigenesis. *The Journal of biological chemistry* **270**, 29176-29181 (1995).
211. J. E. Peterson *et al.*, Src phosphorylates the insulin-like growth factor type I receptor on the autophosphorylation sites. Requirement for transformation by src. *The Journal of biological chemistry* **271**, 31562-31571 (1996).
212. R. Sarfstein, H. Werner, in *Receptor Tyrosine Kinases: Family and Subfamilies,* D. L. Wheeler, Y. Yarden, Eds., pp. XVII, 878 p. 100 illus., 879 illus. in color.
213. A. Morcavallo, M. Stefanello, R. V. Iozzo, A. Belfiore, A. Morrione, Ligand-mediated endocytosis and trafficking of the insulin-like growth factor receptor I and insulin receptor modulate receptor function. *Front Endocrinol (Lausanne)* **5**, 220 (2014).
214. B. Sehat, S. Andersson, L. Girnita, O. Larsson, Identification of c-Cbl as a new ligase for insulin-like growth factor-I receptor with distinct roles from Mdm2 in receptor ubiquitination and endocytosis. *Cancer research* **68**, 5669-5677 (2008).
215. L. Girnita *et al.*, {beta}-Arrestin is crucial for ubiquitination and down-regulation of the insulin-like growth factor-1 receptor by acting as adaptor for the MDM2 E3 ligase. *The Journal of biological chemistry* **280**, 24412-24419 (2005).

216. L. Girnita, A. Girnita, O. Larsson, Mdm2-dependent ubiquitination and degradation of the insulin-like growth factor 1 receptor. *Proceedings of the National Academy of Sciences of the United States of America* **100**, 8247-8252 (2003).
217. G. Monami, V. Emiliozzi, A. Morrione, Grb10/Nedd4-mediated multiubiquitination of the insulin-like growth factor receptor regulates receptor internalization. *Journal of cellular physiology* **216**, 426-437 (2008).
218. A. Vecchione, A. Marchese, P. Henry, D. Rotin, A. Morrione, The Grb10/Nedd4 complex regulates ligand-induced ubiquitination and stability of the insulin-like growth factor I receptor. *Molecular and cellular biology* **23**, 3363-3372 (2003).
219. E. Eden *et al.*, Proteome half-life dynamics in living human cells. *Science (New York, N.Y.)* **331**, 764-768 (2011).
220. T. Gaitanos, I. Dudanova, M. Sakkou, R. Klein, S. Paixao, in *Receptor tyrosine kinases: family and subfamilies,* Y. Y. Deric L Wheeler, Ed. (Springer International Publishing, Switzerland, 2015), pp. 878.
221. Unified nomenclature for Eph family receptors and their ligands, the ephrins. Eph Nomenclature Committee. *Cell* **90**, 403-404 (1997).
222. N. W. Gale *et al.*, Eph receptors and ligands comprise two major specificity subclasses and are reciprocally compartmentalized during embryogenesis. *Neuron* **17**, 9-19 (1996).
223. A. Kania, R. Klein, Mechanisms of ephrin-Eph signalling in development, physiology and disease. *Nature reviews. Molecular cell biology* **17**, 240-256 (2016).
224. P. W. Janes, E. Nievergall, M. Lackmann, Concepts and consequences of Eph receptor clustering. *Seminars in cell & developmental biology* **23**, 43-50 (2012).
225. T. J. Kao, A. Kania, Ephrin-mediated cis-attenuation of Eph receptor signaling is essential for spinal motor axon guidance. *Neuron* **71**, 76-91 (2011).
226. R. F. Carvalho *et al.*, Silencing of EphA3 through a cis interaction with ephrinA5. *Nature neuroscience* **9**, 322-330 (2006).
227. S. Wiesner *et al.*, A change in conformational dynamics underlies the activation of Eph receptor tyrosine kinases. *The EMBO journal* **25**, 4686-4696 (2006).
228. L. E. Wybenga-Groot *et al.*, Structural basis for autoinhibition of the Ephb2 receptor tyrosine kinase by the unphosphorylated juxtamembrane region. *Cell* **106**, 745-757 (2001).
229. J. Nowakowski *et al.*, Structures of the cancer-related Aurora-A, FAK, and EphA2 protein kinases from nanovolume crystallography. *Structure (London, England : 1993)* **10**, 1659-1667 (2002).
230. N. Singla, H. Erdjument-Bromage, J. P. Himanen, T. W. Muir, D. B. Nikolov, A semisynthetic Eph receptor tyrosine kinase provides insight into ligand-induced kinase activation. *Chemistry & biology* **18**, 361-371 (2011).
231. K. L. Binns, P. P. Taylor, F. Sicheri, T. Pawson, S. J. Holland, Phosphorylation of tyrosine residues in the kinase domain and juxtamembrane region regulates the biological and catalytic activities of Eph receptors. *Molecular and cellular biology* **20**, 4791-4805 (2000).
232. D. J. Marston, S. Dickinson, C. D. Nobes, Rac-dependent trans-endocytosis of ephrinBs regulates Eph-ephrin contact repulsion. *Nature cell biology* **5**, 879-888 (2003).
233. G. Mellitzer, Q. Xu, D. G. Wilkinson, Eph receptors and ephrins restrict cell intermingling and communication. *Nature* **400**, 77-81 (1999).
234. Q. Xu, G. Mellitzer, V. Robinson, D. G. Wilkinson, In vivo cell sorting in complementary segmental domains mediated by Eph receptors and ephrins. *Nature* **399**, 267-271 (1999).
235. K. S. Cramer, I. J. Miko, Eph-ephrin signaling in nervous system development. *F1000Res* **5**, (2016).
236. E. B. Pasquale, Eph receptor signalling casts a wide net on cell behaviour. *Nature reviews. Molecular cell biology* **6**, 462-475 (2005).
237. J. J. Campbell, C. J. Watson, Three-dimensional culture models of mammary gland. *Organogenesis* **5**, 43-49 (2009).
238. B. E. Perez White, S. Getsios, Eph receptor and ephrin function in breast, gut, and skin epithelia. *Cell adhesion & migration* **8**, 327-338 (2014).
239. D. M. Brantley-Sieders *et al.*, The receptor tyrosine kinase EphA2 promotes mammary adenocarcinoma tumorigenesis and metastatic progression in mice by amplifying ErbB2 signaling. *The Journal of clinical investigation* **118**, 64-78 (2008).
240. N. Munarini *et al.*, Altered mammary epithelial development, pattern formation and involution in transgenic mice expressing the EphB4 receptor tyrosine kinase. *Journal of cell science* **115**, 25-37 (2002).
241. M. Haldimann *et al.*, Deregulated ephrin-B2 expression in the mammary gland interferes with the development of both the glandular epithelium and vasculature and promotes metastasis formation. *International journal of oncology* **35**, 525-536 (2009).
242. P. Kaenel, S. Hahnewald, C. Wotzkow, R. Strange, A. C. Andres, Overexpression of EphB4 in the mammary epithelium shifts the differentiation pathway of progenitor cells and promotes branching activity and vascularization. *Development, growth & differentiation* **56**, 255-275 (2014).
243. P. Kaenel *et al.*, Deregulated ephrin-B2 signaling in mammary epithelial cells alters the stem cell compartment and interferes with the epithelial differentiation pathway. *International journal of oncology* **40**, 357-369 (2012).
244. W. B. Fang, D. M. Brantley-Sieders, Y. Hwang, A. J. Ham, J. Chen, Identification and functional analysis of phosphorylated tyrosine residues within EphA2 receptor tyrosine kinase. *The Journal of biological chemistry* **283**, 16017-16026 (2008).
245. J. Walker-Daniels, D. J. Riese, 2nd, M. S. Kinch, c-Cbl-dependent EphA2 protein degradation is induced by ligand binding. *Molecular cancer research : MCR* **1**, 79-87 (2002).
246. Y. Wang *et al.*, Negative regulation of EphA2 receptor by Cbl. *Biochemical and biophysical research communications* **296**, 214-220 (2002).
247. D. Dutta *et al.*, EphrinA2 regulates clathrin mediated KSHV endocytosis in fibroblast cells by coordinating integrin-associated signaling and c-Cbl directed polyubiquitination. *PLoS pathogens* **9**, e1003510 (2013).
248. S. Chakraborty, M. V. Veettil, V. Bottero, B. Chandran, Kaposi's sarcoma-associated herpesvirus interacts with EphrinA2 receptor to amplify signaling essential for productive infection. *Proceedings of the National Academy of Sciences of the United States of America* **109**, E1163-1172 (2012).
249. C. Naudin *et al.*, SLAP displays tumour suppressor functions in colorectal cancer via destabilization of the SRC substrate EPHA2. *Nature communications* **5**, 3159 (2014).
250. M. Tandon, S. V. Vemula, S. K. Mittal, Emerging strategies for EphA2 receptor targeting for cancer therapeutics. *Expert opinion on therapeutic targets* **15**, 31-51 (2011).
251. E. B. Pasquale, Eph receptors and ephrins in cancer: bidirectional signalling and beyond. *Nature reviews. Cancer* **10**, 165-180 (2010).
252. M. Macrae *et al.*, A conditional feedback loop regulates Ras activity through EphA2. *Cancer cell* **8**, 111-118 (2005).

253. M. Lu, K. D. Miller, Y. Gokmen-Polar, M. H. Jeng, M. S. Kinch, EphA2 overexpression decreases estrogen dependence and tamoxifen sensitivity. *Cancer research* **63**, 3425-3429 (2003).
254. D. P. Zelinski *et al.*, Estrogen and Myc negatively regulate expression of the EphA2 tyrosine kinase. *Journal of cellular biochemistry* **85**, 714-720 (2002).
255. G. Zhuang *et al.*, Elevation of receptor tyrosine kinase EphA2 mediates resistance to trastuzumab therapy. *Cancer research* **70**, 299-308 (2010).
256. D. P. Zelinski, N. D. Zantek, J. C. Stewart, A. R. Irizarry, M. S. Kinch, EphA2 overexpression causes tumorigenesis of mammary epithelial cells. *Cancer research* **61**, 2301-2306 (2001).
257. K. J. Roux, D. I. Kim, M. Raida, B. Burke, A promiscuous biotin ligase fusion protein identifies proximal and interacting proteins in mammalian cells. *The Journal of cell biology* **196**, 801-810 (2012).
258. J. P. Lambert, M. Tucholska, C. Go, J. D. Knight, A. C. Gingras, Proximity biotinylation and affinity purification are complementary approaches for the interactome mapping of chromatin-associated protein complexes. *J Proteomics* **118**, 81-94 (2015).
259. A. L. Couzens *et al.*, Protein interaction network of the mammalian Hippo pathway reveals mechanisms of kinase-phosphatase interactions. *Sci Signal* **6**, rs15 (2013).
260. E. Coyaud *et al.*, BioID-based Identification of Skp Cullin F-box (SCF)beta-TrCP1/2 E3 Ligase Substrates. *Molecular & cellular proteomics : MCP* **14**, 1781-1795 (2015).
261. J. Cox, M. Mann, MaxQuant enables high peptide identification rates, individualized p.p.b.-range mass accuracies and proteome-wide protein quantification. *Nature biotechnology* **26**, 1367-1372 (2008).
262. J. C. Silva, M. V. Gorenstein, G. Z. Li, J. P. Vissers, S. J. Geromanos, Absolute quantification of proteins by LCMSE: a virtue of parallel MS acquisition. *Molecular & cellular proteomics : MCP* **5**, 144-156 (2006).
263. G. Teo *et al.*, SAINTq: Scoring protein-protein interactions in affinity purification - mass spectrometry experiments with fragment or peptide intensity data. *Proteomics* **16**, 2238-2245 (2016).
264. D. Szklarczyk *et al.*, STRING v10: protein-protein interaction networks, integrated over the tree of life. *Nucleic Acids Res* **43**, D447-452 (2015).
265. M. J. Keuss *et al.*, Characterization of the mammalian family of DCN-type NEDD8 E3 ligases. *Journal of cell science* **129**, 1441-1454 (2016).
266. T. Kurz *et al.*, The conserved protein DCN-1/Dcn1p is required for cullin neddylation in C. elegans and S. cerevisiae. *Nature* **435**, 1257-1261 (2005).
267. M. F. Kleijnen *et al.*, The hPLIC proteins may provide a link between the ubiquitination machinery and the proteasome. *Molecular cell* **6**, 409-419 (2000).
268. E. N. N'Diaye *et al.*, PLIC proteins or ubiquilins regulate autophagy-dependent cell survival during nutrient starvation. *EMBO reports* **10**, 173-179 (2009).
269. R. Heir *et al.*, The UBL domain of PLIC-1 regulates aggresome formation. *EMBO reports* **7**, 1252-1258 (2006).
270. A. L. Wu, J. Wang, A. Zheleznyak, E. J. Brown, Ubiquitin-related proteins regulate interaction of vimentin intermediate filaments with the plasma membrane. *Molecular cell* **4**, 619-625 (1999).
271. N. R. Gangula, S. Maddika, WD repeat protein WDR48 in complex with deubiquitinase USP12 suppresses Akt-dependent cell survival signaling by stabilizing PH domain leucine-rich repeat protein phosphatase 1 (PHLPP1). *The Journal of biological chemistry* **288**, 34545-34554 (2013).
272. Y. Kee *et al.*, WDR20 regulates activity of the USP12 x UAF1 deubiquitinating enzyme complex. *The Journal of biological chemistry* **285**, 11252-11257 (2010).
273. S. Cavadini *et al.*, Cullin-RING ubiquitin E3 ligase regulation by the COP9 signalosome. *Nature* **531**, 598-603 (2016).
274. T. Yasukawa *et al.*, Mammalian Elongin A complex mediates DNA-damage-induced ubiquitylation and degradation of Rpb1. *The EMBO journal* **27**, 3256-3266 (2008).
275. M. Antonioli *et al.*, AMBRA1 interplay with cullin E3 ubiquitin ligases regulates autophagy dynamics. *Developmental cell* **31**, 734-746 (2014).
276. C. J. Greenhalgh *et al.*, Growth enhancement in suppressor of cytokine signaling 2 (SOCS-2)-deficient mice is dependent on signal transducer and activator of transcription 5b (STAT5b). *Molecular endocrinology (Baltimore, Md.)* **16**, 1394-1406 (2002).
277. B. K. Garvalov *et al.*, The conformational state of Tes regulates its zyxin-dependent recruitment to focal adhesions. *The Journal of cell biology* **161**, 33-39 (2003).
278. J. Oldenburg *et al.*, VASP, zyxin and TES are tension-dependent members of Focal Adherens Junctions independent of the alpha-catenin-vinculin module. *Scientific reports* **5**, 17225 (2015).
279. J. Krcmery, T. Camarata, A. Kulisz, H. G. Simon, Nucleocytoplasmic functions of the PDZ-LIM protein family: new insights into organ development. *Bioessays* **32**, 100-108 (2010).
280. K. Mandai *et al.*, Afadin: A novel actin filament-binding protein with one PDZ domain localized at cadherin-based cell-to-cell adherens junction. *The Journal of cell biology* **139**, 517-528 (1997).
281. J. D. Hildebrand, P. Soriano, Shroom, a PDZ domain-containing actin-binding protein, is required for neural tube morphogenesis in mice. *Cell* **99**, 485-497 (1999).
282. J. K. Zalewski *et al.*, Structure of the Shroom-Rho Kinase Complex Reveals a Binding Interface with Monomeric Shroom That Regulates Cell Morphology and Stimulates Kinase Activity. *The Journal of biological chemistry* **291**, 25364-25374 (2016).
283. J. M. Daniel, A. B. Reynolds, Tyrosine phosphorylation and cadherin/catenin function. *Bioessays* **19**, 883-891 (1997).
284. S. M. Feller, Crk family adaptors-signalling complex formation and biological roles. *Oncogene* **20**, 6348-6371 (2001).
285. M. K. Rosen *et al.*, Direct demonstration of an intramolecular SH2-phosphotyrosine interaction in the Crk protein. *Nature* **374**, 477-479 (1995).
286. A. Gautreau, P. Poullet, D. Louvard, M. Arpin, Ezrin, a plasma membrane-microfilament linker, signals cell survival through the phosphatidylinositol 3-kinase/Akt pathway. *Proceedings of the National Academy of Sciences of the United States of America* **96**, 7300-7305 (1999).
287. Q. Chang, C. Jorgensen, T. Pawson, D. W. Hedley, Effects of dasatinib on EphA2 receptor tyrosine kinase activity and downstream signalling in pancreatic cancer. *Br J Cancer* **99**, 1074-1082 (2008).
288. X. Shi *et al.*, A role of the SAM domain in EphA2 receptor activation. *Scientific reports* **7**, 45084 (2017).

289. D. R. Singh *et al.*, The SAM domain inhibits EphA2 interactions in the plasma membrane. *Biochimica et biophysica acta* **1864**, 31-38 (2017).
290. D. R. Singh *et al.*, Unliganded EphA3 dimerization promoted by the SAM domain. *The Biochemical journal* **471**, 101-109 (2015).
291. N. L. Paul, Purdue University, (2007).
292. E. M. Lisabeth, G. Falivelli, E. B. Pasquale, Eph receptor signaling and ephrins. *Cold Spring Harbor perspectives in biology* **5**, (2013).
293. E. L. Eskelinen, Roles of LAMP-1 and LAMP-2 in lysosome biogenesis and autophagy. *Molecular aspects of medicine* **27**, 495-502 (2006).
294. T. Neill *et al.*, EphA2 is a functional receptor for the growth factor progranulin. *The Journal of cell biology* **215**, 687-703 (2016).
295. R. Hjerpe *et al.*, Efficient protection and isolation of ubiquitylated proteins using tandem ubiquitin-binding entities. *EMBO reports* **10**, 1250-1258 (2009).
296. S. B. Shields, R. C. Piper, How ubiquitin functions with ESCRTs. *Traffic (Copenhagen, Denmark)* **12**, 1306-1317 (2011).
297. J. A. Cooper, T. Kaneko, S. S. Li, Cell regulation by phosphotyrosine-targeted ubiquitin ligases. *Molecular and cellular biology* **35**, 1886-1897 (2015).
298. D. Balasubramaniam, L. N. Paul, K. T. Homan, M. C. Hall, C. V. Stauffacher, Specificity of HCPTP variants toward EphA2 tyrosines by quantitative selected reaction monitoring. *Protein Sci* **20**, 1172-1181 (2011).
299. P. A. Kiely, M. Leahy, D. O'Gorman, R. O'Connor, RACK1-mediated integration of adhesion and insulin-like growth factor I (IGF-I) signaling and cell migration are defective in cells expressing an IGF-I receptor mutated at tyrosines 1250 and 1251. *The Journal of biological chemistry* **280**, 7624-7633 (2005).
300. C. Gundry *et al.*, Phosphorylation of Rab-coupling protein by LMTK3 controls Rab14-dependent EphA2 trafficking to promote cell:cell repulsion. *Nature communications* **8**, 14646 (2017).
301. J. J. Senn *et al.*, Suppressor of cytokine signaling-3 (SOCS-3), a potential mediator of interleukin-6-dependent insulin resistance in hepatocytes. *The Journal of biological chemistry* **278**, 13740-13746 (2003).
302. V. C. Calegari *et al.*, Suppressor of cytokine signaling-3 Provides a novel interface in the cross-talk between angiotensin II and insulin signaling systems. *Endocrinology* **146**, 579-588 (2005).
303. C. Pilling, J. A. Cooper, SOCS2 Binds to and Regulates EphA2 through Multiple Mechanisms. *Scientific reports* **7**, 10838 (2017).
304. B. Linggi, G. Carpenter, ErbB receptors: new insights on mechanisms and biology. *Trends Cell Biol* **16**, 649-656 (2006).
305. M. J. Wieduwilt, M. M. Moasser, The epidermal growth factor receptor family: biology driving targeted therapeutics. *Cellular and molecular life sciences : CMLS* **65**, 1566-1584 (2008).
306. F. Pareja, G. Pines, Y. Yarden, in *Receptor Tyrosine Kinases: Family and Subfamilies,* D. L. Wheeler, Y. Yarden, Eds., pp. XVII, 878 p. 100 illus., 879 illus. in color.
307. M. A. Lemmon, J. Schlessinger, K. M. Ferguson, The EGFR family: not so prototypical receptor tyrosine kinases. *Cold Spring Harbor perspectives in biology* **6**, a020768 (2014).
308. N. E. Hynes, H. A. Lane, ERBB receptors and cancer: the complexity of targeted inhibitors. *Nature reviews. Cancer* **5**, 341-354 (2005).
309. G. Tarcic *et al.*, An unbiased screen identifies DEP-1 tumor suppressor as a phosphatase controlling EGFR endocytosis. *Current biology : CB* **19**, 1788-1798 (2009).
310. Y. Mosesson, G. B. Mills, Y. Yarden, Derailed endocytosis: an emerging feature of cancer. *Nature reviews. Cancer* **8**, 835-850 (2008).
311. J. Debnath, J. S. Brugge, Modelling glandular epithelial cancers in three-dimensional cultures. *Nature reviews. Cancer* **5**, 675-688 (2005).
312. S. K. Muthuswamy, D. Li, S. Lelievre, M. J. Bissell, J. S. Brugge, ErbB2, but not ErbB1, reinitiates proliferation and induces luminal repopulation in epithelial acini. *Nature cell biology* **3**, 785-792 (2001).
313. H. D. Soule *et al.*, Isolation and characterization of a spontaneously immortalized human breast epithelial cell line, MCF-10. *Cancer research* **50**, 6075-6086 (1990).
314. A. Levitzki, A. Gazit, Tyrosine kinase inhibition: an approach to drug development. *Science (New York, N.Y.)* **267**, 1782-1788 (1995).
315. N. Osherov, A. Levitzki, Epidermal-growth-factor-dependent activation of the src-family kinases. *European journal of biochemistry* **225**, 1047-1053 (1994).
316. J. A. Cooper, B. Howell, The when and how of Src regulation. *Cell* **73**, 1051-1054 (1993).
317. J. S. Biscardi *et al.*, c-Src-mediated phosphorylation of the epidermal growth factor receptor on Tyr845 and Tyr1101 is associated with modulation of receptor function. *The Journal of biological chemistry* **274**, 8335-8343 (1999).
318. D. A. Tice, J. S. Biscardi, A. L. Nickles, S. J. Parsons, Mechanism of biological synergy between cellular Src and epidermal growth factor receptor. *Proceedings of the National Academy of Sciences of the United States of America* **96**, 1415-1420 (1999).
319. P. S. Hegde *et al.*, Delineation of molecular mechanisms of sensitivity to lapatinib in breast cancer cell lines using global gene expression profiles. *Mol Cancer Ther* **6**, 1629-1640 (2007).
320. G. E. Konecny *et al.*, Activity of the dual kinase inhibitor lapatinib (GW572016) against HER-2-overexpressing and trastuzumab-treated breast cancer cells. *Cancer research* **66**, 1630-1639 (2006).
321. D. W. Rusnak *et al.*, The effects of the novel, reversible epidermal growth factor receptor/ErbB-2 tyrosine kinase inhibitor, GW2016, on the growth of human normal and tumor-derived cell lines in vitro and in vivo. *Mol Cancer Ther* **1**, 85-94 (2001).
322. A. Sorkin, L. K. Goh, Endocytosis and intracellular trafficking of ErbBs. *Experimental cell research* **314**, 3093-3106 (2008).
323. J. Zhang *et al.*, YAP-dependent induction of amphiregulin identifies a non-cell-autonomous component of the Hippo pathway. *Nature cell biology* **11**, 1444-1450 (2009).
324. G. N. Gill *et al.*, Monoclonal anti-epidermal growth factor receptor antibodies which are inhibitors of epidermal growth factor binding and antagonists of epidermal growth factor binding and antagonists of epidermal growth factor-stimulated tyrosine protein kinase activity. *The Journal of biological chemistry* **259**, 7755-7760 (1984).
325. . (R&D Systems a Biotechne Brand, 2015), chap. 1.
326. . (R&D Systems a Biotechne Brand, 2015), chap. 2, pp. 1.
327. . (R&D Systems a Biotechne Brand, 2015), chap. 2, pp. 1.
328. M. F. Favata *et al.*, Identification of a novel inhibitor of mitogen-activated protein kinase kinase. *The Journal of biological chemistry* **273**, 18623-18632 (1998).

329. A. Citri, Y. Yarden, EGF-ERBB signalling: towards the systems level. *Nature reviews. Molecular cell biology* **7**, 505-516 (2006).
330. R. Dobrowolski, E. M. De Robertis, Endocytic control of growth factor signalling: multivesicular bodies as signalling organelles. *Nature reviews. Molecular cell biology* **13**, 53-60 (2011).
331. M. E. Pitulescu, R. H. Adams, Eph/ephrin molecules--a hub for signaling and endocytosis. *Genes & development* **24**, 2480-2492 (2010).
332. A. Yoshimura, M. Suzuki, R. Sakaguchi, T. Hanada, H. Yasukawa, SOCS, Inflammation, and Autoimmunity. *Frontiers in immunology* **3**, 20 (2012).
333. S. Ilangumaran, S. Ramanathan, R. Rottapel, Regulation of the immune system by SOCS family adaptor proteins. *Seminars in immunology* **16**, 351-365 (2004).
334. A. Yoshimura, T. Naka, M. Kubo, SOCS proteins, cytokine signalling and immune regulation. *Nat Rev Immunol* **7**, 454-465 (2007).
335. P. N. Reddy *et al.*, SOCS1 cooperates with FLT3-ITD in the development of myeloproliferative disease by promoting the escape from external cytokine control. *Blood* **120**, 1691-1702 (2012).
336. H. Kouros-Mehr, Z. Werb, Candidate regulators of mammary branching morphogenesis identified by genome-wide transcript analysis. *Developmental dynamics : an official publication of the American Association of Anatomists* **235**, 3404-3412 (2006).
337. B. Kumar *et al.*, ESCRT-I Protein Tsg101 Plays a Role in the Post-macropinocytic Trafficking and Infection of Endothelial Cells by Kaposi's Sarcoma-Associated Herpesvirus. *PLoS pathogens* **12**, e1005960 (2016).
338. N. D. Zantek *et al.*, E-cadherin regulates the function of the EphA2 receptor tyrosine kinase. *Cell growth & differentiation : the molecular biology journal of the American Association for Cancer Research* **10**, 629-638 (1999).
339. W. Kim *et al.*, Systematic and quantitative assessment of the ubiquitin-modified proteome. *Molecular cell* **44**, 325-340 (2011).
340. A. Tomas, C. E. Futter, E. R. Eden, EGF receptor trafficking: consequences for signaling and cancer. *Trends Cell Biol* **24**, 26-34 (2014).
341. C. Sachsenmaier, H. B. Sadowski, J. A. Cooper, STAT activation by the PDGF receptor requires juxtamembrane phosphorylation sites but not Src tyrosine kinase activation. *Oncogene* **18**, 3583-3592 (1999).
342. K. M. Quesnelle, A. L. Boehm, J. R. Grandis, STAT-mediated EGFR signaling in cancer. *Journal of cellular biochemistry* **102**, 311-319 (2007).
343. S. Kermorgant, P. J. Parker, Receptor trafficking controls weak signal delivery: a strategy used by c-Met for STAT3 nuclear accumulation. *The Journal of cell biology* **182**, 855-863 (2008).
344. C. Choudhary *et al.*, Mislocalized activation of oncogenic RTKs switches downstream signaling outcomes. *Molecular cell* **36**, 326-339 (2009).
345. X. Yang *et al.*, A public genome-scale lentiviral expression library of human ORFs. *Nature methods* **8**, 659-661 (2011).
346. N. Hiramoto-Yamaki *et al.*, Ephexin4 and EphA2 mediate cell migration through a RhoG-dependent mechanism. *The Journal of cell biology* **190**, 461-477 (2010).
347. Y. Zhang *et al.*, Time-resolved mass spectrometry of tyrosine phosphorylation sites in the epidermal growth factor receptor signaling network reveals dynamic modules. *Molecular & cellular proteomics : MCP* **4**, 1240-1250 (2005).
348. L. J. Licklider, C. C. Thoreen, J. Peng, S. P. Gygi, Automation of nanoscale microcapillary liquid chromatography-tandem mass spectrometry with a vented column. *Analytical chemistry* **74**, 3076-3083 (2002).
349. S. Tyanova, T. Temu, J. Cox, The MaxQuant computational platform for mass spectrometry-based shotgun proteomics. *Nat Protoc* **11**, 2301-2319 (2016).

VITA

Carissa Pilling attended the University of Colorado, Boulder where she received a Bachelor of Arts with distinction in Molecular, Cellular, and Developmental Biology (MCDB) & Biochemistry in 2009. While at the University of Colorado Carissa completed two and half years of biophysics research in Dr. Joseph J. Falke's lab. In Dr. Falke's lab she studied the methods pleckstrin homology (PH) domains use to bind phosphoinositide lipids on the plasma membrane. Her work in Dr. Falke's lab was written up in an undergraduate honors thesis titled "GRP1 PH Domain Possesses a Gatekeeper Glutamate (Glu 345) that Controls PIP Lipid Affinity and Specificity" and successfully defended for *summa cum laude* honors in Biochemistry. Carissa continued her research in Dr. Falke's lab for one and half years after graduation and published four peer-reviewed papers on her work in Dr. Falke's lab. Carissa joined the Molecular and Cellular Biology Interdisciplinary Graduate Program at the University of Washington in the Fall of 2011. She received the National Science Foundation graduate research fellowship to complete the work contained in this dissertation. While at the University of Washington, she completed 3-month summer internships at Omeros and Seattle Genetics, two local biotechnology companies. During these experiences, she learned about the discovery and use of antibodies as therapeutics. She defended her dissertation describing $CRL5^{SOCS}$ regulation of receptor tyrosine kinases on November 14th, 2017. Passionate about translating breakthrough research into cancer therapeutics Carissa will be pursuing a job in the biotechnology/pharmaceutical sector after graduate school.